Multiplexed transcriptional control strategies for biosynthesis from mixed substrates in *Escherichia coli*

by

Cynthia Ni

M.S. Chemical Engineering Practice
Massachusetts Institute of Technology (2018)

B.A.Sc. Chemical and Biological Engineering
University of British Columbia (2016)

Submitted to the Department of Chemical Engineering
in partial fulfillment of the requirements for the degree of

Doctor of Philosophy in Chemical Engineering

at the

MASSACHUSETTS INSTITUTE OF TECHNOLOGY

May 2022

Author . . . .
Department of Chemical Engineering
April 29, 2022

Certified by. . . . .
Kristala L. J. Prather
Arthur D. Little Professor of Chemical Engineering
Thesis Supervisor

Accepted by . . . .
Patrick S. Doyle
Robert T. Haslam Professor of Chemical Engineering
Chairman, Committee for Graduate Students

Multiplexed transcriptional control strategies for biosynthesis from mixed substrates in *Escherichia coli*

by

Cynthia Ni

Submitted to the Department of Chemical Engineering
on April 29, 2022, in partial fulfillment of the
requirements for the degree of
Doctor of Philosophy in Chemical Engineering

Abstract

Metabolic engineering reprograms microbes to produce value-added chemicals. Microbial production has the potential to use renewable feedstocks, such as conventional waste streams. Metabolic engineers already contend with the metabolic burden of recombinant production pathways; utilizing complex input streams only further complicates allocating cellular resources appropriately for biosynthesis. This thesis aims to develop transcriptional control strategies that sense and respond to changing feedstock conditions for biosynthesis and demonstrate the ability to produce a product of interest from mixed substrate feeds.

We constructed a galacturonate biosensor with the galacturonate-responsive transcription factor, ExuR, from *Bacillus subtilis* and determined the best performer from a selection of biosensor variants. After establishing no interactions with the host *Escherichia coli* native regulatory system, we applied the biosensor to control expression of biosynthetic pathway. It was confirmed that the biosensor activated transcription in the presence of galacturonate, eliminating the need for a chemically-inducible control system.

A second, gluconate biosensor was constructed with GntR, from *B. subtilis*. The two biosensors were shown to be orthogonal and each was used to control the expression of a novel D-glycerate biosynthetic pathway from its cognate substrate. We demonstrated D-glycerate production from single and mixed substrate feeds and showed that mixed substrates in different ratios resulted in fairly consistent titers.

Finally, the pairwise orthogonality of various AHL-based QS systems was characterized to establish multiple controllers for autonomous, cell density activated expression. We determined the the *las* and *tra* systems demonstrated minimal crosstalk, which agreed with literature findings.

This work demonstrates the engineering of expression controllers and a production strain for biosynthesis from mixed substrate feeds.

Thesis Supervisor: Kristala L. J. Prather
Title: Arthur D. Little Professor of Chemical Engineering

Acknowledgments

Thank you Kris, for everything. For helping to develop me as a scientist and giving me the room to grow as a human being. For holding humanity and levity in as high regard as you do good science. For always believing in me as a scientist, even when I thought I was lost. And for all the laughs, from day one. Thank you to my thesis committee, Greg and Jim, for your support and enlightening input on my project.

Thank you to my undergraduate PI, Vikram Yadav, for introducing metabolic engineering into my life and championing me through grad school applications. I would never have applied to MIT if you hadn't adamantly told me to. And thanks to Karen Cheung, my first ever PI, whose lab was the start of my research career.

To Gwen, Lisa, Stephanie, Christina, Bernie, Kevin, Jennifer, K'yal, Mike, Zappi, Yoseb, Wesley, Kristina, and Jason, thanks for making the Prather Lab such a special place. I'm so glad I got to spend my PhD with you all, having exciting and inspiring scientific discussions, asking any stupid question any number of times, receiving encouragement when experiments failed and celebrations when milestones were achieved, and being bolstered by a group that wants to see each member succeed, in and out of the lab.

To the Ni Fam: Neil, Nika, Mickey, Sam, Astrid, Jules, and Tessa, y'all made Camberville (from the Shaft to the Tip, and beyond) home. All the trails, summits, grill outs, card games, and long talks are what fueled the work in this thesis. Cambridge is also where I found ultimate frisbee. To sMITe, Versa, and Beans, and all the teams in between, I owe all of my on land coordination to you.

To my biological and chosen family: Mom, Dad, Lil, Allens, thank you for being the village that raised and continues to raise me. Much of my strength and confidence comes from you all. Mom and Dad, thank you for all your hard work and sacrifice that paved the way for me to get here.

<div align="right">Cynthia Ni</div>

Contents

List of Figures

List of Tables

Chapter 1

Introduction

Abstract

Metabolic engineering reprograms cells to synthesize value-added products. In doing so, endogenous genes are altered and heterologous genes can be introduced to achieve the necessary enzymatic reactions. Dynamic regulation of metabolic flux is a powerful control scheme to alleviate and overcome the competing cellular objectives that arise from the introduction of these production pathways. This chapter discusses dynamic regulation strategies that can alleviate the metabolic burden of production. These tools are particularly useful when tackling complex process parameters such as complex feed streams.

1.1 Dynamic pathway regulation in metabolic engineering

Metabolic engineering reprograms microbial cells to convert renewable or inexpensive feedstocks to value-added products, including compounds from pharmaceuticals to biofuels.These microbial synthesis processes take advantage of cellular machinery to express endogenous and heterologous genes encoding enzymes that carry out chemical conversions to produce desired products. Enzymatic reactions result in a highly specific product pool, simplifying downstream separation procedures, and fermentation processes occur under environmentally friendly conditions. However, cost efficiency relies on achieving high titer, yield, and productivity criteria, which has proven to be difficult for many products for a variety of reasons. In this chapter, we discuss the challenges that can be addressed through dynamic regulation of metabolic fluxes.

Dynamic metabolic flux regulation is one potential method of balancing competing cellular objectives that are beneficial to achieving high titer, yield, and productivity. For example, conditions that achieve high reaction rates on a per-cell basis may result in burdened growth and, thus, low productivity. This conflict can result from diversion of cellular resources to production pathway-related processes in which the limiting resources could be general, such as ribosomes, or pathway specific, such as metabolites involved in both endogenous and production pathways. Additionally, burdened growth can result from toxicity of production pathway metabolites at high concentrations. Microbial cells naturally face similar trade-offs and manage them by dynamically regulating gene expression. In low-nutrient conditions, survival relies on expression of metabolic pathways that do not benefit fitness in high-nutrient conditions in which essential metabolites can be scavenged from the environment. Cells employ dynamic control approaches to address this and similar situations. Zaslaver et al. [1] analyzed dynamic transcription trends in amino acid biosynthesis systems in *Escherichia coli* to show that the presence of amino acids in the media leads

to decreased transcription of the corresponding pathway genes. They saw that there is temporal control within amino acid biosynthesis pathways such that transcription of upstream genes is upregulated before that of downstream ones.

The observation of dynamic regulation in natural systems raises the question of whether synthetic regulatory systems could be used to advance the goals of metabolic engineering (i.e., to increase titer, yield, and/or productivity) in recombinant organisms. Several computational studies exploring the impact of dynamic regulation in production systems suggest that the optimal dynamic regulation scheme at the appropriate metabolic node can improve production over static control at that point. Gadkar et al. [2] conducted two production case studies in silico that are each subject to a trade-off between high growth rate and high production pathway flux. In the first example, glycerol production relies on diversion of metabolic fluxes from glycolysis to the production pathway. The second example considers that an *ackA* knockout improves ethanol production at the expense of ATP generation, resulting in a growth defect. Their bi-level optimization algorithm predicts that dynamic control at the relevant metabolic node to switch from growth to production phases increases the final glycerol and ethanol production by more than 30% and 40%, respectively. Anesiadis et al. [3, 4] incorporated the circuit dynamics of a toggle switch into their model to show that production improvements can be achieved with a more gradual transition from growth to production phases. Based on the predicted production improvements and studies of natural microbial systems, researchers have constructed and implemented regulatory circuits to dynamically control metabolic fluxes in experimental studies.

1.1.1 Externally controlled factors

The earliest dynamic control circuits responded to chemical inducers that are exogenously added to the culture media. Common chemical inducers include isopropyl β-d-1-thiogalactopyranoside (IPTG) and anhydrotetracycline (aTc) (Figure 1-1). Each of these systems contains three main components: (a) a protein repressor that binds to a specific DNA sequence, (b) an inducible promoter that contains the DNA

sequence that binds to the repressor, and (c) the chemical inducer that binds to the protein repressor. Upon binding, the chemical inducer causes a conformational change in the repressor protein to prevent DNA binding, allowing transcription from the inducible promoter [5–12].These and similar circuits have been applied to control gene expression in several contexts and organisms.

Figure 1-1: Examples of stimuli that can trigger transcriptional control include chemical inducers such as IPTG (shown), temperature, light, environmental factors within a fermentation, cell density or physiology, and metabolites. The changes in transcription lead to shifts in metabolic flux that metabolic engineers can program for effective cell growth, metabolite utilization, and biosynthesis.

The chemically inducible regulation systems, along with many others, are derived from natural regulation systems, which may not exhibit desired induction curve characteristics. To address these limitations, researchers have mutated or evolved circuit components to increase the dynamic range of the circuit and improve the specificity of the response to the desired chemical inducer [13, 14]. For example, Meyer et al. [14] developed a generalizable dual-selection directed evolution scheme to identify regulator proteins and inducible promoters with improved characteristics, such as a larger dynamic range and lower half-induction concentrations. Implementation of these evolved parts can result in greater tunability, leading to more precise control of metabolic fluxes and production gains, or lower inducer concentrations, reducing inducer costs. Another approach to improving the

response of chemically inducible control circuits is to assemble two circuits in a toggle switch architecture in which genes encoding regulator proteins mutually inhibit their corresponding target promoters [15]. Under this arrangement, induction of genes controlled under the regulated promoters is bistable such that gene expression can be stably activated by a transient chemical inducer. Additionally, these circuits display a more switch-like response to inducer addition rather than a graded response of an individual control circuit [15–17]. Although chemically inducible systems have been instrumental tools for experimentally demonstrating the potential benefit of dynamic control, this approach is not generally industrially feasible, as the chemical inducers can add significantly to material costs, potentially rendering a process cost prohibitive. In one analysis, IPTG was by far the most expensive component of a defined medium, accounting for more than half of the materials cost [18]. This limitation has motivated the development of circuits that respond to other extracellular factors, such as light and temperature (Figure 1-1). Temperature-dependent dynamic control systems build on the discovery of the temperature-sensitive mutant of the cI repressor, cI1857 [19], which represses expression from the lambda p_R and p_L promoters only at temperatures below 30°C. This circuit has been applied to dynamically repress gene expression by placing the target gene under the control of a lambda promoter and typically shifting the temperature of the fermentation from 37-42°C to 28-30°C [20–22].

1.1.2 Environmental factors

Conditions that trigger a response can be environmental factors that generally change during a fermentation, such as oxygen, pH, and nutrient levels (Figure 1-1). Many studies that regulate expression based on these factors take advantage of the natural response circuitry present in their host strain. For example, the *DAN1* gene of *Saccharomyces cerevisiae* has been found to be expressed in anaerobic conditions. By appending a target gene to the *DAN1* promoter, Nevoigt et al. [23] dynamically controlled expression based on the dissolved oxygen level of the culture. Similar applications have been investigated using pH-, glucose-, and

phosphate-responsive promoters [16, 24–27]. Although it is possible to improve the responses of these systems, studies thus far have only investigated modifications of the responsive promoter, possibly owing to the global implications of modifying regulatory components or owing to the complexity of the underlying regulatory system. Nevoigt et al. [23] performed directed evolution on the *DAN1* promoter to identify a mutant that activates transcription in microaerobic conditions, making its utilization more industrially feasible, and Moreb et al. [28] obtained different response curves and media-dependent characteristics by using different phosphate-responsive promoters in *E. coli.*

1.1.3   Autoinduction

Autoinducible circuits dynamically control gene expression by responding to changes in an organisms physiological state. For example, some circuits up- or downregulate gene expression when the culture reaches a critical cell density, whereas others trigger expression changes as the cells begin to transition to stationary phase (Figure 1-1). Similar to regulatory systems that respond to common environmental factors, autoinducible systems are attractive because they are autonomous and have shown early promise for generalizability across different pathway contexts [29–31]. Here, we divide autoinducible circuits into circuits that respond during growth phase and those that respond during the transition to stationary phase.

Many regulatory systems that respond during growth phase employ quorum-sensing (QS) circuits. QS is a natural bacterial mechanism for controlling gene expression in a cell density dependent manner. These systems are similar to chemically inducible ones in that they are composed of a regulator protein that changes conformation when bound to a small molecule and one of the conformations enables DNA-binding activity. The key difference is that the small, or signaling, molecule is produced via a pathway within the cells such that the cells are self-induced [32–34]. Additionally, whereas the chemically inducible circuits mentioned previously all employ a regulator protein that acts as a repressor in the absence of the inducer molecule, some QS circuits

contain regulator proteins with different roles. The most widely studied category of QS circuits are *lux*-type systems, which contain a regulator protein that activates transcription from its cognate promoter when bound to its signaling molecule [35, 36]. Examples of *lux*-type QS systems are the *lux* system from *Vibrio fischeri* [32, 35–37] and the *las* and *rhl* systems from *Pseudomonas aeruginosa* [33, 34, 38], each of which use a unique acyl-homoserine lactone (AHL) compound as the signaling molecule.

To apply AHL-based QS circuits to dynamically control gene expression in *E. coli*, genes encoding the regulator protein and AHL synthase, responsible for producing the AHL, are expressed under constitutive promoters, such that the signaling molecule concentration increases with cell density. Expression of the gene of interest is dynamically controlled by placing the gene of interest under the control of the cognate QS promoter [29, 39, 40]. Rather than importing a heterologous QS circuit, researchers have alternatively rewired the native *E. coli* QS system that employs a repressor, LsrR, that is released from the *lsrR* promoter when bound to its cognate signaling molecule. This QS system includes many other proteins involved in the synthesis, transport, and modification of the signaling molecule [41]. Similar approaches have been executed in *S. cerevisiae* − both importing a heterologous QS circuit [42] and rewiring a native circuit [43].

In some contexts, the cell density that corresponds to the threshold concentration of the signaling molecule is an important parameter that must be finely tuned to achieve production improvements. To modulate the switching time, Gupta et al. [29] constructed an AHL synthase expression level ladder. Here, stronger promoter-ribosome binding site (RBS) variants resulted in strains that achieved the threshold AHL concentration at lower cell densities. Dinh & Prather [30] showed that the threshold cell density of *lux*-type QS systems can also be controlled by varying the expression level of the gene encoding the regulator protein, and Soma & Hanai [39] demonstrated control of the switching time when the AHL synthase and regulator protein expression levels are varied in a coupled manner.

1.1.4 Metabolites

A metabolite-responsive regulation scheme is the most direct method for addressing the limitations of some metabolic pathways (Figure 1-1). For example, when aiming to minimize accumulation of a production pathway intermediate, the concentration of that intermediate, which might fluctuate over the course of the fermentation, is the most relevant indicator for how the regulation system should behave at that particular time. In this section, we summarize previous work on biosensors that detect the relevant endogenous or pathway metabolites, focusing on studies that demonstrated application to metabolic flux control.

When a production pathway shares a common precursor with an essential endogenous pathway, it is important to maintain a balance between limiting flux through the production pathway to maintain a sustainable pool of the precursor and maximizing production. Farmer & Liao [44] addressed this challenge in the lycopene production pathway that consumes glycolytic intermediates glyceraldehyde 3-phosphate and pyruvate by developing a strategy to sense excess glycolytic flux and trigger upregulation of the production pathway. They controlled their production pathway under the Ntr regulation system native to *E. coli*, which contains the *glnAp2* promoter that is upregulated under conditions of high acetyl phosphate levels, indicative of excess glycolytic flux. Rather than using native regulatory components from *E. coli*, Xu et al. [45, 46] imported a malonyl-CoA-responsive control circuit from *Bacillus subtilis* that contains a FapR regulator protein that exhibits DNA-binding behavior in the absence of malonyl-CoA. Additionally, they constructed two hybrid promoter variants that display opposing responses to malonyl-CoA (i.e., one ON-to- OFF and one OFF-to-ON).With these two promoters, they were able to both turn ON malonyl-CoA production genes and turn OFF fatty acid production pathway genes in low malonyl-CoA conditions and achieve the opposite responses in high malonyl-CoA conditions.

Some production pathways are subject to a challenge that is better addressed by

sensing a pathway metabolite. Zhang et al. [47] developed a strategy to regulate expression of fatty acid ethyl ester (FAEE) pathway genes based on the level of the key intermediate, acyl-CoA. To achieve this response, they used the acyl-CoA regulator FadR that binds to the FadR recognition DNA sequence in the absence of acyl-CoA and hybrid promoters that contain at least one recognition sequence in the core region. This system was used to repress expression of the ethanol biosynthesis branch of the FAEE pathway under low acyl-CoA conditions, which would otherwise be subject to toxicity from ethanol accumulation. Doong et al. [48] addressed the bottleneck caused by an unstable enzyme, MIOX, in the glucaric acid pathway by developing a biosensor that upregulates gene expression in the presence of the substrate of MIOX, *myo*-inositol. Their biosensor was imported from *Corynebacterium glutamicum* and contains a regulator protein, IpsA, which represses expression from an engineered promoter until the level of *myo*-inositol reaches a critical threshold. By controlling expression of MIOX under this promoter, the authors could synchronize periods of high *myo*-inositol and MIOX levels, resulting in production improvements. Additionally, the authors demonstrated that the switching dynamics of their biosensor can be tuned by varying IpsA expression levels.

1.1.5 Transcriptional control

Control of the timing and strength of transcription, through the interactions of promoters, RNA polymerases (RNAPs), and transcription factors (TFs), is the most well-studied [49–52] and commonly used dynamic regulation strategy (Figure 1-1). Synthetic promoter libraries have been developed and well characterized and are readily available engineering tools [53–55]. Hybrid synthetic promoters that are controlled by a TF can be engineered easily owing to the modularity of promoters and TF binding sites [56, 57]. There is also a wide array of characterized metabolite-responsive TFs (MRTFs) that can be used to control expression from these promoters, and over 200 more reported in *E. coli* by various groups [52, 58], which have yet to be further tested. Synthetic MRTFs have been engineered via mutagenesis to respond to new inducers [59] and via fusing the ligand-binding domain of one to

the DNA-binding domain of another [60] or to zinc finger DNA-binding motifs [61]. RNAP-promoter systems from phage confer high transcription rates and function orthogonally from bacterial hosts [62].

Early applications of dynamic transcriptional control employed MRTFs to modulate gene expression in response to pathway intermediates. Zhang et al. [47] developed FadR repressor regulated synthetic promoters, using phage lambda promoter P_L and phage T7 promoter P_{A1}, containing the FadR binding site, which had 10- and 25-fold fluorescence induction in response to endogenously produced fatty acids. The promoters were employed to control expression from two of three modules containing downstream enzymes for FAEE production in response to accumulation of the fatty acyl-CoA intermediate. Xu et al. [46] used the malonyl-CoA responsive FapR TF from *B. subtilis* to downregulate the native *E. coli* promoter, pGAP, expressing malonyl-CoA production enzymes and upregulate T7 with fapO, expressing the malonyl-CoA consumption pathway to make fatty acid products. The promoters exhibited 20-100% activity across the malonyl-CoA range tested. Zhou et al. [63] used temperature as the stimulus to initiate transcription by replacing the chromosomal promoter of *ldhA* in its lactate production strain with the lambda P_R and P_L promoters. Following cell growth at 30°C, the lambda repressor was denatured at 42°C, resulting in twofold-higher LDH activity and dynamic lactate production.

Feed flux responsive dynamic transcription, using the cognate MRTF and promoter, has been employed as a proxy for cell growth to switch to production mode from an initial growth phase. Farmer & Liao (69) repurposed the endogenous Ntr two-component regulon and its controlled *glnAp2* promoter from *E. coli* to activate pathway expression in response to acetyl phosphate, serving as a proxy for glycolytic flux. The regulon natively adapts cells to nitrogen deficiency but was previously reported to respond to acetyl phosphate when the sensor gene is knocked out. Glucose consumption was later sensed more directly with the tandem *TaraF* promoter, a CRP promoter, to express the polyhydroxybutyrate pathway. Autonomous expression from *TaraF* took up to 8 hr after glucose induction [16]. Soma et al. [64] interrupted the

TCA cycle when switching to production mode by using IPTG to induce expression of the TetR repressor, which acted on the $P_L$tetO$_1$ expressing citrate synthase $gltA$, and the isopropanol pathway enzymes expressed from $P_L$lacO$_1$. Lo et al. [27] coupled growth and substrate availability into an AND-gate to express pathway enzymes. Glucose depletion, as a proxy for growth, activated the *E. coli* promoter P_{csiD}, which expressed a CoA ligase. The CoA ligase product was a pathway intermediate and induced the transcription of the rest of the pathway. One variant of the AND-gate circuit showed a 30-fold transcriptional increase 4 h after induction.

Direct transcriptional control induced by cell density occurs naturally through QS systems [65]. Gupta et al. [29] used the *esa* QS system from *Pantoea stewartii* to dynamically divert glucose from glycolysis to their production pathway. The authors replaced the native promoter of the glycolysis flux control gene *pfkA* with P_{esaS}, which deactivates at high cell density, and linked expression to enzyme abundance by appending a strong degradation tag to Pfk-1, encoded by *pfkA*. The switching time and OD were determined by the strength of AHL synthase expression. In a separate application, the *esa* knockdown strategy was applied to dynamically downregulate transcription of the shikimate kinase *aroK* to disrupt endogenous aromatic amino acid production, in order to accumulate the intermediate shikimate as a fermentation product. The cell density induced QS regulation strategy was layered with a *myo*-inositol-responsive IpsA transcriptional repressor and hybrid promoter containing an IpsA binding site to divert glycolytic flux toward the heterologous glucaric acid pathway and couple transcription of the pathway gene MIOX with its substrate. Characterization of the hybrid promoter showed a 16- to 55-fold increase in fluorescence depending on IpsA expression level [48]. Other QS systems have also been engineered to varying levels of complexity, such as the native *E. coli* AI-2 QS system [41] and the *lux* QS system from *V. fischeri* in an AND-gate with the stationary-phase promoter P_{rpoS} [66].

1.2   Thesis Objectives

This work aims to multiplex dynamic pathway regulation for the biosynthesis of value-added products using complex waste streams. We began by developing biosensors that enact transcriptional change in response to abundant substrates in food waste. These biosensors were applied in the context of biosynthesis to mitigate the metabolic burden of recombinant pathways without introducing extrinsic chemical inducers to our fermentations. After construction of novel pathways for each of our substrates, galacturonate and gluconate, to a common product of interest, we used our biosensor controllers to regulate pathway expression as we performed mixed-substrate fermentations. We also explored other tools for dynamic regulation, specifically the autonomous, cell density activated expression control from QS systems. This thesis demonstrates the ability to produce a compound from mixed substrates using a single production strain harboring the pathway regulation that we developed herein.

1.3   Thesis Organization

This thesis is organized into five chapters. Chapter 1 provides background on dynamic flux regulation in metabolic engineering and project motivations. Chapter 2 describes construction and characterization of galacturonate biosensors and their utilization for biosynthetic pathway control. Building off these concepts, Chapter 3 multiplexes the substrate-activated expression approach to two substrates: galacturonate and gluconate, and uses both in its own novel biosynthetic pathway to generate a product of interest from a single production strain. Chapter 4 discusses multiplexing AHL-based QS systems for cell density activated expression control. Lastly, Chapter 5 discusses the implications and outlook of this work.

Chapter 2

Substrate-activated expression of a biosynthetic pathway

Abstract

Microbes can facilitate production of valuable chemicals more sustainably than traditional chemical processes: they utilize renewable feedstocks, require less energy intensive process conditions, and perform a variety of chemical reactions using endogenous or heterologous enzymes. In response to the metabolic burden imposed by production pathways, chemical inducers are frequently used to initiate gene expression after the cells have reached sufficient density. Chemically inducible promoters are a common research tool used for pathway expression, but introduce a compound extrinsic to the process along with the associated costs. We developed an expression control system for a biosynthetic pathway for D-glyceric acid that utilizes galacturonate as both the inducer and the substrate, thereby eliminating the need for an extrinsic chemical inducer. This work demonstrated substrate-activated pathway expression to be an attractive control strategy for more readily scalable biosynthesis.

2.1 Introduction

Metabolic engineering of microbes introduces, alters, and leverages enzymatic reactions to produce value-added chemicals in a host cell. A diverse array of products have been produced through microbial synthesis, including biofuels, polymer precursors, food additives, and pharmaceuticals. These processes operate at mild conditions, which are typically safer and less energy intensive compared to traditional chemical syntheses. The potential for microbes to use renewable feedstocks for synthesis presents an additional environmental benefit.

A challenge within metabolic engineering is that overexpression of pathway enzymes imposes a metabolic burden to the host, resulting in slow growth [67, 68] and product loss [69]. In response, common fermentation practice in research allows cells to dedicate resources to biomass accumulation before expressing pathway enzymes from chemically-inducible promoters, for example, using isopropyl β-D-1-thiogalactopyranoside (IPTG) [70, 71] or arabinose [72, 73]. Due to their simplicity and pathway-independent function, chemically inducible promoters have been widely adopted for pathway expression in recombinant microbial hosts [74]. Despite the broad use of this approach, the practice is undesirable for industrial scale-up due to the introduction of a chemical extrinsic to the process along with the associated costs. IPTG can be the most expensive component in a fermentation by an order of magnitude [18]. Even when less expensive alternative chemical inducers such as arabinose, lactose [75, 76] or galactose [77] are used, the inducer could pose difficulties in separations in a bioprocess. When scaling-up bioproduction, product purification issues are best addressed early [78], thus the introduction of extraneous chemicals for pathway expression is in direct disagreement with bioprocess development heuristics. Industrial bioprocesses use constitutive expression of pathway enzymes to avoid the disadvantages of chemical inducers [79]. However, constitutive expression may impose undue burden to the cells, as mentioned above. Additionally, the only tuning parameter in this scheme is pathway expression strength [79], thus the only way to mitigate burden is to decrease expression strength and perhaps sacrifice

production. These considerations limit the real world relevance of many academically developed pathway expression strategies and hinder commercial bioprocesses from more complex expression control. As an alternative to the use of extrinsic chemical induction or constitutive expression, researchers have leveraged stationary phase promoters to express burdensome genes after substantial cell growth; however, this limits the ability of the user to specify the time of induction [80, 81]. Another approach that has been employed is to use feedback controllers to partially delay pathway expression by activating it in response to a pathway intermediate [47, 82]. This strategy requires an additional mechanism to initiate expression since intermediates must accumulate to trigger the response.

One approach to address these limitations would be to utilize components already present in the culture broth to regulate pathway expression. An example is the use of phosphate-starvation promoters, which trigger gene expression due to phosphate depletion. While used successfully in many cases [28], this approach places restrictions on the medium composition and can, in some cases, impact pathway productivity [29]. In this work, we developed a feed-activated, feed-forward expression control strategy, in which the presence of the pathway substrate induces expression of heterologous pathway genes. Thus, we can achieve user-determined, delayed pathway expression without the introduction of an extrinsic chemical to the process. We accomplished this by constructing a biosensor that utilizes a metabolite-responsive transcription factor (TF), for which the feed is its ligand, to control expression of one or multiple genes of interest. Biosensors employing reporters as the gene of interest are used to easily monitor the status of cells [83], characterize the transcriptional response to inducing conditions [47], or serve as a screening method in directed evolution applications [84]. The gene(s) of interest can also encode one or multiple enzymes to couple expression, and thus enzymatic activity, to relevant cellular metabolic states [85]. TF based biosensors specifically are widely used to sense pathway intermediates or products to trigger a cellular response [47, 82, 86]. Given the wide of array of reported metabolite-responsive TFs [52], the relative ease of tuning transcriptional output

[87–89], and the modularity within TFs themselves [90], this has the potential to be a robust strategy that can be applied to a variety of metabolites, feedstocks, pathways, and transcriptional control applications. We demonstrated our approach with a heterologous biosynthetic pathway to produce D-glyceric acid from galacturonate that was previously developed in our lab [91]. D-glyceric acid holds promise due to its biological activity and for its applications in surfactants and polymers [92]. Furthermore, the pathway's galacturonate feed is the main component of pectin, a ubiquitous plant polysaccharide abundantly found in fruit and vegetable food waste streams [93], that could serve as a renewable feedstock for the process. Pectin makes up 24% of the 25 million metric tons of dried sugar beet pulp byproduct produced globally and 20% of the 1.2 million metric tons of dry citrus peel from Florida each year [94]. Though these two waste streams, and other similar pectin-rich ones, are currently used as animal feed, there is potential for them to be converted into useful products. Thus, galacturonate has emerged as a desirable feedstock for microbial fermentations [95–97].

We began with construction and characterization of a biosensor with a galacturonate dose-dependent super folding green fluorescent protein (sfGFP) signal output. The biosensor utilizes a galacturonate-responsive TF from *Bacillus subtilis* [98]. We tested variants of the biosensor to select for desired response features. With our selected biosensor variant, we showed limited crosstalk with the native *E. coli* regulatory system and demonstrated robust biosensor performance in strains with varied galacturonate utilization abilities. Following a thorough analysis of the biosensor, we replaced the *sfGFP* reporter with genes encoding a heterologous D-glyceric acid pathway. We compared our feed-activated expression strategy to IPTG-inducible and constitutive expression circuits. Cells harboring our control circuit performed identically to those with the IPTG-inducible circuit in growth, pathway expression, and production. Furthermore, we observed that constitutive expression of the pathway resulted in poor cell growth and no production, likely due to its unmitigated metabolic burden. This work demonstrates that feed-activated

pathway expression is an effective strategy for D-glyceric acid biosynthesis, and also confers benefits for scaled-up production.

2.2 Methods

2.2.1 Strains and media

All plasmids were cloned in *E. coli* DH5α. Biosensor variant characterization studies were performed in *E. coli* MG1655. Chromosomal deletion of *exuR* and *uxaC* from *E. coli* MG1655 (Table 2.1) was completed using the respective Keio strain [99] in correspondence with the procedure described by Datsenko and Wanner [100]. The primer pairs dexuR-f and dexuR-r; and duxaC-f and duxaC-r used for the respective knockouts were 200-500 bp away from the target gene (Table 2.2). D-glyceric acid fermentations were conducted in *E. coli* MG1655(DE3) $\Delta garK \Delta hyi \Delta glxK \Delta uxaC$, as previously constructed [91]. All growth and fermentation was done in Luria-Bertani (LB) broth (BD, Franklin Lakes, NJ).

Table 2.1: Deleted endogenous genes and heterologously expressed genes used in this study

Gene	Protein/Enzyme	Usage
exuR	transcriptional repressor ExuR	endogenous deletion
uxaC	D-galacturonate isomerase	endogenous deletion
udh	uronate dehydrogenase	heterologous pathway gene
gli	galactarolactone isomerase	heterologous pathway gene
garD	galactarate dehydratase	endogenous pathway gene
garL	5-keto-4-deoxy-D-glucarate aldolase	endogenous pathway gene
garR	2-hydroxy-3-oxopropionate reductase	endogenous pathway gene

Table 2.2: Primers used for plasmid construction and qRT-PCR

Name	Sequence
dexuR-f	tattggcagtgctgatgattggcccg
dexuR-r	tatttctgtcgcccggtaaaaaggcc
duxaC-f	ttgtagggacattacctgacgacagc
duxaC-r	aatcggcaggccatatttgatgacattg
exuR-Ec-f	aagtcgtctcatcggtctcatatggaaatcactgaaccacgccgtttgtatc
exuR-Ec-r	aagtcgtctcaggtctcaggattcatttactgccgctggtggctgtatc
exuR-Bs-f	aagtcgtctcatcggtctcatatggtaaccataaaagatatcgcaaaactcgcaaac
exuR-Bs-r	aagtcgtctcaggtctcaggattcacgtcgtcaatcgtctgactgaatc
exuO-Ec-XO-f	tgacaagttacaaataattttgtttaactttcag
exuO-Ec-XO-r	tacaacttttccctgaatatattatacgag
exuO-Bs-XO-f	gggatcaaaatgttaacgttaacattttga
exuO-Bs-XO-r	ttgttcaaaatgttaacgttaacattttga
P2-f	ctcagccctaggtattatgctagccgtgc
P2-r	ctagccgtaaaaggggcggccgca
P1-f	ctagggattgtgctagccgtgcaattttaaaattaaaggcgttacccaacacaacacgc
P1-r	gactgagctagctgtcaaaggggcggccgcacggtt
OO-f	gttaacattataatatattcagggatcaaaatg
OO-r	gttaacattcgtaaagttatccagcaac
OX-f	ccacaacggtttccctctacaaataattttgtttaactttcag
OX-r	gggaaaccgttgtggtctccctgaatatattataatgttaac
P1OO-f	ccaggcatcaaataaaacgaaaggc
P1OO-r	ttgtccttaagcgtgaacgaaagttaaacaaaattatttgttcaaaatgttaacgttaac
gli-f	actttcgttcacgcttaaggacaatttataatgagcgaactcgtcagaaaactg
gli-r	tattacctcctaagggcttggacactaggtcgccttgaccgg
udh-f	tgtccaagcccttaggaggtaatacatggcatcggctcataccact
udh-r	actgagcctttcgttttatttgatgcctggttatttatcgccgaacggtccg
lacI-Ec-f	actaatctaaggtagtacaaatgaaaccagtaacgttatacgatgtcg
lacI-Ec-r	tgagcgctcacaattccacatccctgaatatattatattgtgagcgctcacaatcgtaaag ttatccagcaaccactca
lacO-Ec-OO-f	tgtggaattgtgagcgctcacaattccacattgtttaactttcgttcacgcttaagg
lacO-Ec-OO-r	ttgtactaccttagattagttccgagcg
udh-qRTPCR-f	attgcgcgagacattgc
udh-qRTPCR-r	atcgcagacctgcacttc

2.2.2 Cloning and plasmid construction

All primers, genetic parts, and plasmids used in this study are found in Tables 2.2-2.4, respectively. Plasmids pP3XO-Ec and pP3XO-gfp, expressing the TF from promoter P3 and *sfGFP* from the proD promoter [54], were constructed using a modular Golden Gate strategy [101]. pYTK095 from this strategy [101] was used as the plasmid backbone. The *E. coli* and *B. subtilis exuR* genes were isolated by performing PCR with the appropriate genomic DNA as template and primers exuR-Ec-f and exuR-Ec-r; and exuR-Bs-f and exuR-Bs-r, respectively (Table 2.2). Downstream operators were inserted with primer pairs exuO-Ec-XO-f and exuR-Ec-XO-r; and exuR-Bs-XO-f and exuR-Bs-XO-r (Table 2.2) using the Q5® Site-Directed Mutagenesis Kit (NEB, Ipswich, MA).

Table 2.3: Genetic parts used for plasmid construction

Name	Registry Identifier	Sequence	Ref.
P1	BBa_J23117	ttgacagctagctcagtcctagggattgtgctagc	[102]
P2	BBa_J23107	tttacggctagctcagccctaggtattatgctagc	[102]
P3	BBa_J23101	tttacagctagctcagtcctaggtattatgctagc	[102]
ProD	n/a	cacagctaacaccacgtcgtccctatctgctgccc taggtctatgagtggttgctggataactttacgggc atgcataaggctcgtataatatattcagggagacc acaacggtttccctctacaaataattttgtttaacttt	[54]
E. coli exuO	n/a	gatgtggttaaccaattt	[103]
B. subtilis exuO	n/a	tcaaaatgttaacgttaacattttga	[104]
Sadler lacO	n/a	tgtggaattgtgagcgctcacaattccaca	[105]
TF RBS	n/a	acaacacgctcggaactaatctaaggtagtacaa	[106]
sfgfp RBS	n/a	cagcaaactcaaatataaggatctttaatt	[106]
gli RBS	n/a	cgttcacgcttaaggacaatttata	[106]
udh RBS	n/a	tgtccaagcccttaggaggtaatac	[106]
TF terminator	BBa_B1002	cgcaaaaaacccccgcttcggcgggggttttttcgc	[102]
reporter/ pathway terminator	Bba_B0015	ccaggcatcaaataaaacgaaaggctcagtcg aaagactgggcctttcgttttatctgttgtttgtcg gtgaacgctctctactagagtcacactggctca ccttcgggtgggcctttctgcgtttata	[102]

Table 2.4: Plasmids used in this study

Plasmid	Genotype	Ref.
pYTK095	ColE1 origin vector used as backbone for biosensors and pathway plasmids	[101]
pP3XO-Ec	pYTK095 with E. coli exuR expressed from constitutive promoter P1; sfgfp expressed from hybrid ProD promoter with a downstream operator	this study
pP1XO-gfp	pYTK095 with B. subtilis exuR expressed from constitutive promoter P1; sfgfp expressed from hybrid ProD promoter with a downstream operator	this study
pP2XO-gfp	pYTK095 with B. subtilis exuR expressed from constitutive promoter P2; sfgfp expressed from hybrid ProD promoter with a downstream operator	this study
pP3XO-gfp	pYTK095 with B. subtilis exuR expressed from constitutive promoter P3; sfgfp expressed from hybrid ProD promoter with a downstream operator	this study
pP1OO-gfp	pYTK095 with B. subtilis exuR expressed from constitutive promoter P1; sfgfp expressed from hybrid ProD promoter with core and downstream operators	this study
pP1OX-gfp	pYTK095 with B. subtilis exuR expressed from constitutive promoter P1; sfgfp expressed from hybrid ProD promoter with a core operator	this study
pP1XX-gfp	pYTK095 with B. subtilis exuR expressed from constitutive promoter P1; sfgfp expressed from ProD promoter with no operators	this study
pP1OO-empty	pYTK095 with B. subtilis exuR expressed from constitutive promoter P1; nothing expressed from hybrid ProD promoter with core and downstream operators	this study
pP1OO-gli-udh	pYTK095 with B. subtilis exuR expressed from constitutive promoter P1; gli-udh operon expressed from hybrid ProD promoter with core and downstream operators	this study
pP1XX-gli-udh	pYTK095 with B. subtilis exuR expressed from constitutive promoter P1; gli-udh operon expressed from ProD promoter with no operators	this study
pP1lacOO-gli-udh	pYTK095 with E. coli lacI expressed from constitutive promoter P1; gli-udh operon expressed from hybrid ProD promoter with core and downstream Sadler operators	this study

Variants pP2XO-gfp, pP1XO-gfp, pP1OO-gfp, pP1OX-gfp, and pP1XX-gfp (Table 2.4) were constructed using the Q5® Site-Directed Mutagenesis Kit (NEB) and the following primers (Table 2.2): P2-f and P2-r; P1-f and P1-r; OO-f and OO-r; and OX-f and OX-r, respectively. The negative control containing no gene expressed from the hybrid promoter (pP1OO-empty in Table 2.4) was constructed using digestion with NdeI and ligation with T4 DNA Ligase; both enzymes were from NEB.

The biosensor controlled pathway and constitutive pathway plasmids (pP1OO-gli-udh and pP1XX-gli-udh in Table 2.4, respectively) were constructed with the PCR products of P1OO-f and P1OO-r on template pP1OO-gfp or P1XX-gfp, and gli-f and gli-r, plus udh-f and udh-r on the previously constructed pathway plasmid [91], using NEBuilder HiFi DNA Assembly Cloning Kit (NEB). RBS sequences for the operon (Table 2.3), calculated using the Operon Calculator function of the RBS Calculator [107], were included in the primers (Table 2.2). The IPTG-inducible pathway plasmid was constructed by combining the PCR product of lacI-Ec-f and lacI-Ec-r on the *E. coli* genome template and lacO-Ec-OO-f and lacO-Ec-OO-r on template pP1OO-gli-udh, using NEBuilder HiFi DNA Assembly Cloning Kit (NEB).

2.2.3   Fluorescence measurements

Fluorescence characterization experiments were performed in the BioLector microbioreactor system (m2p-labs GmbH, Baesweiler, Germany). Overnight cultures were grown at 37°C with agitation at 250 rpm. 1 mL cultures were inoculated at a 1:100 dilution with the appropriate overnight culture in BioLector 48-well flower plates. Galacturonate was added at inoculation. The BioLector was set to 37°C, 1200 rpm shake speed, and 85% humidity. Continuous biomass (620 nm excitation) and GFP (488 nm excitation, 520 nm emission) measurements were taken in arbitrary BioLector units over a 24 hr period.

2.2.4 D-glyceric acid fermentation

Cultures were grown in LB medium. All chemicals used for medium formulations and analytic standards were purchased from Sigma-Aldrich (St. Louis, MO). Overnight cultures were grown at 37°C with agitation at 250 rpm. 50 mL fermentation cultures in 250 mL baffled flasks were inoculated from overnight cultures to an OD_{600} of 0.05. The fermentation cultures were grown at 37°C with agitation at 250 rpm. 5 g L^{-1} of D-galacturonate was added when the cultures reached an OD_{600} of 0.55-0.75. For IPTG-inducible systems, 0.1 mM of IPTG was added either at inoculation or with D-galacturonate addition, approximately 3 hr after inoculation. Samples were taken at regular intervals for analysis by HPLC, UV-Vis, and qRT-PCR.

2.2.5 Galacturonate and D-glyceric acid quantification

Concentrations of galacturonate and D-glyceric acid in culture supernatants were determined using a 1200 Series Agilent Technologies instrument (Santa Clara, CA) with an Aminex HPX-87H Ion Exclusion Column (Bio-Rad Laboratories, Hercules, CA) and refractive index detector. The 22 minute method ran an isocratic mobile phase of 5 mM sulfuric acid at 0.6 mL min^{-1}, with the column set to 65°C and the detector set to 35°C. Approximate elution times for galacturonate and D-glyceric acid were 8.6 and 11 min, respectively.

2.2.6 Quantification of mRNA levels

Samples of 10^9 cells were taken from the fermentation, assuming a conversion of OD_{600} $\sim 1 = 10^9$ cells mL^{-1}. The illustra RNAspin Kit (Cytiva, Marlborough, MA) was used for mRNA extraction. Reverse transcription was completed with the QuantiTect Reverse Transcription Kit (QIAGEN, Germantown, MD), using the kit specific protocol. Quantitative PCR reactions used Brilliant II SYBR qPCR High ROX Master Mix (Agilent Technologies, Santa Clara, CA), according to the master mix protocol, with primers for *udh* (udh-qRTPCR-f and udh-qRTPCR-r in Table 2.2) and were performed in the ABI 7300 Real Time PCR System (Applied Biosystems,

Foster City, CA). The thermal cycling conditions used are as follows: 50°C for 2 min., 95°C for 10 min., and 40 cycles of 95°C for 30 sec. and 60°C for 1 min. The ABI software determined Ct values and the fold differences were calculated between each sample and the uninduced biosensor controlled pathway at 3 hr after inoculation.

2.3 Results and Discussion

2.3.1 Design and selection of a TF-based galacturonate biosensor

Galacturonate is a sugar acid naturally metabolized by several microorganisms. In *E. coli*, expression of galacturonate transport and catabolic genes is activated in the presence of the substrate and controlled by the transcriptional repressor ExuR [108, 109]. *B. subtilis* has an ExuR that regulates its galacturonate catabolism through a repression mechanism analogous to that of *E. coli* [98]. These naturally occurring transcription regulators provide a basis for our galacturonate-responsive biosensor. The possibility of interactions between the host *E. coli* K-12 MG1655 endogenous regulatory proteins and the engineered biosensor motivates construction of a biosensor from genetic parts taken from heterologous microbes. Thus, we constructed two versions of the galacturonate biosensor: one with the ExuR from *E. coli* and one with the *B. subtilis* equivalent. Each biosensor comprised a constitutively expressed *exuR* using promoter BBa_J23101 from the Anderson promoter library (http://parts.igem.org/Promoters/Catalog/Anderson) and a hybrid promoter controlling the expression of an sfGFP reporter (Figure 2-1A). We designed the hybrid promoter using the insulated proD promoter [54] and the corresponding ExuR DNA binding site (i.e., the operator), placed downstream of the transcriptional start site (Figure 2-2). When placed downstream of or within a promoter, the operator allows ExuR to repress or de-repress transcription in the absence or presence of galacturonate, respectively. The *E. coli* ExuR operator sequence was found in the native galacturonate regulon and confirmed through DNA footprinting [109];

37

similarly, the *B. subtilis* operator was isolated experimentally [98].
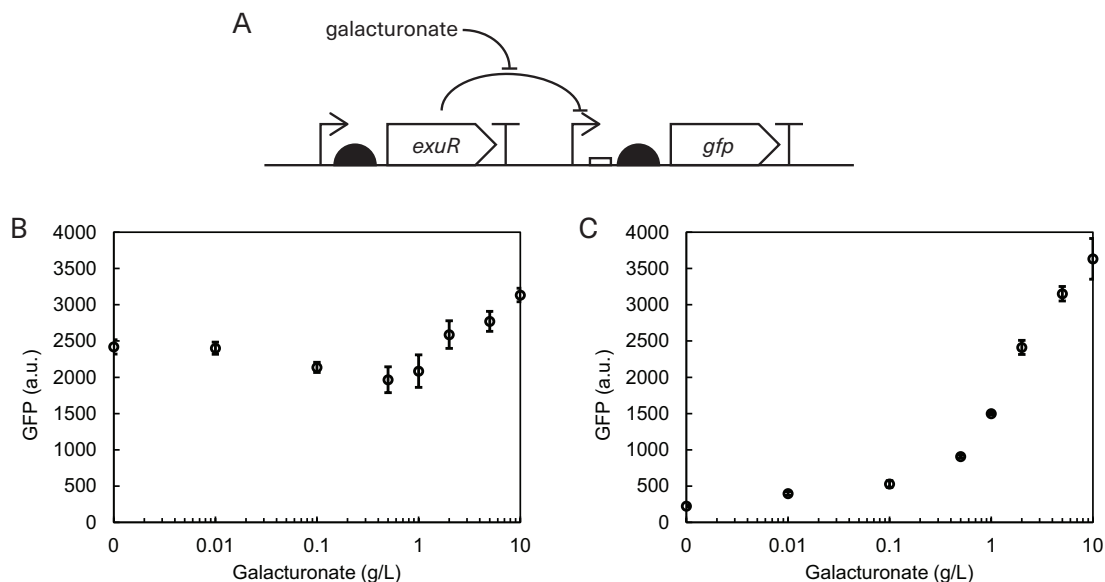
Figure 2-1: Overview of galacturonate biosensors. (A) Biosensor circuit design. A constitutively expressed *exuR* represses *gfp* expression by binding to its downstream operator in the hybrid promoter. De-repression and *gfp* expression occur in the presence of galacturonate. (B) GFP fluorescence response of the *E. coli exuR* biosensor to galacturonate. (C) GFP fluorescence response of the *B. subtilis exuR* biosensor to galacturonate. Data points are mean $\pm$ 1 SD of biological triplicates, taken 24 hr after inoculation.

We measured GFP fluorescence as a response to varying concentrations of galacturonate addition to characterize the *E. coli* ExuR biosensor (Figure 2-1B) and the *B. subtilis* biosensor (Figure 2-1C). Both biosensors exhibit dose-dependent responses, in which higher concentrations of galacturonate achieve more de-repression of *sfGFP*, thus a higher fluorescence output. It is evident from these dose-response curves that the *B. subtilis* ExuR biosensor is superior, as the uninduced and maximal outputs were 225 and 3632 a.u., compared to 2419 and 3134 a.u. for the *E. coli* ExuR biosensor. Given our concerns with orthogonality between our biosensor and the host, and superior performance of the *B. subtilis* biosensor compared to the otherwise identical *E. coli* counterpart, we made variants of the *B. subtilis* biosensor for further characterization and application.

A
CACAGCTAACACCACGTCGTCCCTATCTGCTGCCCTAGGTCTATGAGTGGTTGCTGGATAAC

TTTACGGGCATGCATAAGGCTCG**TATAAT**ATATTCaGGGAGATGTGGTTAACCAATTTACAA

ATAATTTTGTTTAACTTTCAGCAAACTCAAATATAAGGATCTTTAATTATGCGTAAAGGCGA

B
CACAGCTAACACCACGTCGTCCCTATCTGCTGCCCTAGGTCTATGAGTGGTTGCTGGATAAC

TTTACGGGCATGCATAAGGCTCG**TATAAT**ATATTCaGGGATCAAAATGTTAACGTTAACATT

TTGAACAAATAATTTTGTTTAACTTTCAGCAAACTCAAATATAAGGATCTTTAATTATGCGT

C
CACAGCTAACACCACGTCGTCCCTATCTGCTGCCCTAGGTCTATGAGTGGTTGCTGGATAAC

TTTACGAATGTTAACGTTAACAT**TATAAT**ATATTCaGGGAGACCACAACGGTTTCCCTCTAC

AAATAATTTTGTTTAACTTTCAGCAAACTCAAATATAAGGATCTTTAATTATGCGTAAAGGC

D
CACAGCTAACACCACGTCGTCCCTATCTGCTGCCCTAGGTCTATGAGTGGTTGCTGGATAAC

TTTACGAATGTTAACGTTAACAT**TATAAT**ATATTCaGGGATCAAAATGTTAACGTTAACATT

TTGAACAAATAATTTTGTTTAACTTTCAGCAAACTCAAATATAAGGATCTTTAATTATGCGT

E
CACAGCTAACACCACGTCGTCCCTATCTGCTGCCCTAGGTCTATGAGTGGTTGCTGGATAAC

TTTACGGGCATGCATAAGGCTCG**TATAAT**ATATTCaGGGAGACCACAACGGTTTCCCTCTAC

AAATAATTTTGTTTAACTTTCAGCAAACTCAAATATAAGGATCTTTAATTATGCGTAAAGGC

Figure 2-2: Hybrid promoter schematics. Bold text indicates the -35 and -10 σ^{70} RNA polymerase binding sites. The lowercase a indicates the putative transcription start site. Pink highlight indicates an operator sequence. White boxes indicate the insulating upstream and downstream sequences, the grey box indicates the proD promoter core, the blue box is the RBS, and the green box indicates the beginning of the *sfgfp* gene. (A) *E. coli exuR* biosensor hybrid promoter from pP3XO-Ec. (B) Hybrid promoter from pP1XO-gfp, pP2XO-gfp, and pP3XO-gfp. (C) Hybrid promoter from pP1OX-gfp. (D) Hybrid promoter from pP1OO-gfp. (E) Hybrid promoter from pP1XX-gfp.

2.3.2   Characterization of *B. subtilis* ExuR biosensor variants

We constructed variants of the *B. subtilis exuR* biosensor to select for two performance metrics: high dynamic range and low leakiness. We defined dynamic range as the

highest GFP fluorescence output divided by the uninduced output; leakiness was quantified as the uninduced GFP signal divided by the no GFP control. Our variants employed a range of constitutive promoter strengths from the Anderson promoter library (http://parts.igem.org/Promoters/Catalog/Anderson) to express *exuR* and altered the number and placement of operator sites in the hybrid promoter (Figure 2-3A). The promoters have reported relative strengths of 0.06, 0.36, and 0.7 and are referred to as P1, P2, and P3, respectively (Table 2.3). The placement of an operator is denoted with an O in our naming convention and a place without an operator is denoted with an X. The hybrid promoters had operators downstream of the promoter (XO), in the core position between the -35 and -10 σ^{70} RNA polymerase binding sites (OX), or in both positions (OO) (Figure 2-2). We did not test upstream placement of the operator as this position yields the least effective repression [57]. The absence of an operator (XX) should leave nowhere for the ExuR to bind and regulate transcription, and acts as our constitutive, positive control (Figure 2-2). Figure 2-3B shows the galacturonate dose response and Hill fit curves of the biosensor variants. Decreasing the exuR promoter strength results in weaker repression and higher leakiness, as expected, since there are fewer repressor molecules in the cell (Figure 2-3C). The downstream operator variants have similar maximal GFP outputs, which was expected given that the hybrid promoter is identical among them. The placement of a core operator decreases the leakiness and results in stronger overall repression of the hybrid promoter, even with weak *exuR* expression. When there is an operator in both positions, the strong repression and low leakiness matches that of the core operator variant, but the maximum fluorescence is higher. Thus, the P1OO variant is our best performer, with the highest dynamic range and lowest leakiness (Figure 2-3C). These results are in agreement with previously characterized hybrid and natural promoter systems [56, 57].
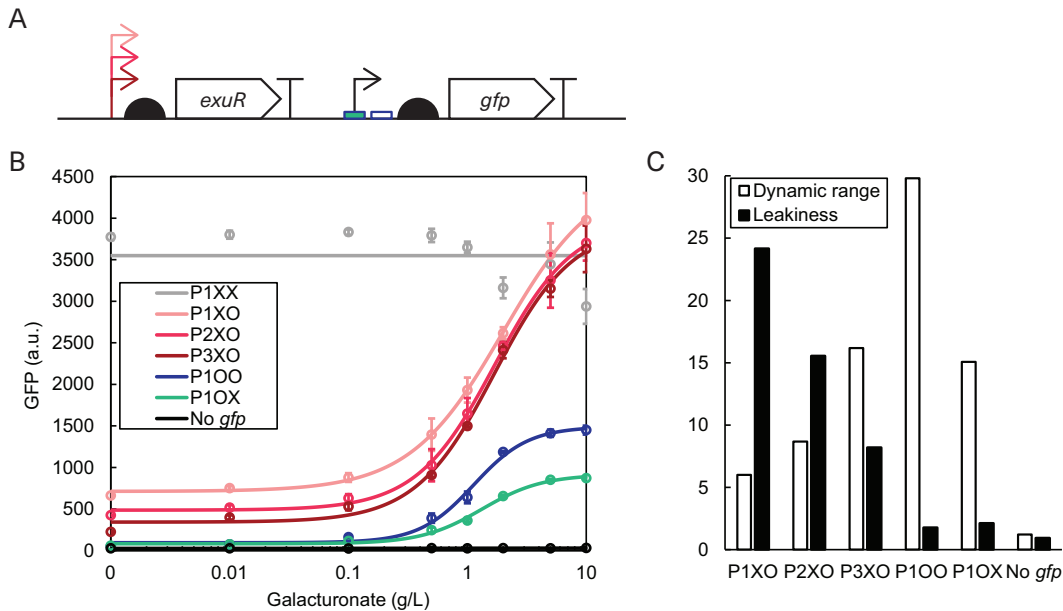
Figure 2-3: Comparison of *B. subtilis exuR* biosensor variants. (A) Overview of biosensor variant circuit. Variants expressed a constitutive *exuR* from a weak (P1/light pink), medium (P2/pink), or strong (P3/red) promoter. The presence or absence of an operator in the core or downstream of the -35 and -10 RNAP binding sites is denoted with an O or X, respectively. Variants of hybrid promoters contained an operator downstream of the 35 and 10 RNAP binding sites (XO/open rectangle), in the core position between the RNAP binding sites (OX/filled rectangle), or two operators placed in both positions (OO/blue rectangles). The hybrid promoter variant with no operators (XX) serves as a constitutive expression positive control. See Figure 2-2 for a more detailed schematic of the hybrid promoters used. (B) GFP fluorescence response of the biosensor variants to galacturonate. Data points are mean ± 1 SD of biological triplicates, taken 24 hr after inoculation. (C) The average dynamic range and leakiness of each variant from its dose response curve.

2.3.3 Effect of endogenous regulation and catabolism on biosensor response

Though we identified robust biosensor variants with desirable performance in the wild type (WT) *E. coli* MG1655 host, we sought to characterize the effects of endogenous regulation and catabolism of the substrate on biosensor response. The homology of the *B. subtilis* putative galacturonate regulon to that of *E. coli* aided in the elucidation

of its ExuR regulatory functions [98]. Thus, it is plausible that the synthetic biosensor could have crosstalk with the *E. coli* host and its endogenous galacturonate-response ExuR. To examine the effect of the endogenous *E. coli* ExuR on our P1OO biosensor, we compared fluorescence characterization in *E. coli* MG1655Δ*exuR* to the response in WT (Figure 2-4A). Using a Students *t*-test with α=0.01 and a Bonferroni correction for each of the eight concentrations tested, we determined that the response in these two strains is not significantly different. These data indicate that the endogenous ExuR has no appreciable effect on the biosensor. The dynamic range and leakiness in the WT and Δ*exuR* strains are also highly similar: 29.8 and 28.9 -fold average dynamic range and leakiness values of 1.8 and 1.6, respectively (Figure 2-4B). We conclude that endogenous transcriptional regulation does not directly affect biosensor performance and the biosensor acts orthogonally to its host.
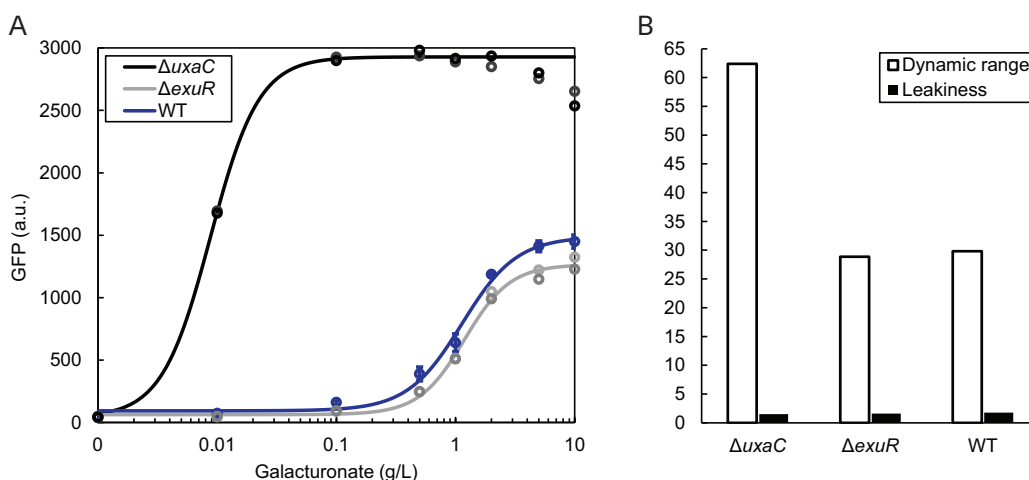
Figure 2-4: Effect of endogenous *exuR* and *uxaC* on biosensor response. (A) GFP fluorescence response of the P1OO biosensor to galacturonate, in *E. coli* MG1655Δ*uxaC* (black) and MG1655Δ*exuR* (grey), compared to *E. coli* MG1655 WT(blue). Data points from the knockout strains are of individual biological duplicates, taken 24 hr after inoculation. (B) The average dynamic range and leakiness of P1OO in each strain from the corresponding dose response curve.

In addition to the endogenous *exuR*, the galacturonate catabolic genes remain intact in the WT host. Though the enzymes encoded by these genes do not directly interact

with our biosensor, native catabolism of the substrate reduces the availability of the inducer to de-repress *sfGFP* expression. Galacturonate was fully consumed by 24 hr, regardless of initial concentration added, in all characterization experiments performed in the WT strain (data not shown). We expect galacturonate consumption in the end application of the biosensor, since it was constructed to control expression of a galacturonate-utilizing pathway. However, knocking out the endogenous *uxaC*, the galacturonate isomerase that implements the first step of catabolism, allowed us to compare P1OO biosensor induction in the presence and absence of galacturonate catabolism. The latter represents a performance ceiling for the biosensor where galacturonate can achieve its full de-repression potential. From the dose response curves of the biosensor in *E. coli* MG1655 and *E. coli* MG1655Δ*uxaC* (Figure 2-4A), we see that more initial galacturonate is required to achieve higher GFP fluorescence in the WT strain containing *uxaC*. This result is expected since catabolism of galacturonate lowers the effective concentration within the cell. Though there is a stark difference between the response curves of the two strains, both have favorable performance metrics, as defined above: 29.8 and 62.4 -fold average dynamic range and leakiness values of 1.8 and 1.5, for *E. coli* MG1655 and *E. coli* MG1655Δ*uxaC*, respectively (Figure 2-4B). The favorable performance of the biosensor in both the WT and Δ*uxaC* strains demonstrates that the choice of strain is flexible, regardless of whether *uxaC* is necessary for the desired application. Additionally, the biosensor could serve as a chemical induction system in which galacturonate induces expression, similarly to IPTG.

2.3.4 Feed activated expression of a D-glyceric acid production pathway

The galacturonate biosensor can be used to control the expression of a galacturonate-utilizing pathway in a feed responsive manner, as demonstrated by the high dynamic range of sfGFP reporter output; the low leakiness prevents unwanted expression of pathway enzymes before galacturonate addition. We

demonstrated this application with the D-glyceric acid production pathway previously developed in our group [91]. The pathway utilizes enzymes encoded by two heterologous genes, uronate dehydrogenase (*udh*) and galactarolactone isomerase (*gli*), to generate the intermediate D-galactarate. D-galactarate is converted to D-glyceric acid by enzymes encoded by the endogenous genes galactarate dehydratase (*garD*), 5-keto-4-deoxy-D-glucarate aldolase (*garL*), and 2-hydroxy-3-oxopropionate reductase (*garR*) (Figure 2-5A, Table 2.1). The *udh* and *gli* genes were expressed from the P1OO biosensor circuit as an operon (Figure 2-5B). Consequently, the presence of the galacturonate feed de-represses ExuR from the hybrid promoter and induces transcription of the heterologous pathway genes (Figure 2-5A). To characterize this system, we conducted fermentations with the MG1655(DE3) $\Delta garK \Delta hyi \Delta glxK \Delta uxaC$ strain used previously [91].
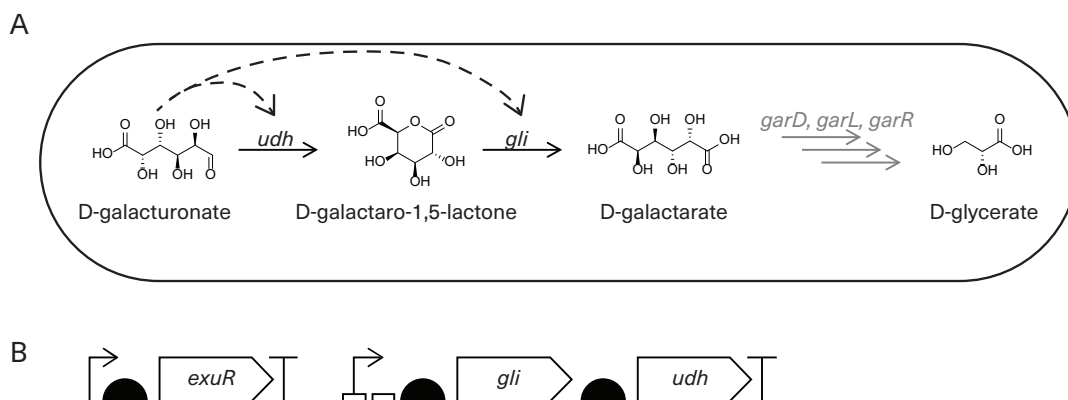
Figure 2-5: Overview of galacturonate activated expression of D-glyceric acid biosynthetic pathway. (A) Schematic of feed activated pathway expression. Galacturonate induces the expression of the heterologous pathway genes, *udh* and *gli*; endogenous enzymes complete the pathway to produce D-glyceric acid. (B) Genetic circuit of P1OO controlling the D-glyceric acid pathway. The heterologous pathway genes form an operon.

We verified that the control circuit modulates transcription in response to galacturonate by quantifying the relative mRNA levels of *udh*, the second gene in the operon, over the course of a fermentation using qRT-PCR (Figure 2-6A). For

all samples, the fold change of mRNA was analyzed relative to P1OO levels before galaturonate addition. We constructed an IPTG-inducible variant of the P1OO control circuit that employs LacI in place of ExuR and two *lac* operators [105] to benchmark the galacturonate-inducible circuit. IPTG addition was tested in two conditions: at inoculation and 3 hr after inoculation. Both cases show an increase in *udh* expression over time. The 3 hr IPTG addition resulted in higher overall *udh* levels (3.9±0.6 fold change compared to 3±1 for 0 hr addition, at 9 hr post inoculation), likely due the growth advantage of delayed pathway induction, discussed further below. Galacturonate added at 3 hr post inoculation to the P1OO controlled pathway resulted in a 3.4±0.2 udh fold change at 9 hr post inoculation. The sample taken just after induction with galacturonate shows a spike in *udh* expression that falls slightly as cell growth slows. The 5 hr *udh* level matches those of the IPTG induced cells. We can conclude that the changes in pathway mRNA expression result from the transcription factor and hybrid promoter interactions in response to galacturonate. Thus, the galacturonate controlled circuit is a direct and effective replacement for the IPTG inducible expression system.

As expected, the uninduced P1OO-controlled pathway maintains consistently low levels of *udh* transcript, which drops over the course of the fermentation as is common with constitutive type expression [110]. This behavior is also seen in the constitutive P1XX case. While the drop in transcription was expected, the low values of mRNA present in the P1XX containing cells surprised us. We expected high relative *udh* levels based on the sfGFP fluorescence characterization. The cause of this became clear as we looked at the biomass, and galacturonate and D-glyceric acid concentrations profiles taken throughout the fermentations (Figure 2-6B-D).
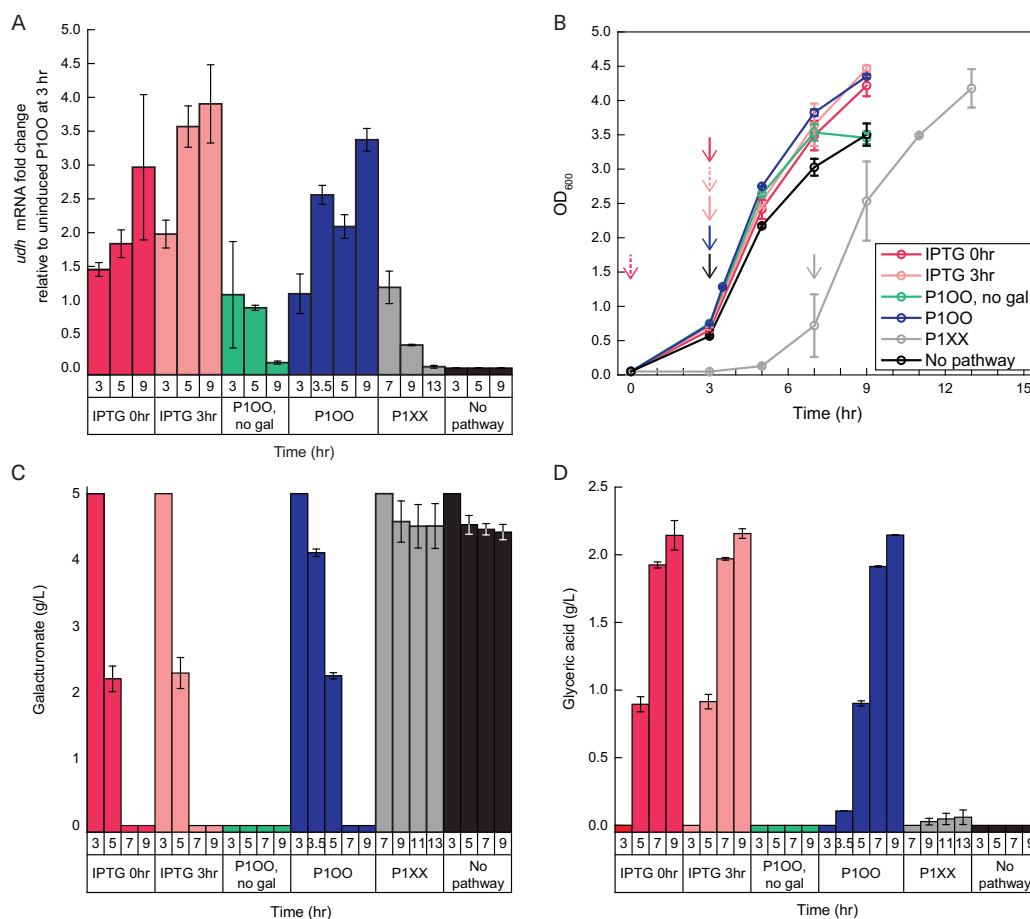
Figure 2-6: Fermentation time series data of mRNA fold change, biomass, galacturonate, and D-glyceric acid. (A) *udh* mRNA fold change relative to the uninduced P1OO levels 3 hr after inoculation, over time. (B)OD_{600} over time. Dotted arrows indicate IPTG addition; solid arrows indicate galacturonate addition. (C) Galacturonate concentration over time. (D) D-Glyceric acid concentration over time. Data are mean $\pm$ 1 SD of biological duplicates.

The growth profiles of all the strains are similar (Figure 2-6B), with the exception of the constitutive pathway harboring strain. The final OD is lower for the strain with no pathway and the strain that was not fed galacturonate. This can be explained by the pyruvate byproduct produced by the D-glyceric acid pathway, which gives cells a growth advantage. We see a substantial lag in the constitutive expression strain, suggesting the pathway introduces significant burden to cell growth. The slow growth and low mRNA presence in the constitutive pathway strain indicate that the

perpetual presence and generation of the heterologous enzymes is detrimental to cell health. This is further supported by observed inability of the strain to consume galacturonate and produce D-glyceric acid (Figure 2-6C-D). Thus, cell health and D-glyceric acid production require an inducible production pathway, as demonstrated by the IPTG-inducible and P1OO controlled cases. The galacturonate utilization and D-glyceric acid production profiles are almost identical when the pathway is induced (Figure 2-6C-D). These strains consumed all 5 g L^{-1} of galacturonate within 6 hr of addition. IPTG induction at inoculation, 3 hr after inoculation, and galacturonate induction 3 hr after inoculation resulted in titers of 2.1±0.1, 2.16±0.04, and 2.146±0.003 g L^{-1} D-glyceric acid and molar yields of 78%, 79%, and 78%, respectively. From these results, we see that we can effectively replace the IPTG-inducible system controlling the D-glyceric acid pathway with one that only requires the pathway feed, galacturonate. This was achieved without compromising pathway performance, as observed by feed utilization and product formation.

2.4 Conclusion

Metabolite-responsive regulatory systems can be leveraged to build substrate-induced, feed-forward expression control strategies. We constructed a galacturonate biosensor with a heterologous metabolite-responsive TF from *B. subtilis* and its cognate DNA binding sites, and used fluorescence characterization to select a top performing variant. The biosensor has minimal crosstalk with the native *E. coli* galacturonate-responsive regulator and exhibits favorable output despite full consumption of the galacturonate feed. Thus, the biosensor is an effective induction system that removes extrinsic chemical inducers for applications in which galacturonate is the feed substrate, but it could also be used generally as a chemical induction system. To demonstrate the former case, we used the biosensor to activate expression of a D-glyceric acid production pathway in the presence of its galacturonate feed. We determined that pathway induction is necessary, as constitutive expression resulted in poor cell growth and no product formation. Strains harboring the

D-glyceric acid pathway expressed from our galacturonate-induced system performed identically to an IPTG-induced system in growth, feed utilization, and production. This work demonstrates that feed-activated pathway expression enables product biosynthesis while removing extrinsic chemical inducers from a microbial production system.

Chapter 3

Biosynthesis from mixed substrates using multi-substrate expression control

Abstract

The use of waste streams and other renewable feedstocks in microbial biosynthesis has long been a goal for metabolic engineers. Microbes can utilize the substrates found in waste streams, though they are more technically challenging to convert to useful products compared to the single substrates of standard practice. It is difficult to control biosynthesis in the face of the temporally changing nature of waste streams. Furthermore, the expression of all the enzymes necessary to convert mixed substrates into a product likely presents great metabolic burden, which already plagues processes that utilize a single substrate. We developed an approach to utilize mixed substrates for production by activating expression of each biosynthetic pathway in the presence of its substrate. This expression control was used on two novel pathways that converted our substrates, galacturonate and gluconate, into D-glycerate. We demonstrated D-glycerate biosynthesis from single and mixed substrates as an example of conversion of complex feedstocks like waste streams.

3.1 Introduction

An attractive feature of utilizing microorganisms for biosynthesis through metabolic engineering is the potential to use renewable feeds or waste streams as process inputs. Biomass byproduct and waste streams from agriculture, food and dairy industry, or municipal organic waste, are rich in carbon and nutrients that microorganisms can utilize for growth and metabolite production [111, 112]. For example, municipal food waste is abundant in carbohydrates such as glucose, galacturonate, gluconate, galactose, and fructose, among others [93, 113, 114]. While waste stream feedstocks are desirable for sustainability and cost, they are technically challenging to implement due to their complexity and temporal variation [111, 114]. Traditionally, microbial production processes utilize a consistent and defined feed stream, wherein a single substrate gets converted into the desired product [115]. However, the ability to maintain consistent production while sensing and responding to feed deviations would allow for more complex, waste streams to be utilized as feeds, which can decrease production costs and carbon footprint [111].

The utilization of waste streams for microbial production has been garnering interest among metabolic engineers. Due to the complexity and incompatibility of waste streams to most existing biosynthetic platforms, much of the effort has been focused on metabolizing the substrates, either through strain engineering [116] or selecting organisms that can naturally consume the prevalent compounds [112, 117–119]. These approaches often limit the resulting product to ones that naturally exist in the host metabolome. In order to expand the product portfolio of these systems, recombinant pathways need to be introduced into the strains. The overexpression of a single pathway often leads to metabolic burden [67, 68]; multiplexing pathways further increases the potential burden to the host. Many systems for expression control have been developed to mitigate burden in production strains such as chemical induction [70, 72], stationary phase activation [80, 81], and activation in response to cell density [30].

In our lab's previous work, we selected a food waste abundant substrate, galacturonate, and engineered an expression control strategy to utilize it as a transcriptional inducer for a recombinant biosynthetic pathway for which it was also the substrate [120]. We were thus able to mediate pathway burden without adding an extrinsic chemical to the fermentation, which is advantageous for scaling up a bioproduction [78]. We expanded on that strategy herein to utilize two substrates, galacturonate and gluconate, for biosynthesis of D-glycerate. D-glycerate is a product of interest due to its applications in surfactants and polymers and its biological activity [92]. We developed a novel pathway for each substrate and induced expression of the heterologous pathway genes with their cognate substrate. By consolidating the recombinant pathways into a single production strain, we achieved mixed-substrate biosynthesis of D-glycerate. Our approach achieved the co-utilization of food waste abundant substrates for biosynthesis in novel recombinant pathways.

3.2   Results

3.2.1   Construction of a gluconate-responsive biosensor

We constructed a transcription-factor (TF) based, substrate-responsive biosensor for gluconate with the same genetic framework our lab used previously to construct a galacturonate biosensor [120]. The gluconate biosensor circuit comprised a constitutively expressed *gntR* TF from *Bacillus subtilis* and a sfGFP reporter expressed from a hybrid promoter containing the DNA binding sequence (i.e., the operator) for GntR. GntR regulates the genes for gluconate transport and catabolism in *B. subtilis* [121, 122] by binding its cognate operator in the gluconate operon [123].

As with our galacturonate biosensor variants (Chapter 2), we varied the constitutive Anderson promoter strength expressing *gntR*. The promoters, denoted P1, P2, and P3, have reported relative strengths of 0.06, 0.36, and 0.7, respectively. Within the hybrid promoter expressing the *sfGFP*, the presence or absence of an operator in each of two potential sites is denoted with an O or X, respectively. Thus, the variants

have an operator downstream of the promoter (XO), in the core position between the -35 and -10 σ^{70} RNA polymerase binding sites (OX), or in both positions (OO). The gluconate biosensor variants responses are influenced by both the TF promoter strength and operator placement (Figure 3-1A). Though variant P2XO has the highest absolute fluorescence and dynamic range (Figure 3-1B), we chose to use variant P3OO as it has a high dynamic range and the lowest leakiness. These qualities are both important and advantageous for pathway expression applications.
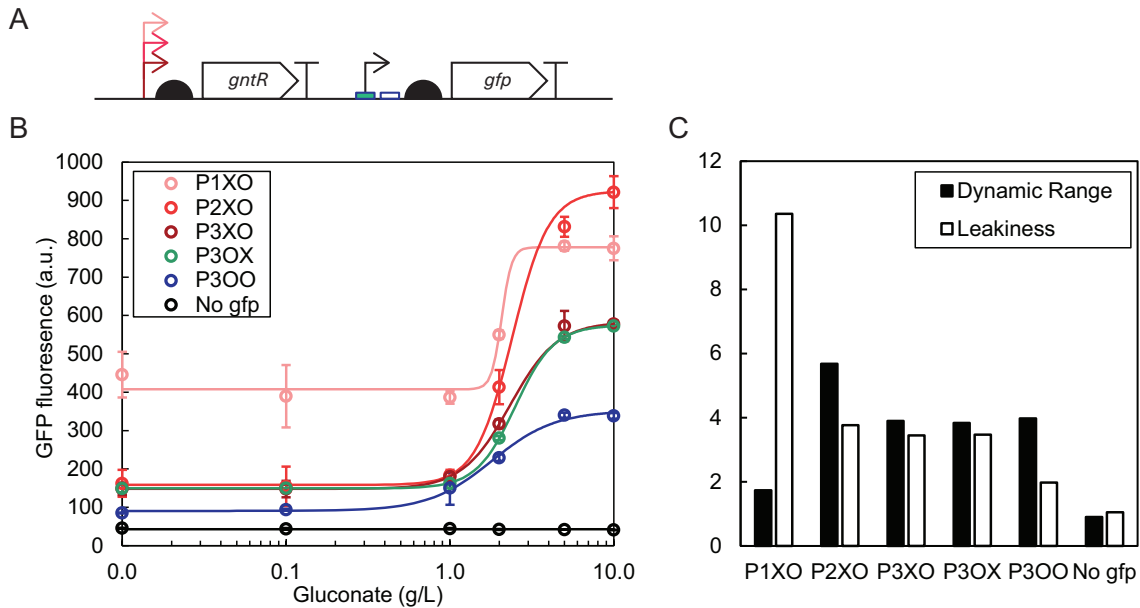
Figure 3-1: Comparison of gluconate biosensor variants. (A) Overview of biosensor variant circuit. Variants expressed a constitutive *gntR* from a weak (P1/light pink), medium (P2/pink), or strong (P3/red) promoter. The presence or absence of an operator in the core or downstream of the -35 and -10 RNAP binding sites is denoted with an O or X, respectively. Variants of hybrid promoters contained an operator downstream of the 35 and 10 RNAP binding sites (XO/open rectangle), in the core position between the RNAP binding sites (OX/green filled rectangle), or two operators placed in both positions (OO/blue rectangles). (B) Fluorescent dose response curves of the biosensor variants to gluconate. Data points are mean $\pm$ 1 SD of biological triplicates, taken 24 hr after inoculation. (C) The average dynamic range and leakiness of each variant from its dose response curve.

3.2.2 Characterization of biosensor orthogonality

A consolidated biosensor for galacturonate and gluconate was constructed by including the selected variant of each on a single plasmid. An *mCherry* reporter was used for the gluconate biosensor to differentiate its output from that of the galacturonate biosensor (Figure 3-2A). We fed varying concentrations of galacturonate and gluconate and mixtures of the two. The resulting fluorescence outputs show that the dynamic range of the two biosensors is maintained, even in the presence of the non-cognate substrate (Figure 3-2B-C). The orthogonality of the two biosensors is a desired characteristic since we wish to have independent transcriptional control of the biosynthetic pathway that utilizes each substrate for mixed-substrate production applications.
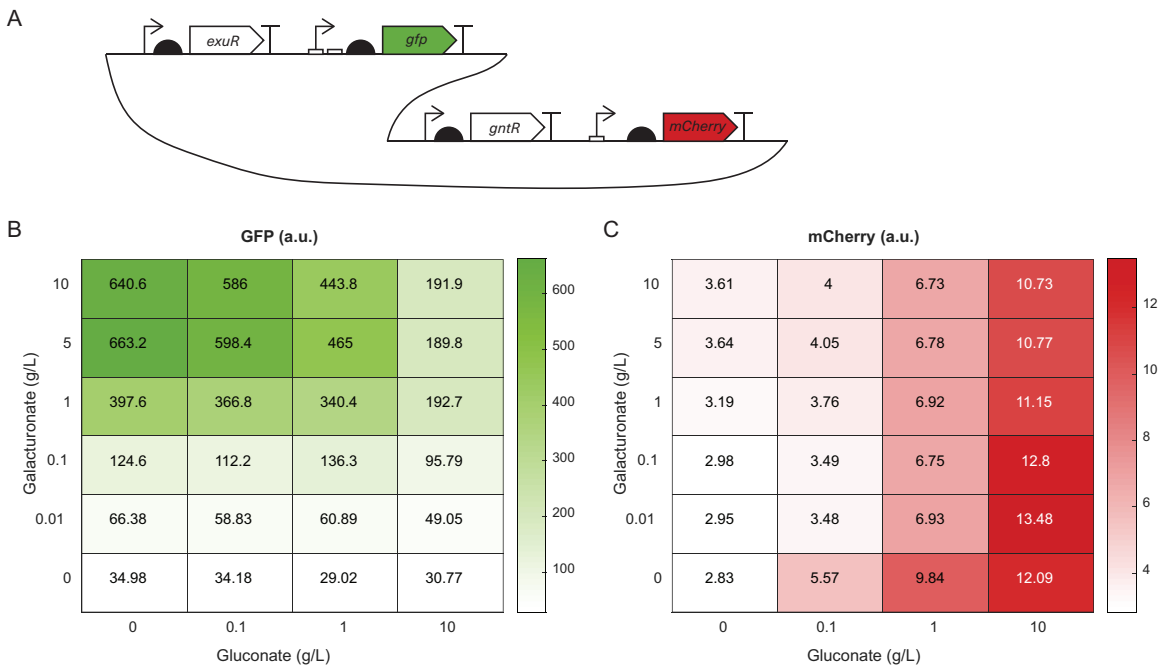
Figure 3-2: Fluorescence response of the consolidated galacturonate and gluconate biosensors. (A) Overview of biosensors' genetic circuit, comprising *exuR* under the P1 promoter and *gfp* under the double exuO operator hybrid ProD promoter, and *gntR* under the P3 promoter and *mCherry* under the core gntO operator hybrid ProD promoter. (B) GFP flourescence response of the consolidated biosensor to varying combinations of galacturonate and gluconate. (C) mCherry flourescence response of the consolidated biosensor to varying combindations of galacturonate and gluconate.

3.2.3 Construction of a novel D-glycerate biosynthetic pathway from galacturonate

We developed a novel glycerate production pathway from galacturonate to demonstrate a mixed substrate biosynthesis application (Figure 3-3A). The pathway from galacturonate comprises endogenous UxaC, UxaB, and UxaA; and two heterologous steps from the non-phosphorylative Entner-Doudoroff pathway found in thermophilic Archea [124]: KdgA from *Sulfolobus solfataricus* [125]; and GadH from *Thermoplasma acidophilum* [126]. The heterologous pathway enzymes were expressed in an operon from our galacturonate biosensor circuit [120] (Figure 3-3B).
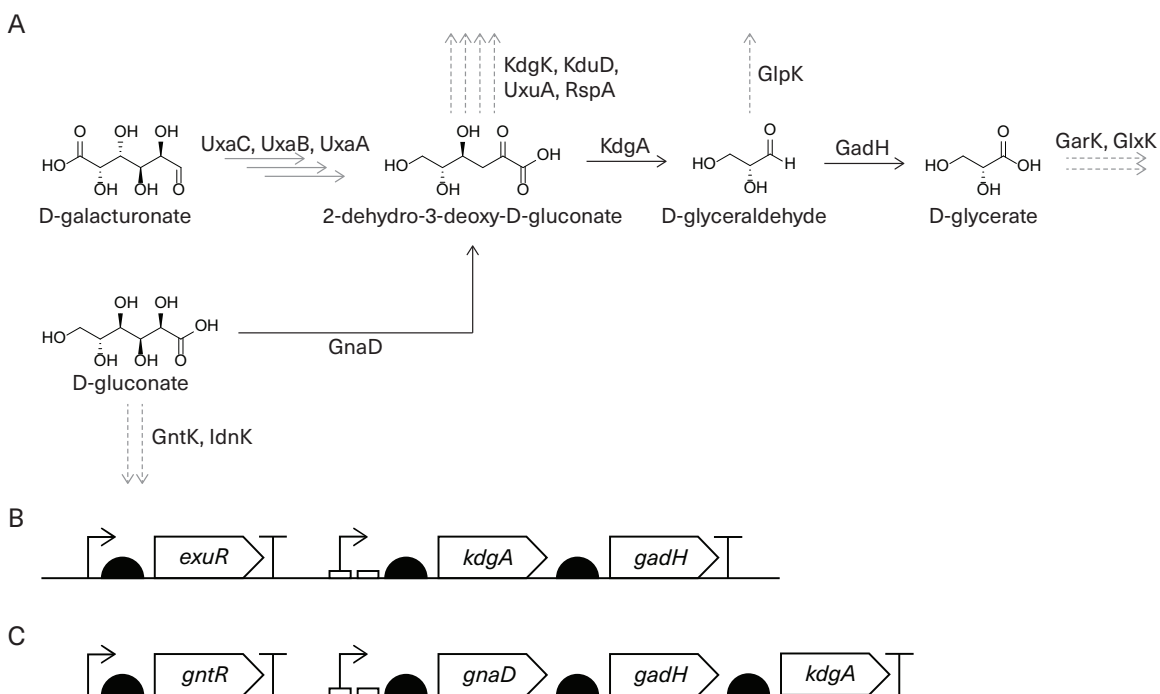
Figure 3-3: Overview of D-glycerate pathways. (A) Schematic of novel D-glycerate pathways from galacturonate and gluconate. Black arrows show heterologous enzymes; grey arrows show endogenous enzymes; dotted grey arrows show endogenous enzymes that may consume pathway metabolites. (B) Genetic circuit of the galacturonate-utilizing pathway's heterologous genes expressed in an operon, under the control of the galacturonate biosensor. (C) Genetic circuit of the gluconate-utilizing pathway's heterologous genes expressed in an operon, under the control of the gluconate biosensor.

We identified endogenous genes in *E. coli* MG1655 (DE3) that encode enzymes which may consume our pathway intermediates or product (Figure 3-3A). We characterized the effect of sequentially knocking out these genes on D-glycerate production with our initial production plasmid, which had a ColE1 origin of replication and *kdgA* and *gadH* in an operon, each with a ~10,000 a.u. translation initiation rate (TIR) RBS calculated by the Operator Calculator within the RBS Calculator [107] (Figure 3-4). Deletion of the glycerate kinase *garK* alone did not lead to improvement of D-glycerate titer. As we added on deletions for *kdgK, glpK,* and *glxK*, whose enzymatic products consume 2-dehydro-3-deoxy-D-gluconate, D-glyceraldehyde, and D-glycerate, respectively, we saw a 6.2-fold titer increase with all four knockouts over the starting *E. coli* MG1655 (DE3) strain. Next, we had to knock out the gluconate kinases, *gntK* and *idnK*, to prevent gluconate catabolism in our future applications, even though it resulted in a drop in D-glycerate titer from galacturonate. The additional deletions of *kduD* and *uxuA* further improved titer, while *rspA* deletion was detrimental to D-glycerate acculumation; all three of the enzymes encoded by these genes have report activity on 2-dehydro-3-deoxy-D-gluconate. We selected *E. coli* MG1655 (DE3) $\Delta garK \Delta kdgK \Delta glpK \Delta glxK \Delta gntK \Delta idnK \Delta kduD$ as our production strain as it resulted in the highest D-glycerate titer of 1.3 ± 0.3 g L^{-1}, with fewer knockouts, and a 9.5-fold improvement of D-glycerate titer compared to *E. coli* MG1655 (DE3).

Next, we changed the production plasmid configuration by increasing each RBS to ~50,000 a.u. TIR, then both, then changed the operon order with the higher RBS strengths (Figure 3-4). From these conditions, we concluded that the expression strength of *gadH* was limiting in our initial production plasmid since increasing its RBS strength and moving it to the first position in the operon resulted in higher titers. Finally, we tested the impact of copy number by changing the origin of replication from ColE1 (~20 copies per cell), to RSF (~100 copies per cell) and pMB1* (~500 copies per cell) (Figure 3-4). The increase in copy number did not produce higher glycerate titers. From these results, we found that the production plasmid with the

ColE1 ori, higher RBS strengths, and *gadH* placed ahead of *kdgA* in the operon gave us 2.4 ± 0.1 g L^{-1} of D-glycerate and 45% molar yield, the highest results from galacturonate and a 17-fold increase from our starting conditions.

ΔgarK		×	×	×	×	×	×	×	×	×	×	×	×	×	×
ΔkdgK			×	×	×	×	×	×	×	×	×	×	×	×	×
ΔglpK			×	×	×	×	×	×	×	×	×	×	×	×	×
ΔglxK				×	×	×	×	×	×	×	×	×	×	×	×
ΔgntK					×	×	×	×	×	×	×	×	×	×	×
ΔidnK					×	×	×	×	×	×	×	×	×	×	×
ΔkduD						×	×	×	×	×	×	×	×	×	×
ΔuxuA							×	×							
ΔrspA								×							
kdgA	1/10	1/10	1/10	1/10	1/10	1/10	1/10	1/10	1/50	1/10	1/50	2/50	2/50	2/50	2/50
gadH	2/10	2/10	2/10	2/10	2/10	2/10	2/10	2/10	2/10	2/50	2/50	1/50	1/50	1/50	1/50
ori	ColE1	ColE1	ColE1	ColE1	ColE1	ColE1	ColE1	ColE1	ColE1	ColE1	ColE1	ColE1	ColE1	RSF	pMB1*
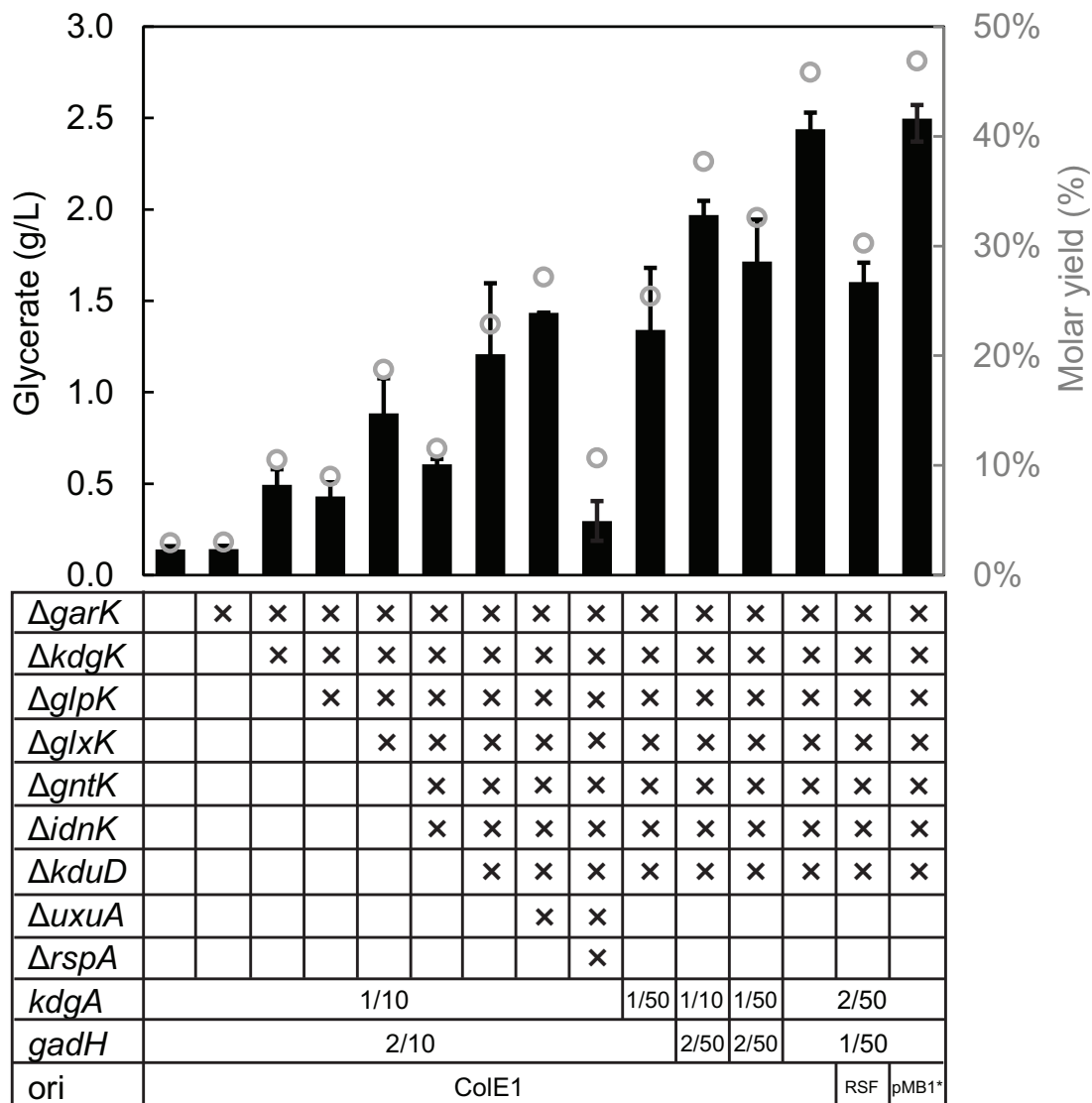
Figure 3-4: D-glycerate production from galacturonate. Endogenous gene knockouts were tested in *E. coli* MG1655 (DE3), as indicated in the table. The rows labeled *kdgA* and *gadH* depict which operon position each gene was in (1 or 2) and the RBS strength of the gene, in ~10,000 a.u. TIR; e.g. "1/10" indicates that the corresponding pathway gene is first in the operon, with a ~10,000 a.u. TIR RBS. The origins of replication tested were ColE1, RSF, and pMB1* (~20, ~100, and ~500 copies per cell, respectively). Bars show mean titer ± 1 SD of biological triplicates and open circles show average molar yield (%), 72 hr after inoculation.

3.2.4 Construction of a novel D-glycerate biosynthetic pathway from gluconate

The pathway from gluconate comprises the same heterologous enzymes as that from galacturonate, with the addition of a gluconate dehydratase, GnaD from *Achromobacter xylosoxidans* [127] (Figure 3-3A). Natively, *A. xylosoxidans* consumes D-glucose via the GnaD in the modified, non-phosphorylative, Entner-Doudoroff pathway. The heterologous pathway enzymes of this pathway are expressed from our gluconate biosensor circuit (Figure 3-3C).

The starting pathway plasmid had a p15A origin of replication. The heterologous genes were contained in an operon; the configuration of the galacturonate-fed pathway that led to the highest titer was conserved and the additional *gnaD* gene was added to the front of the operon with a ~50,000 a.u. TIR RBS, calculated by the RBS Calculator [107]. We hypothesized, as mentioned above, that the endogenous gluconate kinases, *gntK* and *idnK*, needed to be knocked out to accumulate product. This was supported by the 4.6-fold increase in D-glycerate titer in *E. coli* MG1655 (DE3) $\Delta garK\Delta kdgK\Delta glpK\Delta glxK\Delta gntK\Delta idnK$ compared to the starting strain *E. coli* MG1655 (DE3) $\Delta garK\Delta kdgK\Delta glpK\Delta glxK$ (Figure 3-5). The additional, sequential deletions of genes encoding enzymes that consume 2-dehydro-3-deoxy-D-gluconate, *kduD, uxuA,* and *rspA*, led to improved, sustained, and decreased D-glycerate titers compared to the previous strain, respectively (Figure 3-5). As above, we selected *E. coli* MG1655 (DE3) $\Delta garK\Delta kdgK\Delta glpK\Delta glxK\Delta gntK\Delta idnK\Delta kduD$ as our production strain since it produced 0.8 ± 0.2 g L^{-1} of D-glycerate and the addition of the $\Delta uxuA$ does not result in a significant improvement, with a resulting titer of 0.8 ± 0.1 g L^{-1}.

Next, we increased the RBS strength on *gnaD* to determine the impact of higher expression of the gene on titer (Figure 3-5). The higher RBS strength of ~100,000 did not change the final D-glycerate titer. Finally, we investigated the impact of copy number on D-glycerate titer by varying the origins of replication. We compared ~10

(p15A), $\sim$20 (ColA), and $\sim$100 (RSF) copies per cell (Figure 3-5). The additional copies from the RSF origin resulted in the highest D-glycerate titer and yield out of all the conditions tested, 1.11 ± 0.04 g L^{-1} and 24%, respectively, and a 7-fold improvement in titer compared to our starting strain.

ΔglxK	×	×	×	×	×	×	×	×
ΔgntK		×	×	×	×	×	×	×
ΔidnK		×	×	×	×	×	×	×
ΔkduD			×	×	×	×	×	×
ΔuxuA				×	×			
ΔrspA					×			
gnaD	50					100	50	
ori	p15A						ColA	RSF
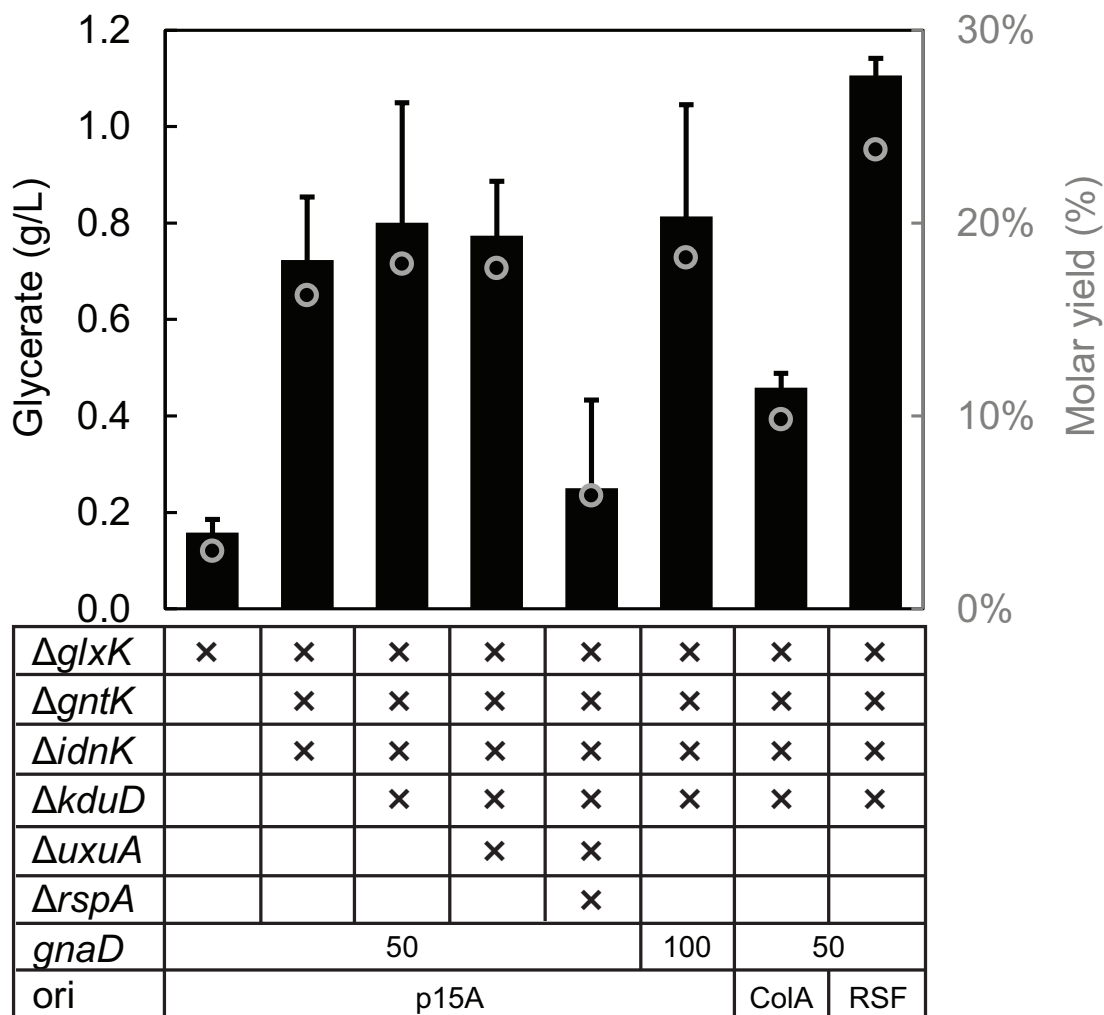
Figure 3-5: D-glycerate production from gluconate. Endogenous gene knockouts were tested in *E. coli* MG1655 (DE3) $\Delta garK \Delta kdgK \Delta glpK$, as indicated in the table. The row labeled *gnaD* indicates the RBS strength of said gene, in $\sim$10,000 a.u. TIR; the gene is the first in the pathway operon. The origins of replication tested were p15A, ColA, and RSF ($\sim$10, $\sim$20, and $\sim$100 copies per cell, respectively). Bars show mean titer $\pm$ 1 SD of biological triplicates and open circles show average molar yield (%), 72 hr after inoculation.

3.2.5 D-glycerate biosynthesis from single and mixed substrates

Having shown biosynthesis of D-glycerate from galacturonate and gluconate in single substrate fermentations, we sought to demonstrate mixed substrate biosynthesis. The biosynthetic pathways that achieved the highest titer from galacturonate (pColE1-P1exuR-OO-50gadH-50-kdgA in Table 3.3), and gluconate (pRSF-P3-OO-50gnaD-50gadH-50kdgA in Table 3.3), described above, were on compatible origins of replication, so they were co-transformed into a single *E. coli* MG1655 (DE3) $\Delta garK \Delta kdgK \Delta glpK \Delta glxK \Delta gntK \Delta idnK \Delta kduD$ production strain. We performed mixed substrate fermentations with our co-transformed production strain (Figure 3-6).
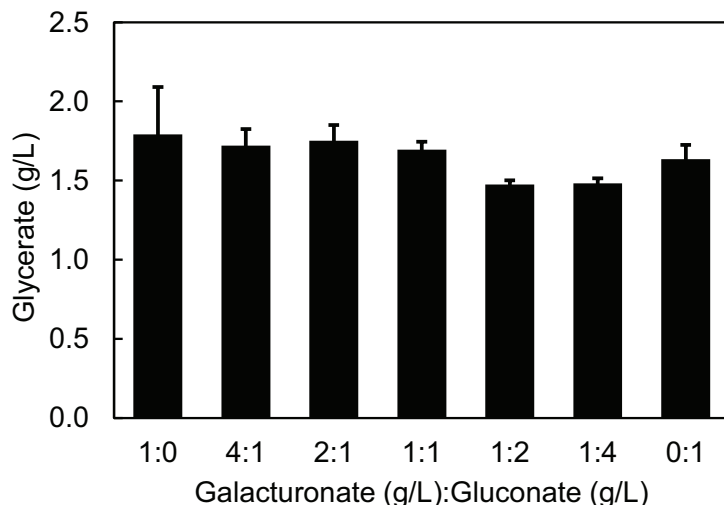
Figure 3-6: D-glycerate production from mixed substrates. Substrate concentration totalled 10 g L^{-1} in all cases. The ratio of galacturonate to gluconate intial concentrations is labelled at the bottom. Data are the mean $\pm$ 1 SD of biological triplicates, taken 72 hr after inoculation.

Above, in our single substrate, single pathway plasmid fermentations, we acheived D-glycerate titers of 2.4 $\pm$ 0.1 g L^{-1} and 1.11 $\pm$ 0.04 g L^{-1} from galacturonate and gluconate, respectively. In fermentations with the co-transformed production strain, all resultant titers stayed at intermediate levels between these two bounds, as though the co-transformed strain dampened the effects of either single substrate with a single

pathway plasmid. The co-transformant still achieved the highest titer, of 1.8 ± 0.3 g L^{-1} D-glycerate, from galacturonate alone. Though the titer from galacturonate alone decreased, that from gluconate alone increased compared to the production strain harboring only the gluconate pathway plasmid, to 1.64 ± 0.09 g L^{-1} D-glycerate. When both substrates were fed in a 1:1 ratio, the resulting D-glycerate titer of 1.70 ± 0.05 g L^{-1} was the average of the single substrate fermentations, for both single- and co- transformant conditions. In conditions where more galacturonate was fed than gluconate, the titers were slightly higher than that of the 1:1 fermentation, and when more gluconate was fed than galacturonate, the resulting D-glycerate produced was lower. Though for each set of conditions, we tested two feed ratios, the results of both were almost identical. The feed ratios of 4:1 and 2:1 galacturonate to gluconate resulted in titers of 1.7 ± 0.1 and 1.8 ± 0.1 g L^{-1} D-glycerate, respectively. For feed ratios of 1:2 and 1:4, D-glycerate was produced at 1.48 ± 0.03 g L^{-1} for both conditions. Thus, we were able to produce D-glycerate from single and mixed substrate feeds. Furthermore, the resulting titer from these fermentations remained consistent and within the bounds of those achieved in single substrate fermentations.

3.3   Discussion

In this study, we developed a scheme for multi-substrate utilization for biosynthesis as an approach to feeding complex input streams. To reduce the burden of the recombinant pathways required for each of the individual substrates, the expression of the heterologous genes for each were induced by their respective substrate. The biosensors we developed for expression control showed minimal crosstalk when consolidated into a single host cell. We previously demonstrated minimal interaction with the host cell's native regulatory system as well [120]. This biosensor construction approach could be taken for other substrates that are abundant in a waste stream of interest, especially for substrates for which microbes natively have regulatory responses using transcription factors or other control elements. As we established in our previous work, there is utility to using the substrate to double as the inducer

for pathway expression and these expression control circuits function as general chemically-inducible expression controllers.

For each of our selected substrates, galacturonate and gluconate, we developed novel pathways to produce D-glycerate using non-phosphorylative Entner-Doudoroff pathway enzymes. The pathways converged onto the intermediate 2-dehydro-3-deoxy-D-gluconate (KDG), which presents the possibility of introducing promoter logic schemes in the expression of the downstream genes. For example, an AND-gate, which requires the presence of both substrates, could express an additional copy of *gadH* and *kdgA* to help process the flux from both pathways.

Interestingly, the presence of both of our production pathway plasmids in a single production strain resulted in consistent D-glycerate production from mixed substrates, without the need for additional genetic logic or control mechanisms. The need may arise if we could achieve higher yields from the pathways. Production from galacturonate led to a higher titer of 2.4 ± 0.1 g L^{-1} compared to gluconate which resulted in 1.11 ± 0.04 g L^{-1} of D-glycerate, in single pathway plasmid fermentations. The co-transformed production strain, harboring both pathways, produced D-glycerate titers of 1.8 ± 0.3 and 1.64 ± 0.09 g L^{-1} from galacturonate and gluconate, respectively. A 1:1 ratio of the substrates led to an intermediate level of production compared to single substrate fermentations; when more galacturonate was present in the mixed feed, the output skewed towards the higher end, and when more gluconate was added in the mixture, the titer skewed lower. The presence of both substrates led to less varation in titer than for single substrate fermentations, which could be a desirable quality of our co-transformed production strain and utilizing mixed substrate feeds. We demonstrated the ability to biosynthesize a product of interest, D-glycerate, from mixtures of two substrates using novel recombinant pathways. This work brings us closer to managing the complexity of waste streams that could be used as feeds for biosynthsis, as the substrates are both abundant in food waste. Our approach also expands the possibilities of products to make outside of the native metabolism of our host.

3.4 Methods

3.4.1 Strains and media

All plasmids were cloned in Stellar Competent Cells from Takara Bio (San Jose, CA). Biosensor characterization studies were performed in *E. coli* MG1655. Chromosomal deletion of endogenous genes from *E. coli* MG1655(DE3) (Table 3.1) was completed using the procedure described by Datsenko and Wanner [100]. The primer pairs for each knockout included ∼50 bp homology arms outside of the target gene (Table 3.1). D-Glyceric acid fermentations were conducted in *E. coli* MG1655(DE3) with the chromosomal knockouts of the specified genes. All growth and fermentation was done in Luria-Bertani (LB) broth (BD, Franklin Lakes, NJ).

Table 3.1: Endogenous gene knockouts and associated primers

Endogenous gene	f primer	r primer
garK	[91]	[91]
kdgK	GACCAGCAAACCACCACAGCGCAAACTAAC GCTAATTTTTTACAGATCAGGTTCACGACTGT GTAGGCTGGAGCTGCTTC	ATTTATGGATGAGCTGGATAGAGGGGTAAC ACTTTATCCAGCCTTTTGCATATGCTGCGTT CCGTCGACCTGCAGTT
glpK	TCCTTCAGAACAAAAAGCTTCGCTGTAATAT GACTACGGGACAATTAAACGTGTAGGCTGG AGCTGCTTC	ACGTTTCGGGACTACCGGATGCGGCATAAA CGCTTCATTCGGCATTTACATCCGTCGACCT GCAGTT
glxK	[91]	[91]
gntK	AGTATTGGCGCTGAACGCCTG	TCGACTGCGCCGGTTTCATG
idnK	AAATTATTATGCCGCCAGGCGTAGTATCGCA GCAGGTAAGATGATTCAGGAGATTTTAAAG TGTAGGCTGGAGCTGCTTC	CAGCATGTGCGCGACGGTAAGGCGCGTTAC CGCGTGGTGTTGAAAGCCGATTTTTGAAAA TCCGTCGACCTGCAGTT
kduD	GCCGTTAAAGATTTGCGCTAGTTGTGGGCA TAAACGAATAAGGTATTGTTGTGTAGGCTG GAGCTGCTTC	GTATAAAAAACCCTGCCATGCGGCAGGGTC ATAAAAGTAAGAAGAATGAATCCGTCGACC TGCAGTT
uxuA	GGTTCCGCGTCTCTTTGCTGTGGAACCCAC TATGTGAAAGAGGAAAAATCGTGTAGGCT GGAGCTGCTTC	GACGGCAAGGAAGAAGGAACCGGCACGG CGCGCAGCCATGCCGGTGGATATCCGTCGA CCTGCAGTT
rspA	TCAGTTGCGTAGATTTCATGCATCACGACA AGCGATGCAAGGAATCGAACGTGTAGGCT GGAGCTGCTTC	CGCCAGTTGATTCGGTTTTTTCAATTAATATG CTTTTCATTATCTTACTCCTCCGTCGACCTG CAGTT

3.4.2   Cloning and plasmid construction

The gluconate biosensor variants were constructed in the same way as the galacturonate ones in our previous work in Chapter 2 [120], with *gntR* and its cognate operator. All cloning primers and plasmids used in this study are found in Tables 3.2 and 3.3, respectively.

The consolidated galacturonate and gluconate double biosensor plasmid (pP1exuR-OOgfp-P3gntR-OOmCherry) was constructed using the PCR products of 2gal-f and 2gal-r, and 2glcn-f and 2glcn-r on their respective biosensor template, mCherry-f and mCherry-r on the *mCherry* gene template, and 2BB-f and 2BB-r on pYTK001 [101], with the NEBuilder HiFi DNA Assembly Cloning Kit (NEB, Ipswich, MA).

Table 3.2: Primers used for cloning

Name	Sequence
gntR-f	AAGTCGTCTCATCGGTCTCATATGCTAGACTCCAAAGACCTGTTGTATCCC
gntR-r	AAGTCGTCTCAGGTCTCAGGATCTAGTCATTGTTGTATTCAGCTCCTTTTGCCAG
gntO-XO-f	GGGAATGTTACCCGTATCAT
gntO-XO-r	TTGTATGATACGGGTAACAT
P2-f	[120]
P2-r	[120]
P1-f	[120]
P1-r	[120]
OO-f	ATACTTGTATACAAGTATATAATATATTCAGGGACGTTATCATACTTG
OO-r	CTTGTATACAAGTATCGTAAAGTTATCCAGCAACCA
OX-f	ATACTTGTATACAAGTATATAATATATTCAGGGAGACAACAA
OX-r	CTTGTATACAAGTATCGTAAAGTTATCCAGCAACCA
mCherry-f	ATGGACGAGCTGTACAAGTAACCAGGCATCAAATAAAACGAAAGG
mCherry-r	TCGCCCTTGCTCACCATAATTAAAGATCCTTATATTTGAGTTTGCTGAA
2BB-f	ATGGACGAGCTGTACAAGTAACCAGGCATCAAATAAAACGAAAGG
2BB-r	TCGCCCTTGCTCACCATAATTAAAGATCCTTATATTTGAGTTTGCTGAA
2gal-f	TAACCGTAGTCGGCGAGACGTTGACAGCTAGCTCAGTCCTAGG
2gal-r	GGGCGGCCGCTATAAACGCAGAAAGGCCCACC
2glcn-f	TGCGTTTATAGCGGCCGCCCCTTTTACAG
2glcn-r	TATTGGTCTGGTCAGAGACGTATAAACGCAGAAAGGCCCACCC
kdgA-f	ACTTTCGTTCACGCTTAAGGACAATTTATAATGCCAGAAATCATAACTCCAATCATAACC
kdgA-r	TATTACCTCCTAAGGGCTTGGACACTATTCTTTCAATATTTTAAGCTCTACAAGTTTCGC
gadH-f	AATAGTGTCCAAGCCCTTAGGAGGTAATACATGGACACAAAGTTGTACATCGACG

63

gadH-r	ACTGAGCCTTTCGTTTTATTTGATGCCTGGTTAATGGTGGTGGTGGTGGTG
exuR-biosensor-f	CCAGGCATCAAATAAAACGAAAGGC
exuR-biosensor-r	TTGTCCTTAAGCGTGAACGAAAGTTAAACAAAATTATTTGTTCAAAATGTTAACGTTAAC
50k-1kdgA-f	ATAAGCCCCCCATAAGAGAGAAATTAAATGCCAGAAATCATAACTCCAATCATAAC
50k-1kdgA-r	ATTTCTCTCTTATGGGGGGCTTATAAACGTCAAACACCATAATTCTTCCAGGTTC
50k-2gadH-f	GGAAGTAAGTCCTATTAAGAGAGGTAGATAATGGACACAAAGTTGTACATCGAC
50k-2gadH-r	TCTTAATAGGACTTACTTCCCTATTCTTTCAATATTTTAAGCTCTACAAGTTTCG
50k-1gadH-f	AAATAATTTTGTTTAACTTTGGAAGTAAGTCCTATTAAGAGAGGTAGATAATG
50k-1gadH-r	TTATGGGGGGCTTATAAACGTTAATGGTGGTGGTGGTGGTG
50k-2kdgA-f	CGTTTATAAGCCCCCCATAAGAGA
50k-2kdgA-r	TCGTTTTATTTGATGCCTGGCTATTCTTTCAATATTTTAAGCTCTACAAGTTTCG
RSFgal-f	TCCCCGAAAAGTGCCACCTGCTTCCGCTTCCTCGCTCA
RSFgal-r	GCTGTAAAAGGGGCGGCCGCAACGGAATAGCTGTTCGTTGACT
pMB1*gal-f	TCCCCGAAAAGTGCCACCTGTTGAGATCCTTTTTTTCTGCGCG
pMB1*gal-r	GCTGTCAAAGGGGCGGCCGCTTTCCATAGGCTCCGCCC
p15A-f	TTTTATCTGATTAATAAGATGATCTTCTTGAGATCGTTTTG
p15A-r	TGTATACTGGCTTACTATGTTGGCACTG
gntR-biosensor-f	ACATAGTAAGCCAGTATACAGCGGCCGCCCCTTTTAC
gntR-biosensor-r	AATTAAAGATCCTTATATTTGAGTTTGCTGAAAGTTAAACA
gnaD-f	TAGATACGCCGAGAAGGAGAGAATATATGACGGACACCCCTCGT
gnaD-r	TCTTAATAGGACTTACTTCCTCAGTGCGAATGGCGCG
kdgA-gadH-f	CGTTCACGCTTAAGGACAATTTATAATGC
kdgA-gadH-r	GCCGGGCGTTTTTTATTGGTGCGGCCGCTGTATATAAACGC
100k-gnaD-f	CATACATAACTTGTATAAGGAGGATATTCATGACGGACACCCCTCGT
100k-gnaD-r	CCTTATACAAGTTATGTATGAAAGTTAAACAAAATTATTTGTAGGAGTATACTTGT
ColAglcn-f	CCTCTTACGTGCCCGATCAAAAACGTCCTAGAAGATGCCAGG
ColAglcn-r	GCTGTAAAAGGGGCGGCCGCTGGTGTCGGGAATCCGTAAAG
RSFglcn-f	CCTCTTACGTGCCCGATCAACTTCCGCTTCCTCGCTCA
RSFglcn-r	GCTGTAAAAGGGGCGGCCGCAACGGAATAGCTGTTCGTTGACT

Table 3.3: Plasmids used in this study

Plasmid	Genotype	Ref
pYTK095	empty vector, backbone for biosensors and pathway plasmids	[101]
pYTK001	empty vector, backbone for consolidated biosensor	[101]
pP1XO-gfp	pYTK095 with gntR under the P1 promoter; sfgfp under the hybrid ProD promoter with a downstream operator	this study
pP2XO-gfp	pYTK095 with gntR under the P2 promoter; sfgfp under the hybrid ProD promoter with a downstream operator	this study
pP3XO-gfp	pYTK095 with gntR under the P3 promoter; sfgfp under the hybrid ProD promoter with a downstream operator	this study
pP3OX-gfp	pYTK095 with gntR under the P3 promoter; sfgfp under the hybrid ProD promoter with a core operator	this study
pP3OO-gfp	pYTK095 with gntR under the P3 promoter; sfgfp under the hybrid ProD promoter with core and downstream operators	this study
pP3XX-gfp	pYTK095 with gntR under the P3 promoter; sfgfp under the hybrid ProD promoter with no operators	this study
pP3OO-empty	pYTK095 with gntR under the P3 promoter; no gene under the hybrid ProD promoter with core and downstream operators	this study
pP1exuR-OOgfp-P3gntR-OOmCherry	pYTK001 with exuR under the P1 promoter; sfgfp under the hybrid ProD promoter with core and downstream exuO operators; gntR under the P3 promoter; mCherry under the hybrid ProD promoter with core and downstream gntO operators	this study
pColE1-P1exuR-OO-10kdgA-10gadH	exuR under the P1 promoter; ProD with 2 exuO operators expressing a 10k RBS kdgA and 10k RBS gadH operon	this study
pColE1-P1exuR-OO-50kdgA-10gadH	exuR under the P1 promoter; ProD with 2 exuO operators expressing a 50k RBS kdgA and 10k RBS gadH operon	this study
pColE1-P1exuR-OO-10kdgA-50gadH	exuR under the P1 promoter; ProD with 2 exuO operators expressing a 10k RBS kdgA and 50k RBS gadH operon	this study
pColE1-P1exuR-OO-50kdgA-50gadH	exuR under the P1 promoter; ProD with 2 exuO operators expressing a 50k RBS kdgA and 50k RBS gadH operon	this study
pColE1-P1exuR-OO-50gadH-50kdgA	exuR under the P1 promoter; ProD with 2 exuO operators expressing a 50k RBS gadH and 50k RBS kdgA operon	this study
pRSF-P1exuR-OO-50gadH-50kdgA	exuR under the P1 promoter; ProD with 2 exuO operators expressing a 50k RBS gadH and 50k RBS kdgA operon	this study
pMB1*-P1exuR-OO-50gadH-50kdgA	exuR under the P1 promoter; ProD with 2 exuO operators expressing a 50k RBS gadH and 50k RBS kdgA operon	this study
p15A-P3gntR-OO-50gnaD-50gadH-50kdgA	gntR under the P3 promoter; ProD with 2 gntO operators expressing a 50k RBS gnaD, 50k RBS gadH, and 50k RBS kdgA operon	this study
p15A-P3gntR-OO-100gnaD-50gadH-50kdgA	gntR under the P3 promoter; ProD with 2 gntO operators expressing a 10k RBS gnaD, 50k RBS gadH, and 50k RBS kdgA operon	this study
pColA-P3gntR-OO-50gnaD-50gadH-50kdgA	gntR under the P3 promoter; ProD with 2 gntO operators expressing a 50k RBS gnaD, 50k RBS gadH, and 50k RBS kdgA operon	this study
pRSF-P3gntR-OO-50gnaD-50gadH-50kdgA	gntR under the P3 promoter; ProD with 2 gntO operators expressing a 50k RBS gnaD, 50k RBS gadH, and 50k RBS kdgA operon	this study

Heterologous pathway genes, in Table 3.4 were synthesized from Integrated DNA

Technologies (Coralville, IA). All pathway plasmids were constructed with the NEBuilder HiFi DNA Assembly Cloning Kit (NEB) and PCR products as described here. The initial galacturonate-fed pathway, pColE1-P1exuR-OO-10kdgA-10gadH, was constructed with the PCR products of kdgA-f and kdgA-r, and gadH-f and gadH-r, on their respective synthesized gene templates, and exuR-biosensor-f and exuR-biosensor-r on the galacturonate biosensor template pP1OO-gfp from our previous work [120]. The genes' RBS strengths were changed using the [RBS strength]-[gene name]-f and -r primers; origins of replication were changed using [ori]gal-f and -r.

The initial gluconate-fed pathway, p15A-P3gntR-OO-50gnaD-50gadH-50kdgA, was constructed with the PCR products of gnaD-f and gnaD-r on its synthesized gene template, kdgA-gadH-f and kdgA-gadH-r on template pColE1-P1exuR-OO-50gadH-50kdgA, and gntR-biosensor-f and gntR-biosensor-r on template pP3OO-gfp from this study. The RBS strength of *gnaD* was increased using the 100k-gnaD-f and -r primers; origins of replication were changed using [ori]glcn-f and -r.

Table 3.4: Sequences of custom synthesized genes

Gene	Sequence
kdgA	ATGCCAGAAATCATAACTCCAATCATAACCCCATTCACTAAAGATAATAGAATAGAT
	AAGGAAAAATTAAAGATACATGCGGAGAATCTCATTAGGAAGGGAATAGATAAGT
	TGTTCGTCAACGGTACTACTGGTCTTGGTCCTTCGTTATCTCCAGAGGAGAAGTTA
	GAGAACTTAAAGGCAGTTTATGACGTCACCAATAAGATAATATTTCAAGTTGGTGG
	ATTGAATCTAGACGATGCTATAAGATTGGCTAAATTAAGTAAAGACTTTGATATTGT
	CGGTATAGCCTCGTATGCTCCATATTATTACCCAAGAATGTCTGAGAAGCATTTGGT
	AAAGTATTTTAAGACCTTGTGTGAAGTATCTCCACACCCTGTCTATTTGTACAATTA
	CCCGACGGCAACGGGAAAAGACATAGATGCAAAAGTCGCTAAAGAGATAGGCTG
	TTTTACTGGAGTAAAGGATACTATTGAAAACATAATTCACACCTTAGACTACAAAC
	GTCTAAATCCTAACATGTTAGTATATAGTGGCTCTGATATGTTAATAGCAACGGTAG
	CTTCTACGGGTTTAGATGGTAATGTTGCAGCAGGTTCGAATTATCTTCCAGAGGTT
	ACTGTGACAATTAAGAAATTGGCTATGGAAAGGAAAATTGATGAAGCACTTAAGT
	TACAATTCCTTCATGACGAGGTAATAGAGGCGTCTAGAATATTTGGGAGCTTATCTT
	CAAATTACGTATTAACCAAGTATTTCCAAGGATACGATTTAGGATATCCTAGACCTC
	CAATATTCCCACTAGATGATGAAGAAGAAAGGCAGCTAATTAAGAAAGTTGAGGG
	TATAAGGGCGAAACTTGTAGAGCTTAAAATATTGAAAGAATAG

gadH	ATGGACACAAAGTTGTACATCGACGGTCAATGGGTTAACTCGTCTTCAGGGAAGA
	CAGTGGATAAATACAGCCCTGTAACGGGACAAGTAATCGGTCGCATGGAGGCTGC
	CACACGTGATGATGTTGACCGTGCGATTGATGCCGCAGAGGATGCGTTCTGGGCT
	TGGAATGACCTGGGGTCGGTGGAACGCTCCAAAATTATTTACCGTGCGAAGGAGT
	TGATCGAGAAGAACCGTGCTGAGCTTGAAAATATCATTATGGAGGAAAATGGTAA
	ACCCGTAAAAGAGGCGAAAGAGGAGGTTGACGGGGTAATCGATCAGATTCAGTA
	CTATGCAGAATGGGCGCGCAAACTGAATGGTGAGGTGGTAGAGGGTACTAGCTCC
	CATCGTAAGATTTTTCAGTACAAGGTGCCGTATGGCATTGTAGTCGCCTTGACTCCT
	TGGAATTTCCCCGCTGGAATGGTGGCGCGCAAATTAGCTCCGGCGTTGTTAACGGG
	CAACACCGTCGTGCTGAAACCCAGTTCGGACACTCCTGGGTCTGCGGAGTGGATC
	GTGCGTAAGTTCGTAGAGGCTGGGGTCCCTAAGGGCGTGCTGAACTTCATTACCGG
	GCGTGGATCTGAAATCGGCGATTATATCGTGGAGCACAAGAAAGTAAACTTGATTA
	CGATGACCGGCTCAACGGCCACTGGCCAACGTATTATGCAAAAAGCAAGCGCGAA
	CATGGCAAAGTTAATTCTGGAGCTGGGAGGTAAGGCCCCATTTATGGTATGGAAGG
	ACGCGGACATGGATAACGCTTTGAAAACCCTGTTGTGGGCGAAGTACTGGAATGC
	AGGGCAATCCTGTATTGCAGCCGAACGCCTTTACGTACACGAAGACATTTATGACA
	CTTTTATGAGTCGTTTCGTCGAACTTTCACGTAAGTTGGCCTTGGGCGATCCGAAG
	AACGCCGATATGGGACCACTTATCAACAAAGGAGCCCTTCAAGCGACTTCGGAAA
	TTGTTGAAGAAGCGAAGGAGTCTGGAGCGAAGATTTTGTTTGGAGGAAGTCAGCC
	TTCACTGAGCGGACCGTACCGTAACGGCTACTTCTTCTTGCCTACCATCATCGGAAA
	CGCCGACCAGAAGTCCAAGATTTTCCAAGAAGAGATTTTTGCTCCTGTAATCGGCG
	CACGCAAAATTTCGTCTGTAGAGGAGATGTGCGATTTAGCAAACGATAATAAGTATG
	GTCTGGCTTCCTACCTTTTCACGAAGGACCCCAACATTATTTTCGAAGCCTCCGAAC
	GCATTCGTTTTGGCGAATTGTATGTGAACATGCCCGGGCCAGAGGCAAGCCAAGGC
	TACCATACGGGTTTTCGCATGACGGGACAGGCTGGTGAGGGCTCTAAATACGGTATT
	TCTGAGTATTTAAAGTTAAAGAATATCTACGTCGACTATAGTGGTAAACCACTGCACA
	TCAACACTGTACGTGATGATTTGTTTCAAAGCGGTCGTCCGGTGCTGTCCTCTCACC
	ACCACCACCACCATTAA

gnaD	ATGACGGACACCCCTCGTAAACTGCGTTCGCAAAAATGGTTTGACGATCCCGCGCA CGCGGACATGACGGCTATTTACGTTGAGCGTTACCTGAATTACGGACTTACGCGCCA AGAGTTACAGTCAGGCCGCCCAATCATCGGCATCGCGCAAACCGGAAGTGACCTTG CTCCATGTAACCGTCATCATCTGGCGCTGGCAGAACGCATTAAGGCTGGCATTCGTG ATGCCGGGGGTATCCCGATGGAGTTCCCGGTGCATCCGCTGGCTGAGCAGGGCCGT CGTCCGACAGCGGCCTTAGACCGTAATCTGGCCTACCTTGGTCTGGTGGAGATCTTA CATGGTTATCCTCTTGATGGCGTAGTTTTAACGACAGGTTGTGACAAGACTACGCCT GCATGTTTGATGGCCGCAGCGACCGTGGACATTCCGGCCATCGTGCTGTCGGGTGG ACCGATGCTGGACGGTTGGCACGATGGGCAGCGCGTAGGAAGTGGTACCGTCATTT GGCATGCTCGTAATCTTATGGCCGCCGGGAAATTAGACTATGAAGGGTTTATGACGT TAGCCACGGCATCATCGCCGTCCATTGGACATTGCAACACTATGGGTACGGCTTTAA GCATGAATAGCCTTGCAGAAGCATTAGGCATGAGTCTGCCCACATGCGCGAGTATTC CTGCACCCTACCGTGAGCGTGGACAAATGGCGTACGCAACCGGCTTACGCATCTGC GATATGGTTCGCGAGGACTTACGTCCTTCGCGTATTTTAACACGTGAAGCATTTGAA AATGCGATTGTAGTTGCTTCGGCCCTTGGTGCGAGTAGTAATTGTCCGCCTCATCTG ATTGCGATGGCTCGCCATGCGGGAATCGACCTTTCTTTAGATGACTGGCAGCGCCTG GGCGAGGATGTCCCTTTGTTAGTCAATTGTGTCCCCGCAGGTGAGCATTTAGGTGAA GGATTTCATCGCGCAGGTGGCGTCCCAGCCGTAATGCACGAGCTGCTGGCCGCAGG TCGCTTACATGCAGATTGTGCGACCGTGTCAGGAAAGACCATCGGGGAGATCGCTG CGGGGGCGAAAACACACGATGCGGACGTAATCCGCGGTTGCGACGCGCCGCTTAA ACACCGTGCAGGATTTATCGTGCTTTCAGGAAACTTCTTTGATAGCGCCGTCATTAA GATGTCAGTTGTGGGGGAAGCGTTCCGCCGTGCCTATTTATCGGCGCCCGGCGACG AAAATGCCTTCGAGGCTCGCGCTATTGTCTTCGAAGGGCCCGAGGATTATCATGCCC GTATCGAAGATCCGGCGTTAAACATCGACGAGCATTGTATCTTGGTTATTCGTGGAG CAGGAACAGTGGGCTACCCCGGGAGTGCCGAAGTGGTCAACATGGCACCGCCCTC CCATCTTATTAAGCGTGGCATTGATTCACTGCCTTGTTTGGGAGACGGTCGTCAATC AGGCACGTCAGCGTCTCCCTCGATCCTTAACATGTCACCTGAAGCCGCAGTAGGTG GGGGCCTGGCACTGTTACGTACCGGGGACCGCATCCGTGTAGACTTGAATCAGCGT TCTGTCATCGCATTAGTCGATGAAGCAGAGCTGGCCCGCCGCCGCCAAGACCCTCC TTATCAGCCTCCACCGGCACAGACCCCTTGGCAAGAGTTGTACCGTCAGTTGGTGG GACAACTGTCCACAGGCGGTTGTCTGGAACCAGCAACCTTATATTTAAAAGTCGTT GAAACACGTGGTGACCCGCGCCATTCGCACTGA

3.4.3 Fluorescence measurements

Fluorescence characterization experiments were performed in the BioLector microbioreactor system (m2p-labs GmbH, Baesweiler, Germany). Overnight cultures were grown at 37°C with agitation at 250 rpm. One milliliter cultures were inoculated in BioLector 48-well flower plates at a 1:100 dilution with the appropriate overnight culture. Gluconate, and galacturonate where indicated, were added at inoculation.

The BioLector was set to 37°C, 1200 rpm shake speed, and 85% humidity. Continuous biomass (620 nm excitation), GFP (488 nm excitation, 520 nm emission), and where mentioned, mCherry (550 nm excitation, 610 nm emission), measurements were taken in arbitrary BioLector units over a 24 hr period.

3.4.4   D-glyceric acid fermentations

All cultures were grown in LB medium. All chemicals used for medium formulations and analytic standards were purchased from Sigma-Aldrich (St. Louis, MO). Overnight cultures were grown at 37°C and 250 rpm agitation. 50 mL fermentation cultures were grown in 250 mL baffled flasks at 30°C and 250 rpm agitation. An initial OD_{600} of 0.05 was inoculated into each flask from its corresponding overnight culture. The appropriate concentration of substrate was added at inoculation, unless otherwise stated. Cultures were sampled at 4, 24, 48, and 72 hr for analysis by UV-Vis and HPLC.

3.4.5   Galacturonate, gluconate, and D-glyceric acid quantification

In the single substrate fermentations, concentrations of galacturonate or gluconate, and D-glyceric acid in culture supernatants were determined using a 1200 Series Agilent Technologies instrument (Santa Clara, CA) with an Aminex HPX-87H Ion Exclusion Column (Bio-Rad Laboratories, Hercules, CA) and refractive index detector. The 22 min method ran an isocratic mobile phase of 5mM sulfuric acid at 0.6 mL min[1], with the column set to 65°C and the detector set to 35°C. Approximate elution times for galacturonate, gluconate, and D-glyceric acid were 8.9, 9.3, and 11.2 min, respectively.

Chapter 4

Multiplexed, autonomous, cell density activated expression control using quorum sensing

Abstract

QS systems coordinate behavior in response to cell density natively in microorganisms. While this is a distinct function from the transcription factors used in our metabolite-responsive biosensors, we can use these systems in a similar way to activate transcription of some gene(s) of interest in response to cell density as the stimulus. Furthermore, consolidating multiple engineered QS systems into one cell provides independent expression controllers that can be individually tuned for the user's application. This chapter summarizes the characterization of QS expression controllers in their transcriptional output and orthogonality for the purposes of multiplexed activation of expression by cell density.

4.1 Introduction

Quorum sensing (QS) systems are an attractive autonomous, cell density responsive, pathway independent expression control tool that have piqued the interest of many synthetic biologists and metabolic engineers. The Prather Lab has leveraged QS systems for dynamic pathway regulation to improve the titers of various products including glucaric acid, naringenin, salicylic acid, and shikimate [30, 128]. While Dinh and Prather utilized two QS regulatory systems, *lux* and *esa*, they respond to the same signaling molecule, 3-oxohexanoyl homoserine lactone [30], which limits the independent tunability of each expression circuit. Other groups have studied the orthogonality and multiplexing of QS systems; characterizations have been done with exogenously added acyl-homoserine lactone (AHL) signaling molecules [129, 130] and with individual QS systems or components in separate cells [131, 132]. Recently, Jiang et al. demonstrated two orthogonal, *in vivo* QS systems [133] and Wu et al. did the same and applied the regulatory system towards pathway expression control [134]. These studies use two systems that are engineered and ensured to be orthogonal in the inducer ranges utilized. Though they are successful demonstrations, they do not provide comprehensive understanding of how the systems interact *in vivo*. I sought to do a comprehensive study on the crosstalk between *in vivo* AHL-based QS systems. The knowledge could be useful to the field; although not all systems can be orthogonal, the characteristics of their crosstalk could be leveraged for metabolic engineering applications.

4.2 Results and Discussion

4.2.1 Construction of individual QS systems

I constructed individual *lux, las, rpa, tra,* and *esa* QS systems using the same genetic circuitry: the regulatory protein (R protein) was constitutively expressed and the promoter which it regulates (P_{QS}) expressed a *gfp* fluorescent reporter (Figure 4-1). The fluorescent output of the systems were measured in the BioLector with

exogenously added AHLs (Figure 4-1). Of these QS systems, the *rpa* and *tra* systems behaved favorably, with dynamic ranges over 10.
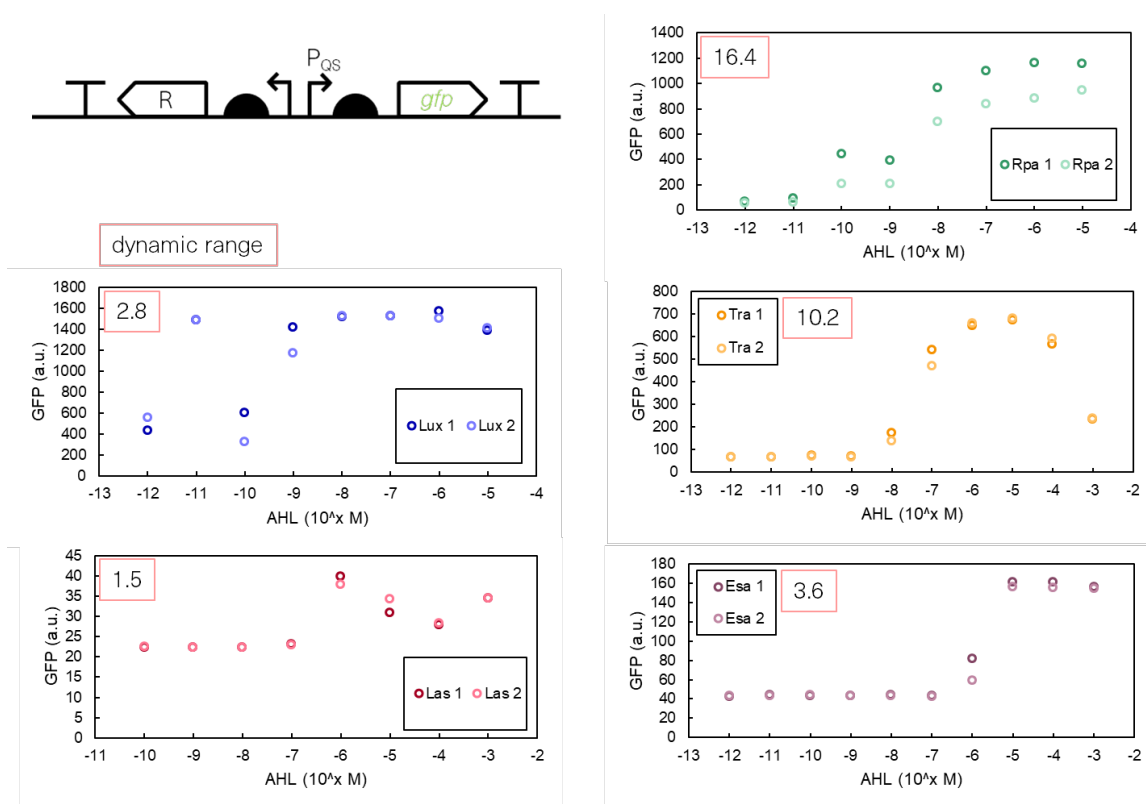

Figure 4-1: Schematic of the QS circuit and dose response curves of the single QS systems. The constitutively expressed regulatory (R) protein regulates its cognate promoter (P$_{QS}$), which controls *gfp* expression. Data points show the GFP fluorescence of biological duplicates in response to exogenous additional of the cognate AHL, 24 hr after inoculation. The average dynamic range of the duplicates is boxed in pink.

To remedy the low dynamic ranges of the remaining QS systems, I re-constructed the *lux, las, and esa* systems with higher RBS strengths on the *gfp* (Figure 4-2). This approach worked for the *lux* system, but was not effective for the other two. However, *las* and *esa* had previously been used and characterized in the Prather Lab, so I used those constructs from the Strain Database for further testing.
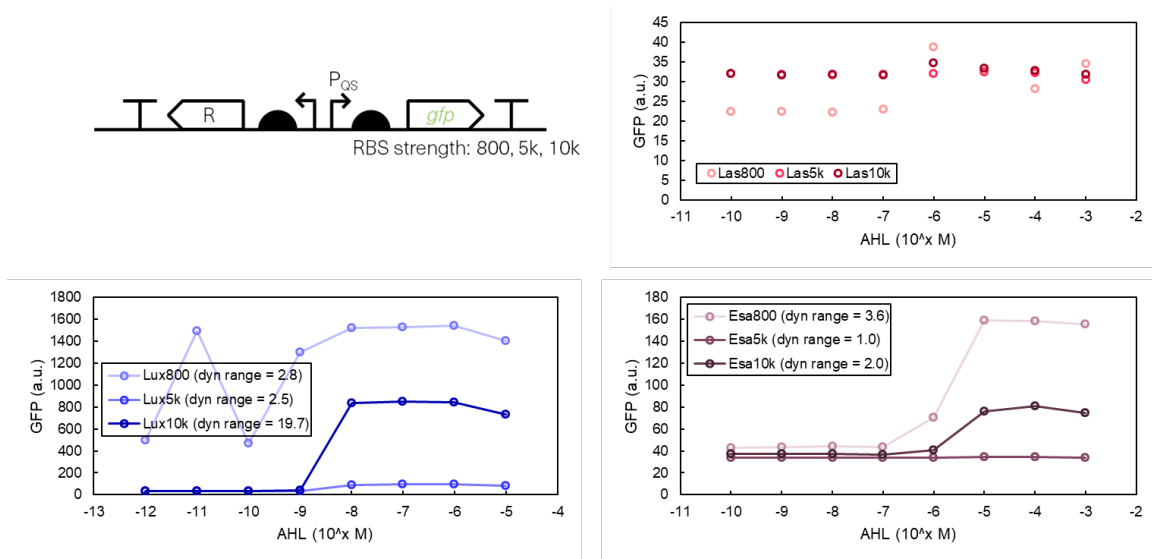
Figure 4-2: Schematic of the modified QS circuit with differing RBS strengths and dose response curves of the single QS systems. Data points show the GFP fluorescence in response to exogenous addition of the cognate AHL, 24 hr after inoculation. The dynamic range of the constructs, where application, are indicated in the legend.

4.2.2   Characterization of TraI with the *tra* QS system

Fully autonomous QS systems require the cognate synthase in the host cell to generate the AHL. I tested the synthase for the *tra* system, TraI, in a plasmid co-transformed with the single QS system characterized above. The data show that when the *traI* is expressed, with no exogenous addition of 3O-C8-HSL (C8), the synthase generates enough C8 to activate the GFP fluorescence to a similar level as when 10^{-7} M C8 is exogenously added (Figure 4-3). When *traI* is expressed and 10^{-5} M C8 is added exogenously, the GFP fluorescence further increases above the level from TraI alone, though only to the same level as 10^{-5} M C8 exogenously added without TraI. This saturation of GFP signal could be due to full activation of the *gfp* promoter, P_{tra}. Given that the *tra* synthase works in our hands, the *traI* could be chromosomally integrated into future host cells for autonomous activation from P_{tra}.
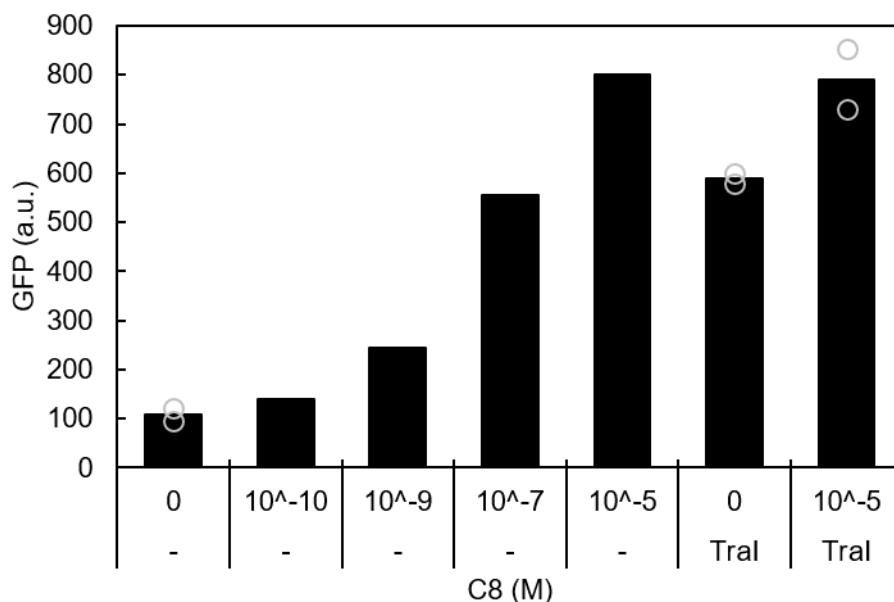
Figure 4-3: GFP fluorescence output from *tra-gfp* at varying exogenously added 3O-C8-HSL (C8) concentrations, 24 hr after inoculation; when the TraI synthase is present; and when TraI is present and exogenous C8 is added. The grey circles are individual values of biological replicates and their corresponding bar is their average; bars without grey circles show single replicate values.

4.2.3 Evaluating the crosstalk between pairwise QS systems

I developed a plan to test pairwise combinations of all of the individual QS systems that I had characterized that used distinct AHL molecules. I would construct pairwise QS plasmids by consolidating the individual systems and use *gfp* as the reporter for the system with the lower dynamic range and *mCherry* for the higher dynamic range system. This is because we get higher GFP signal in the BioLector. I planned to generate a mixed-inducer heat map for each pairwise plasmid, similar to the analysis for my galacturonate and gluconate biosensors in Chapter 3. I then would have taken the pairs with the least crosstalk or most interesting interactions and introduced their respective AHL synthases to the strain for a fully autonomous dual QS system. Finally, the fluorescent reporters could be replaced by relevant genes for pathway applications.

I only had time to characterize a few pairs of QS systems: *las-gfp+rpa-mCherry*,

las-gfp+lux-mCherry, and *las-gfp+tra-mCherry*, which exhibited a range of crosstalk. The worst performing was *las-gfp+rpa-mCherry*, in which the response of both reporters did not follow a trend for their respective AHL (Figure 4-4). We saw an unreliable increase in GFP response to 3O-C12-HSL (C12), its cognate AHL in the *las-gfp+lux-mCherry* system, coupled with a reverse induction trend in *mCherry*, in which the fluorescence decreased with its cognate AHL, 3O-C6-HSL (C6), concentration increasing (Figure 4-5). Lastly, for the *las-gfp+tra-mCherry* pair, each fluorescent reporter signal increased with increase cognate AHL concentration (Figure 4-6). This result is consistent with the literature, as these are the two systems Jiang et al. used in their orthogonal application [133].
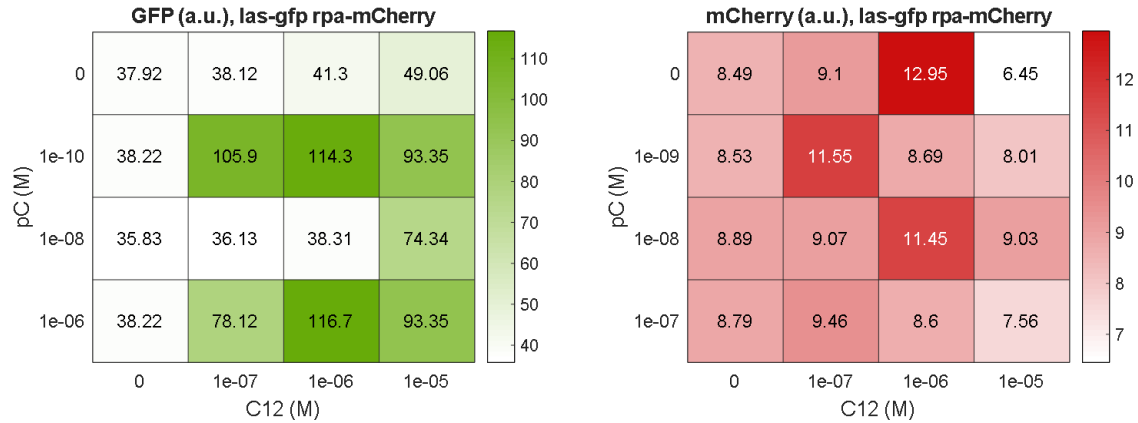

Figure 4-4: GFP (left) and mCherry (right) fluorescence output from *las-gfp+rpa-mCherry* at varying exogenously added AHL concentrations, 24 hr after inoculation. The cognate AHL for *las* and *rpa* are 3O-C12-HSL (C12) and p-coumaroyl-HSL (pC), respectively.
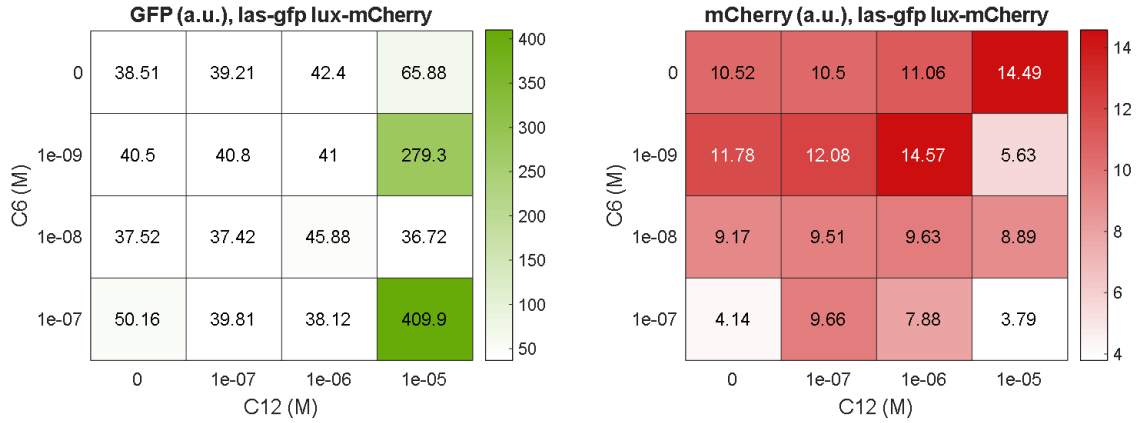
Figure 4-5: GFP (left) and mCherry (right) fluorescence output from *las-gfp+lux-mCherry* at varying exogenously added AHL concentrations, 24 hr after inoculation. The cognate AHL for *las* and *lux* are 3O-C12-HSL (C12) and 3O-C6-HSL (C6), respectively.
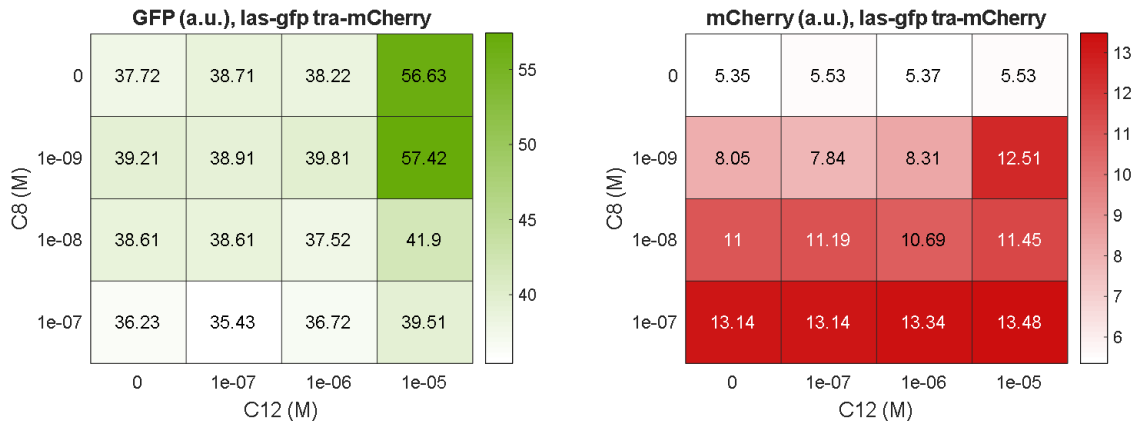

Figure 4-6: GFP (left) and mCherry (right) fluorescence output from *las-gfp+tra-mCherry* at varying exogenously added AHL concentrations, 24 hr after inoculation. The cognate AHL for *las* and *tra* are 3O-C12-HSL (C12) and 3O-C8-HSL (C8), respectively.

4.2.4   Investigation of an RpaR(K196N) mutant

At one point during the cloning process, I discovered that the *rpaR* I had been using in the *las-gfp+rpa-mCherry* construct had a missense mutation: 588C>A, which changed the wild type asparagine into a lysine (K196N). The mutant and wild type *rpaR* were verified to work in a single *rpa* system context, with adequate dynamic range (Figure 4-7).
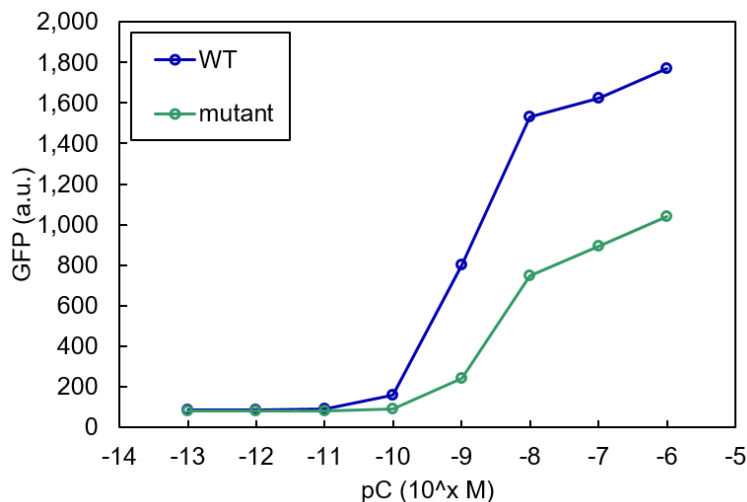
Figure 4-7: Fluorescence dose response of the *rpa* single system with wild type (WT) and mutant *rpaR*, 24 hr after inoculation.

Given that the mutant RpaR seemed to enhance the the fluorescence output from both QS systems, both the mutant and wild type were further tested and compared, in the context of a pairwise system with *las-gfp* (Figure 4-8). Though crosstalk was evident from both the wild type of mutant RpaR, the increased fluorescence was interesting and could be useful for pathway control. I hypothesized from initial data that while both versions of RpaR were functional in the *rpa* system, the enhanced GFP signal resulted from different interactions with the *las* system, specifically forming multimers with LasR in the presence of 3O-C12-HSL.

To investigate this, the systems were split onto two plasmids, and combinations of lasR, P$_{las}$-*gfp*, rpaR(WT/mut), and P$_{rpa}$-*mCherry* were co-transformed into *E. coli* MG1655 and characterized. These results showed that there is no appreciable difference in P$_{las}$-*gfp* response between the presence of RpaR WT or mutant in the context of the full *las* and *rpa* system, each in its own plasmid (Figure 4-9). mCherry activation was negligible in both cases, but the presence of both AHLs with the mutant RpaR may have led to higher mCherry expression compared to the WT.

To fully tease apart the interactions between all the *las* and *rpa* system components, subsets of the QS components were co-transformed into *E. coli* MG1655 and
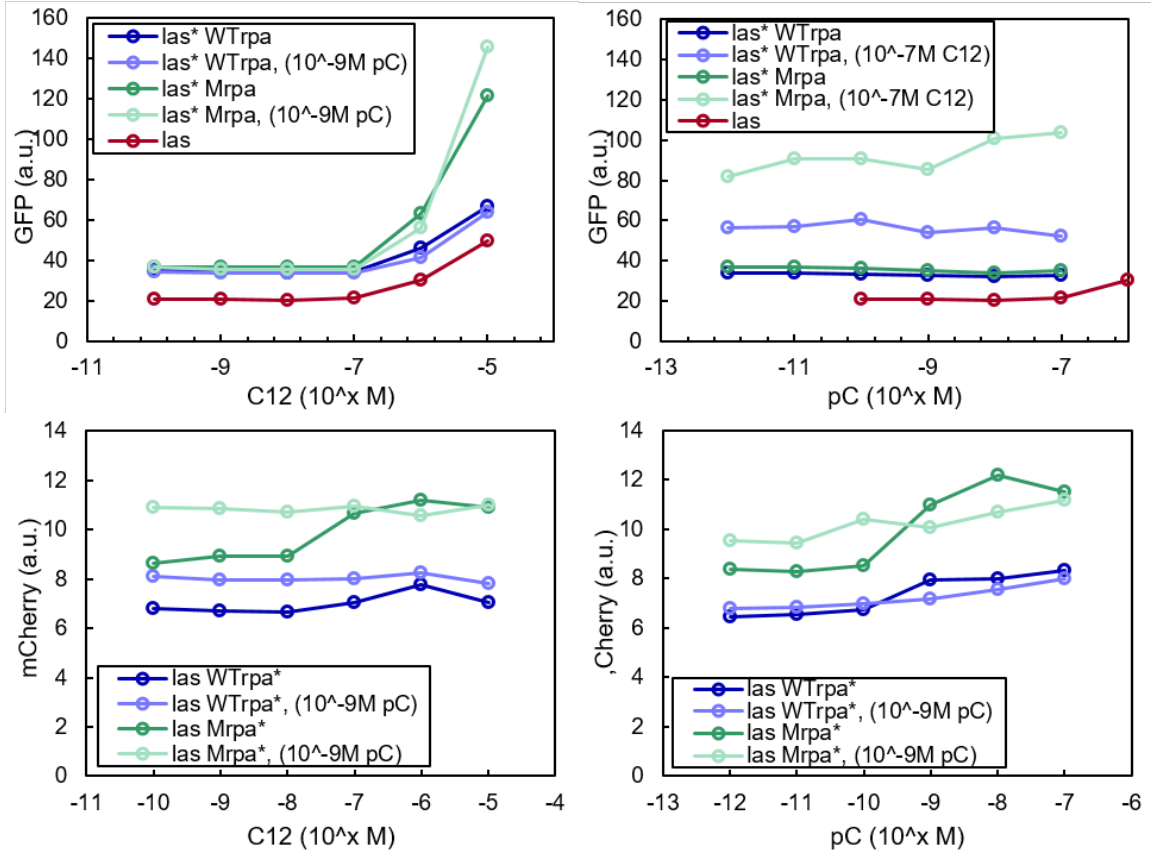
78

Figure 4-8: Fluorescence response of *las-gfp+rpa-mCherry* on a single plasmid with wild type (WTrpa) and mutant (Mrpa) *rpaR*, 24 hr after inoculation. The asterisk (*) indicates which system is controlling the reported fluorescence.

characterized. I first characterized P$_{las}$-*gfp*, with combinations of the R-proteins. Both the WT and mutant RpaR appeared to further activate P$_{las}$ when LasR and C12 were also present (Figure 4-10). There was p-coumaroyl-HSL (pC) crosstalk over 10^{-9} M with LasR, but not when an RpaR variant was present. Next, looking at P$_{rpa}$-*mCherry* with combinations of the R-proteins, the response curves to pC were weak (Figure 4-10). LasR alone showed activation of P$_{rpa}$, in response to both C12 and pC. Some of the response curves to C12 seemed to be fully activated across the concentration range tested. I do not currently have an explanation for this. From the investigation of the *las* and *rpa* systems, they appear have moderate crosstalk, though performed better than in the data from Section 4.2.3. Though the RpaR variants may activate P$_{rpa}$ to different degrees, they have not shown useful differences. Though this avenue of investigation did not lead to a useful multiplexed expression control circuit,
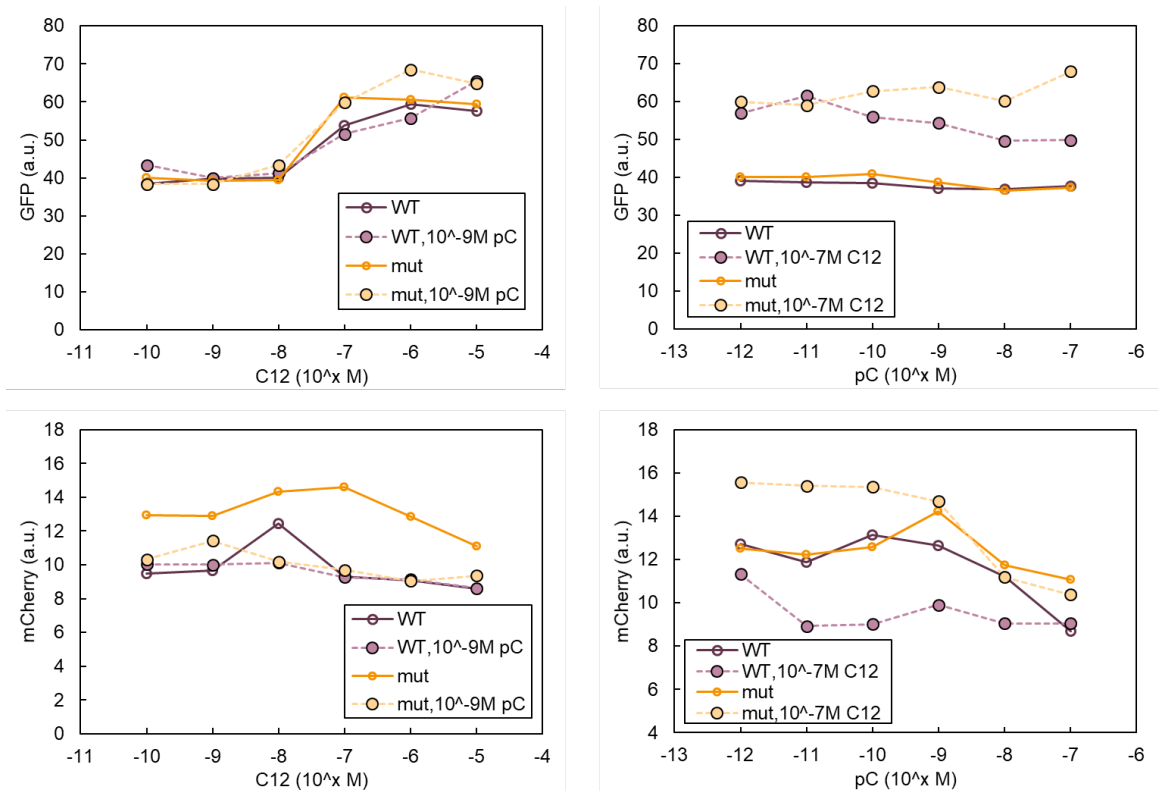
Figure 4-9: Fluorescence response of p15A-lasR-Plas-gfp and pCOLE1-rpaR(wt/mut)-Prpa-mCherry co-transformed into *E. coli* MG1655, 24 hr after inoculation. 3-oxo-C12-HSL (C12) activates *las*, while p-coumaroyl-HSL (pC) activates *rpa*. WT and mut denote which RpaR variant is used.

the approach taken can be used in future work. Using mulitple, full, *in vivo* QS systems in one cell for expression control presents many potential cross interactions, and the above presented work flow of isolating system components to characterize their interactions may offer resolution to said interactions.

Figure 4-10: The top row depicts the GFP response of subsets of p15A-lasR-Plas-gfp and pColE1-rpaR(wt/mut) co-transformed into MG1655, 24 hr after inoculation. The present R-proteins and promoters are shown in the legend; empty means an empty ColE1 plasmid containing only the origin of replication and the antibiotic resistance gene. The bottom row depicts the mCherry response o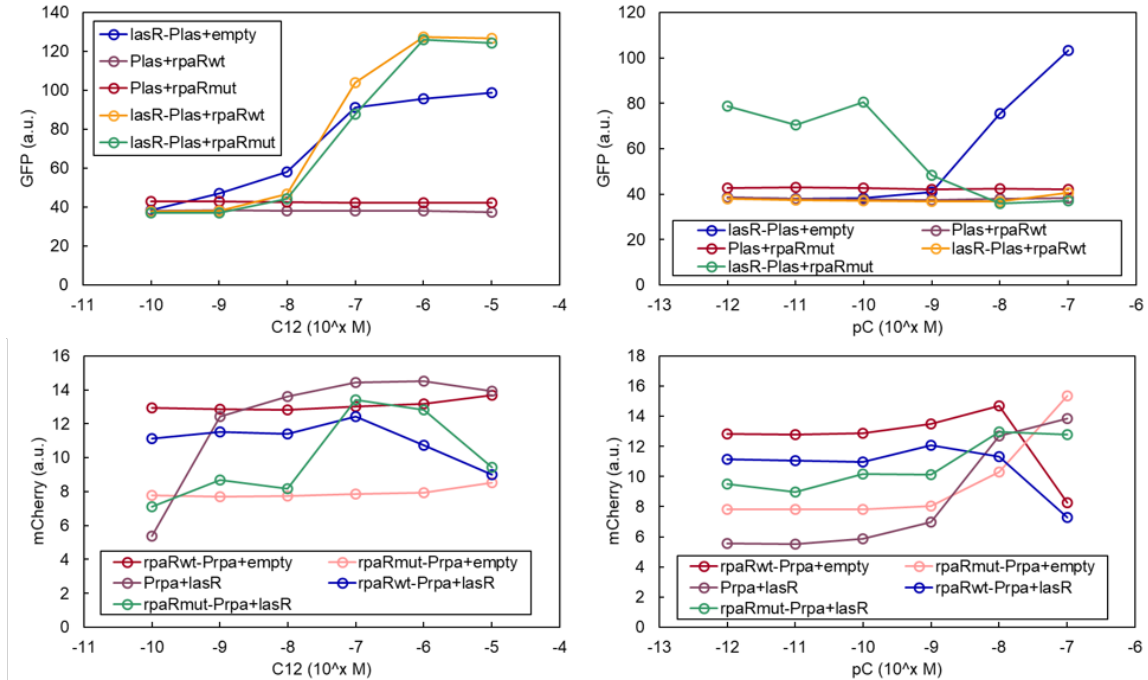f subsets of p15A-lasR and pColE1-rpaR(wt/mut)-Prpa-mCherry co-transformed into MG1655, 24 hr after inoculation. The present R-proteins and promoters are shown in the legend; empty means an empty 15A plasmid containing only the origin of replication and the antibiotic resistance gene.

4.3   Methods

4.3.1   Strains and media

All plasmids were cloned in Stellar Competent Cells from Takara Bio (San Jose, CA). Fluorescence characterization studies were performed in *E. coli* MG1655. All growth and fermentation was done in Luria-Bertani (LB) broth (BD, Franklin Lakes, NJ).

4.3.2   Plasmids used in this study

All plasmids used in this chapter are found in Table 4.1 and in the Prather Lab Strain Database, with sequence files.

4.3.3   Fluorescence measurements

Fluorescence characterization experiments were performed in the BioLector microbioreactor system (m2p-labs GmbH, Baesweiler, Germany). Overnight cultures were grown at 37°C with agitation at 250 rpm. One milliliter cultures were inoculated in BioLector 48-well flower plates at a 1:100 dilution with the appropriate overnight culture. Exogenous AHLS were added at inoculation. The BioLector was set to 37°C, 1200 rpm shake speed, and 85% humidity. Continuous biomass (620 nm excitation), GFP (488 nm excitation, 520 nm emission), and where mentioned, mCherry (550 nm excitation, 610 nm emission), measurements were taken in arbitrary BioLector units over a 24 hr period.

Table 4.1: Plasmids used in this study

Plasmid	Genotype
p15A-luxR-Plux-gfp	luxR under BioFAB104 promoter; GFPmut3b under Plux and RBS0034
p15A-lasR-Plas-gfp	lasR under BioFAB104 promoter; GFPmut3b under Plas and RBS0034
p15A-rpaR(588C>A)-Prpa*-gfp	rpaR(rpaR(588C>A) under BioFAB104 promoter; GFPmut3b under Prpa* and RBS0034
p15A-traR-Ptra*-gfp	traR under BioFAB104 promoter; GFPmut3b under Ptra* and RBS0034
p15A-luxR-Plux-5kRBS-gfp	luxR under BioFAB104 promoter; GFPmut3b under Plux and 5k TIR RBS
p15A-luxR-Plux-10kRBS-gfp	luxR under BioFAB104 promoter; GFPmut3b under Plux and 10k TIR RBS
p15A-lasR-Plas-5kRBS-gfp	lasR under BioFAB104 promoter; GFPmut3b under Plas and 5k TIR RBS
p15A-lasR-Plas-10kRBS-gfp	lasR under BioFAB104 promoter; GFPmut3b under Plas and 10k TIR RBS
p15A-esaR-PesaR-5kRBS-gfp	esaR under BioFAB104 promoter; GFPmut3b under Pesa and 5k TIR RBS
p15A-esaR-PesaR-10kRBS-gfp	esaR under BioFAB104 promoter; GFPmut3b under Pesa and 10k TIR RBS
pMMB206-traI	pMMB206-traI
pColE1-las-GFP+rpa(588C>A)-mCherry	lasR and Plas expressing GFPmut3B and rpaR(588C>A) and Prpa* expressing mCherry
pColE1-las-GFP+lux-mCherry	lasR and Plas expressing GFPmut3B and luxR and Plux expressing mCherry
pColE1-las-GFP+tra-mCherry	lasR and Plas expressing GFPmut3B and traR and Ptra* expressing mCherry
p15A-rpaR-Prpa*-gfp	rpaR under BioFAB104 promoter; GFPmut3b under Prpa* and RBS0034
pColE1-las-GFP+rpa-mCherry	lasR and Plas expressing GFPmut3B and rpaR and Prpa* expressing mCherry
p15A-rpaR-Plas-gfp	rpaR under BioFAB104 promoter; GFPmut3b under Plas
p15A-rpaR(588C>A)-Plas-gfp	rpaR(588C>A) under BioFAB104 promoter; GFPmut3b under Plas
p15A-lasR-Prpa*-gfp	constitutive lasR and GFPmut3b under Prpa* and RBS0034
pColE1-rpaR-lasR-Plas-gfp	constitutive lasR; rpaR under BioFAB104 promoter; GFPmut3b under Plas
pColE1-rpaR(588C>A)-lasR-Plas-gfp	constitutive lasR; rpaR(588C>A) under BioFAB104 promoter; GFPmut3b under Plas
pColE1-rpaR-lasR-Prpa*-gfp	constitutive lasR; rpaR under BioFAB104 promoter; GFPmut3b under Prpa*
pColE1-rpaR(588C>A)-lasR-Prpa*-gfp	constitutive lasR; rpaR(588C>A) under BioFAB104 promoter; GFPmut3b under Prpa*
pColE1-rpaR	rpaR under BioFAB104 promoter
pColE1-rpaR(588C>A)	rpaR(588C>A) under BioFAB104 promoter
pColE1-Prpa*-mCherry	mCherry under Prpa*
p15A-lasR	constitutive lasR
p15A-Plas-gfp	GFPmut3b under Plas
pColE1-rpaR-Prpa*-mCherry	rpaR under BioFAB104 promoter; mCherry under Prpa* and 60k TIR RBS
pColE1-rpaR(588C>A)-Prpa*-mCherry	rpaR(588C>A) under BioFAB104 promoter; mCherry under Prpa* and 60k TIR RBS

4.4 Conclusion

In the work from this chapter, the significant results were (1) constructing a *las-tra* dual QS controller with minimal crosstalk in our hands and (2) establishing a workflow for investigating the interactions between the individual elements of two QS systems. What has emerged from the characterization of many dual QS systems is that crosstalk is extrememly likely between two AHL-based QS systems. This makes sense, as the signaling molecules are very similar, as are the components and mechanism of

the QS systems. Even in instances where orthogonality is achieved, it is only in specific concentrations ranges. These results are in agreement with the literature as well [129]. While the endeavor to construct orthogonal, autonomous QS transcriptional controllers remains valuable for metabolic engineering applications, broadening the search beyond AHL-based systems will increase the likelihood of finding usable pairs. This work is already being undertaken in the Prather lab.

Chapter 5

Conclusions and outlook

5.1 Summary and future directions

In this thesis, we developed biosensors for two substrates that are abundantly present in food waste: galacturonate and gluconate. The transcription factors, *exuR* and *gntR*, respectively, utilized in the biosensors came from *B. subtilis*. We employed the biosensors to activate the expression of novel recombinant pathways for D-glycerate production. The pathways were used for production with single susbtrate feeds, then co-transformed into our selected production strain for mixed substrate feeds.

5.1.1 Biosensor development

The biosensor development work conducted in Chapters 2 and 3 of this thesis can be applied to other substrates and metabolites of interest, especially those that are prevalent in food waste and organic byproduct streams. *E. coli* alone has over 200 reported metabolite-responsive TFs [52, 58]. Our biosensors used *B. subtilis* TFs, demonstrating that importing TFs into our *E. coli* host is an attainable and attractive option. Add to that the options to mutate or combine binding domains for novel TFs [59], there is a massive search space to find or create TFs for any substrate of interest.

When porting over heterologous TFs from other organisms, verifying the expression

in the *E. coli* host is a valuable double check. I encountered many failed biosensors constructs for other substrates and relied on the GFP dose-response as the indicator for biosensor function. In hindsight, it would have been worthwhile to check if the TF was truly being expressed as part of the biosensor construction workflow, especially since there is no consensus on whether or not codon optimization helps or hurts protein expression [135, 136]. Additionally, issues of protein solubility could impact an otherwise functional protein [137].

5.1.2   Increasing the yield of the D-glycerate pathways

While we were able to achieve up to 18-fold improvement in our novel D-glycerate production pathways, the highest molar yields we achieved in flasks at 30°C were 48% and 24%, from galacturonate and gluconate, respectively. We got almost identical results for the galacturonate-fed pathway when culturing in 4 mL working volume in 14 mL tubes at 37°C. However, gluconate-fed tubes cultured at 37°C achieved up to 100% molar yield from our best performing pathway (Figure 5-1). This is most likely due to the pathway enzymes having higher activity at higher temperatures [127, 138]. We observed that gluconate was generally consumed slower in tube fermentations compared to galacturonate. This leads to the hypothesis that imbalanced flux up- and down- stream of the D-glyceraldehyde intermediate leads to diminished molar yield. Given that D-glyceraldehyde is volatile, excess flux that cannot be converted by GadH likely evaporates out of the culture. Preliminary experiments using a dodecane organic cap to trap the volatile compound showed no difference between cultures with and without the cap; at the time those experiments were conducted, there may have been bigger bottlenecks to the pathways, since they were not conducted on the best performing pathway for either substrate.
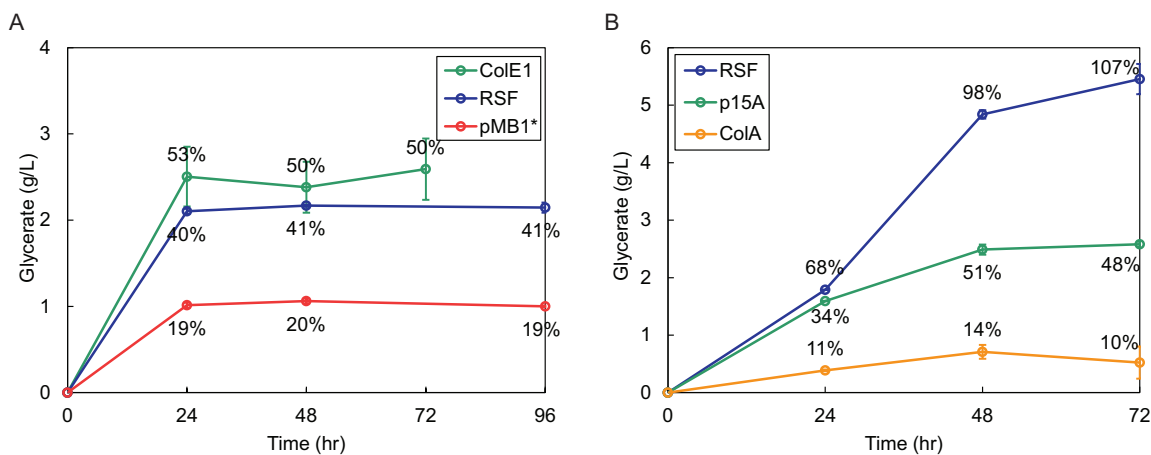
Figure 5-1: D-glycerate production in tubes from 10 g L^{-1} of substrate at 37°C. (A) D-glycerate production from galacturonate. The origins of replication tested were ColE1, RSF, and pMB1* ($\sim$20, $\sim$100, and $\sim$500 copies per cell, respectively). (B) D-glycerate production from gluconate. The origins of replication tested were p15A, ColA, and RSF ($\sim$10, $\sim$20, and $\sim$100 copies per cell, respectively). Data show mean titer $\pm$ 1 SD of biological duplicates; data labels show average molar yield (%)

The flux imbalance hypothesis is further supported by the fact that the two pathways converge on the KDG intermediate. Thus the main difference between the two that could lead to the difference in yields was the rate at which the substrate was consumed. To test this, *uxaC*, the endogenous, first step of the galacturonate-fed pathway could be knocked out and placed on the pathway plasmid at a lower expression strength in an effort to reduce the upstream flux. Similarly, an extra copy of *gadH* could be tested for both pathways.

5.1.3 Scale up of mixed substrate biosynthesis

The full robustness of our mixed substrate production strain has not been demonstrated. Given that these biosensors, in theory, could go for OFF-to-ON and ON-to-OFF, it would be an interesting exploration of functionality to demonstrate the expression and production response to temporally changing substrate concentrations in a bioreactor. This experiment would also more closely mimic a food waste utilization application. A bioreactor could be run for a few days, in which time,

different concentrations of galacturonate, or gluconate, or both could be fed. At regular intervals, samples should be taken for qRT-PCR and HPLC analysis to see if transcription of the appropriate pathway(s) is taking place and how production is impacted by the feeding schedule. A non-coding DNA sequence could be added to the galacturonate pathway operon to distinguish it for qRT-PCR analysis since the entirety of the pathway is included in the gluconate pathway.

5.2 Outlook

5.2.1 Waste stream specific production strains

At the start of this thesis project, general residential food waste was the targeted feed stream. Thus, a wide net was cast to develop biosensors for multiple compounds found in food waste. While food waste is an abundant source of carbon and nutrients for microbial production processes, it is a big jump from the defined, pure feed streams used for biosyntheses, and the complex, variable nature of food waste. A middle ground that could be employed for biosynthesis are waste or byproduct streams with a smaller number of compounds compared to general food waste, such as whey from the dairy industry that primarily contains lactose [139], or the pectin from orange peel waste specifically, that contains mostly galacturonate and arabinose [93]. Constructing a production strain and biosynthetic pathway(s) specific to one of these waste streams would result in a more tailored organism that could carry out production in a more effective manner. The work in this thesis developed a proof of concept for designing a production strain that can utilize a highly diverse waste stream as a feed; future work should focus on waste streams with fewer potential substrates to convert into a product for higher yield of the biosynthetic process.

5.2.2 Construction of an autonomously regulated production strain encoding substrate activated biosynthesis

Given the numerous dynamic control tools that use a wide array of stimuli to actuate, an autonomous production strain could be engineered for minimal required user involvement. Such an organism would be one part of a process that takes in a waste stream and outputs a product of interest. The conversion of the bulk waste into the monomeric substrates could be performed by existing technologies such as degradation by anaerobic fungi [140]. The waste input may be batch fed, as is done with household- or municipal- scale compost. Thus, it would be advantageous for the production strain to be engineered to respond to both cell density and substrate availability, by using QS and biosensor genetic circuits to control pathway expression. This could be achieved by engineering AND-gates, in which the QS element must be activated in the presence of the cognate substrate of the biosensor for the strain to begin transcription of the recombinent biosynthetic pathway. More complex genetic logic gates could be explored for specific applications. Such logic gates were constructed by Moser et al. [141] to control expression in response to glucose feedstock consumption, dissolved oxygen, and acetate by-product accumulation; logic gates were used to knock down endogenous genes responsible for acetate production at the relevant points of a batch fermentation. The resulting organism could grow in response to available carbon and nutrients, and begin expressing pathway genes when the cells reach sufficient density and the pathway's cognate substrate is present. For further stability in the imagined process, synthetic auxotrophic elements could be engineered into the co-culture organism to ensure the continued growth of the fungi and production strain, as has been done in the past [142, 143]. Specified, synthetic, interaction modes between co-culture and consortium members have been engineered by Kong et al. [144].

5.2.3 Incentivization of waste stream use for biosynthesis

Research exploring ways to utilize waste streams for biosynthesis, or other applications, is important; I believe this to be true even outside the fact that it was a motivation for this thesis. Moving towards a more sustainable society will require technological innovations such as these, however the technology alone is necessary but not sufficient. Funding, including federal funding, is critical to sustain research and allow for new avenues of research to be explored [145]. Supportive policy is needed, not only to sustain the research, but to develop such technologies beyond labs. Especially if we hope to see innovations deployed at societally relevant scales, they must first bridge the so-called "valley of death" between scientific research and commercialization [146]. Not only is the availability of funding important, social factors such as public and governmental support can aid in the crossing of this bridge as well [147]. In a, hopefully one day usable in a bioprocess, nutshell, the joint push of technology and policy in support of sustainable biosynthesis is required for the longevity and applicability of the technology. The policy and funding side will be critical to continue to incentivize such work, both academically and societally.

References

[1] Alon Zaslaver, Avi E Mayo, Revital Rosenberg, Pnina Bashkin, Hila Sberro, Miri Tsalyuk, Michael G Surette, and Uri Alon. Just-in-time transcription program in metabolic pathways. *Nature Genetics*, 36(5):486–491, 2004.

[2] Kapil G Gadkar, Francis J Doyle Iii, Jeremy S Edwards, and Radhakrishnan Mahadevan. Estimating Optimal Profiles of Genetic Alterations Using Constraint-Based Models. *Biotechnology and Bioengineering*, 89(2):243–251, 2004.

[3] Nikolaos Anesiadis, William R Cluett, and Radhakrishnan Mahadevan. Dynamic metabolic engineering for increasing bioprocess productivity. *Metabolic Engineering*, 10(5):255–266, 2008.

[4] Nikolaos Anesiadis, Hideki Kobayashi, William R Cluett, and Radhakrishnan Mahadevan. Analysis and Design of a Genetic Circuit for Dynamic Metabolic Engineering. *ACS Synthetic Biology*, (2):442–452, 2013.

[5] François Jacob and Jacques Monod. Genetic regulatory mechanisms in the synthesis of proteins. *Journal of Molecular Biology*, 3(3):318–356, 1961.

[6] Yasumi Ohshima, Michiko Matsuura, and Tadao Horiuchi. Conformational change of the lac repressor induced with the inducer. *Biochemical and Biophysical Research Communications*, 47(6):1444–1450, 1972.

[7] Benno Müller-Hill. Lac repressor and Lac operator. *Progress in Biophysics and Molecular Biology*, 30:227–252, 1976.

[8] H L Yang, G Zubay, and S B Levy. Synthesis of an R plasmid protein associated with tetracycline resistance is negatively regulated. *Proceedings of the National Academy of Sciences*, 73(5):1509 LP–1512, 5 1976.

[9] U Deuschle, R Gentz, and H Bujard. lac Repressor blocks transcribing RNA polymerase and terminates transcription. *Proceedings of the National Academy of Sciences*, 83(12):4134 LP–4137, 6 1986.

[10] Laurie D Smith and Kevin P Bertrand. Mutations in the Tn10 tet represser that

interfere with induction: Location of the tetracycline-binding domain. *Journal of Molecular Biology*, 203(4):949–959, 1988.

[11] U Deuschle, R A Hipskind, and H Bujard. RNA polymerase II transcription blocked by Escherichia coli lac repressor. *Science*, 248(4954):480 LP–483, 4 1990.

[12] J Degenkolb, M Takahashi, G A Ellestad, and W Hillen. Structural requirements of tetracycline-Tet repressor interaction: determination of equilibrium binding constants for tetracycline analogs with the Tet repressor. *Antimicrobial Agents and Chemotherapy*, 35(8):1591 LP–1595, 8 1991.

[13] Cynthia H Collins, Jared R Leadbetter, and Frances H Arnold. Dual selection enhances the signaling specificity of a variant of the quorum-sensing transcriptional activator LuxR. *Nature Biotechnology*, 24(6):708–712, 2006.

[14] Adam J Meyer, Thomas H Segall-Shapiro, Emerson Glassey, Jing Zhang, and Christopher A Voigt. Escherichia coli Marionette strains with 12 highly optimized small-molecule sensors. *Nature Chemical Biology*, 15(2):196–204, 2019.

[15] Timothy S. Gardner, Charles R. Cantor, and James J. Collins. Construction of a genetic toggle switch in Escherichia coli. *Nature*, 403(6767):339–342, 1 2000.

[16] William Bothfeld, Grace Kapov, and Keith E J Tyo. A Glucose-Sensing Toggle Switch for Autonomous, High Productivity Genetic Control. *ACS Synthetic Biology*, 6(7):1296–1304, 2017.

[17] Naveen Venayak, Kaushik Raj, Rohil Jaydeep, and Radhakrishnan Mahadevan. An Optimized Bistable Metabolic Switch To Decouple Phenotypic States during Anaerobic Fermentation. *ACS Synthetic Biology*, 7(12):2854–2866, 12 2018.

[18] Valdemir M. Cardoso, Gilson Campani, Maurício P. Santos, Gabriel G. Silva, Manuella C. Pires, Viviane M. Gonçalves, Roberto de C. Giordano, Cíntia R. Sargo, Antônio C.L. Horta, and Teresa C. Zangirolami. Cost analysis based on bioreactor cultivation conditions: Production of a soluble recombinant protein using Escherichia coli BL21(DE3). *Biotechnology Reports*, 26:e00441, 6 2020.

[19] Margaret Lieb. Studies of heat-inducible lambda bacteriophage: I. Order of genetic sites and properties of mutant prophages. *Journal of Molecular Biology*, 16(1):149–163, 1966.

[20] Erik Remaut, Patrick Stanssens, and Walter Fiers. Plasmid vectors for high-efficiency expression controlled by the PL promoter of coliphage lambda. *Gene*, 15(1):81–93, 1981.

[21] Han Saem Cho, Sang Woo Seo, Young Mi Kim, Gyoo Yeol Jung, and Jong Moon

Park. Engineering glyceraldehyde-3-phosphate dehydrogenase for switching control of glycolysis in escherichia coli. *Biotechnology and Bioengineering*, 109(10):2612–2619, 2012.

[22] Björn-Johannes Harder, Katja Bettenbrock, and Steffen Klamt. Temperature-dependent dynamic control of the TCA cycle increases volumetric productivity of itaconic acid production by <i>Escherichia coli</i>. *Biotechnology and Bioengineering*, (May):1–9, 2017.

[23] Elke Nevoigt, Curt Fischer, Oliver Mucha, Falk Matthaus, Ulf Stahl, and Gregory Stephanopoulos. Engineering Promoter Regulation. *Biotechnology and Bioengineering*, 96(3):550–558, 2006.

[24] Xian Yin, Hyun-Dong Shin, Jianghua Li, Guocheng Du, Long Liu, and Jian Chen. Pgas, a Low-pH-Induced Promoter, as a Tool for Dynamic Control of Gene Expression for Metabolic Engineering of Aspergillus niger. *Applied and Environmental Microbiology*, 83(6):03222–16, 3 2017.

[25] Wenping Xie, Lidan Ye, Xiaomei Lv, Haoming Xu, and Hongwei Yu. Sequential control of biosynthetic pathways for balanced utilization of metabolic intermediates in Saccharomyces cerevisiae, 2015.

[26] Romel MenachoMelgar, Eirik A. Moreb, John P. Efromson, Tian Yang, Jennifer N. Hennigan, Ruixin Wang, and Michael D. Lynch. Improved twostage protein expression and purification via autoinduction of both autolysis and auto DNA/RNA hydrolysis conferred by phage lysozyme and DNA/RNA endonuclease. *Biotechnology and Bioengineering*, 117(9):2852–2860, 9 2020.

[27] Tat Ming Lo, Si Hui Chng, Wei Suong Teo, Han Saem Cho, and Matthew Wook Chang. A Two-Layer Gene Circuit for Decoupling Cell Growth from Metabolite Production. *Cell Systems*, 3(2):133–143, 2016.

[28] Eirik Adim Moreb, Zhixia Ye, John P. Efromson, Jennifer N. Hennigan, Romel Menacho-Melgar, and Michael D. Lynch. Media Robustness and Scalability of Phosphate Regulated Promoters Useful for Two-Stage Autoinduction in E.ǎcoli. *ACS synthetic biology*, 9(6):1483–1486, 2020.

[29] Apoorv Gupta, Irene M.Brockman Reizman, Christopher R. Reisch, and Kristala L.J. Prather. Dynamic regulation of metabolic flux in engineered bacteria using a pathway-independent quorum-sensing circuit. *Nature Biotechnology*, 35(3):273–279, 3 2017.

[30] Christina V. Dinh and Kristala L.J. Prather. Development of an autonomous and bifunctional quorum-sensing circuit for metabolic flux control in engineered Escherichia coli. *Proceedings of the National Academy of Sciences of the United States of America*, 116(51):25562–25568, 12 2019.

[31] Jianshen Hou, Cong Gao, Liang Guo, Jens Nielsen, Qiang Ding, Wenxiu Tang, Guipeng Hu, Xiulai Chen, and Liming Liu. Rewiring carbon flux in Escherichia coli using a bifunctional molecular switch. *Metabolic Engineering*, 61:47–57, 2020.

[32] A Eberhard, A L Burlingame, C Eberhard, G L Kenyon, K H Nealson, and N J Oppenheimer. Structural identification of autoinducer of Photobacterium fischeri luciferase. *Biochemistry*, 20(9):2444–2449, 4 1981.

[33] J G Cao and E A Meighen. Purification and structural identification of an autoinducer for the luminescence system of Vibrio harveyi. *Journal of Biological Chemistry*, 264(36):21670–21676, 1989.

[34] J P Pearson, K M Gray, L Passador, K D Tucker, A Eberhard, B H Iglewski, and E P Greenberg. Structure of the autoinducer required for expression of Pseudomonas aeruginosa virulence genes. *Proceedings of the National Academy of Sciences of the United States of America*, 91(1):197–201, 1 1994.

[35] J Engebrecht and M Silverman. Identification of genes and gene products necessary for bacterial bioluminescence. *Proceedings of the National Academy of Sciences of the United States of America*, 81(13):4154–4158, 7 1984.

[36] B L Hanzelka and E P Greenberg. Evidence that the N-terminal region of the Vibrio fischeri LuxR protein constitutes an autoinducer-binding domain. *Journal of bacteriology*, 177(3):815–817, 2 1995.

[37] Joanne Engebrecht, Kenneth Nealson, and Michael Silverman. Bacterial bioluminescence: Isolation and genetic analysis of functions from Vibrio fischeri. *Cell*, 32(3):773–781, 1983.

[38] U A Ochsner and J Reiser. Autoinducer-mediated regulation of rhamnolipid biosurfactant synthesis in Pseudomonas aeruginosa. *Proceedings of the National Academy of Sciences of the United States of America*, 92(14):6424–6428, 7 1995.

[39] Yuki Soma and Taizo Hanai. Self-induced metabolic state switching by a tunable cell density sensor for microbial isopropanol production. *Metabolic Engineering*, 30:7–15, 2015.

[40] Eun-Mi Kim, Han Min Woo, Tian Tian, Suzan Yilmaz, Pouya Javidpour, Jay D Keasling, and Taek Soon Lee. Autonomous control of metabolic state by a quorum sensing (QS)-mediated regulator for bisabolene production in engineered E. coli. *Metabolic Engineering*, 44(July):325–336, 2017.

[41] Chen Yu Tsao, Sara Hooshangi, Hsuan Chen Wu, James J. Valdes, and William E. Bentley. Autonomous induction of recombinant proteins by minimally rewiring native quorum sensing regulon of E. coli. *Metabolic Engineering*, 12(3):291–297, 5 2010.

[42] Ming-Tang Chen and Ron Weiss. Artificial cell-cell communication in yeast Saccharomyces cerevisiae using signaling elements from Arabidopsis thaliana. *Nature Biotechnology*, 23(12):1551–1555, 2005.

[43] Thomas C Williams, Lars K Nielsen, and Claudia E Vickers. Engineered Quorum Sensing Using Pheromone-Mediated Cell-to-Cell Communication in Saccharomyces cerevisiae. *ACS Synthetic Biology*, 2(3):136–149, 3 2013.

[44] W R Farmer and J C Liao. Improving lycopene production in Escherichia coli by engineering metabolic control. *Nature biotechnology*, 18(5):533–537, 2000.

[45] Peng Xu, Wenya Wang, Lingyun Li, Namita Bhan, Fuming Zhang, and Mattheos a G Koffas. Design and kinetic analysis of a hybrid promoter-regulator system for malonyl-CoA sensing in E. coli Design and kinetic analysis of a hybrid promoter-regulator system for malonyl-CoA sensing in E . coli. *ACS Chemical Biology*, 9:451–458, 2014.

[46] Peng Xu, Lingyun Li, Fuming Zhang, Gregory Stephanopoulos, and Mattheos Koffas. Improving fatty acids production by engineering dynamic pathway regulation and metabolic control. *Proceedings of the National Academy of Sciences*, 111(31):11299–11304, 2014.

[47] Fuzhong Zhang, James M Carothers, and Jay D Keasling. Design of a dynamic sensor-regulator system for production of chemicals and fuels derived from fatty acids. *Nature Biotechnology*, 30(4):354–359, 3 2012.

[48] Stephanie J. Doong, Apoorv Gupta, and Kristala L.J. Prather. Layered dynamic regulation for improving metabolic pathway productivity in Escherichia coli. *Proceedings of the National Academy of Sciences of the United States of America*, 115(12):2964–2969, 3 2018.

[49] Jay D. Gralla. Transcriptional controlLessons from an E. coli promoter data base. *Cell*, 66(3):415–418, 8 1991.

[50] M Lanzer and H Bujard. Promoters largely determine the efficiency of repressor action. *Proceedings of the National Academy of Sciences of the United States of America*, 85(23):8973–7, 12 1988.

[51] K S Matthews and J C Nichols. Lactose repressor protein: functional properties and structure. *Progress in nucleic acid research and molecular biology*, 58:127–64, 1998.

[52] Martin Lempp, Niklas Farke, Michelle Kuntz, Sven Andreas Freibert, Roland Lill, and Hannes Link. Systematic identification of metabolites controlling gene expression in E. coli. *Nature Communications*, 10(1):1–9, 12 2019.

[53] Jason R. Kelly, Adam J. Rubin, Joseph H. Davis, Caroline M. Ajo-Franklin,

John Cumbers, Michael J. Czar, Kim de Mora, Aaron L. Glieberman, Dileep D. Monie, and Drew Endy. Measuring the activity of BioBrick promoters using an in vivo reference standard. *Journal of Biological Engineering*, 3(1):4, 4 2009.

[54] Joseph H. Davis, Adam J. Rubin, and Robert T. Sauer. Design, construction and characterization of a set of insulated bacterial promoters. *Nucleic Acids Research*, 39(3):1131–1141, 2011.

[55] Karin Hammer, Ivan Mijakovic, and Peter Ruhdal Jensen. Synthetic promoter libraries - Tuning of gene expression, 2006.

[56] J. Collado-Vides, B. Magasanik, and J. D. Gralla. Control site location and transcriptional regulation in Escherichia coli. *Microbiological Reviews*, 55(3):371–394, 9 1991.

[57] Robert Sidney Cox, Michael G Surette, Michael B Elowitz, and Michael B Elowitz. Programming gene expression with combinatorial promoters. *Molecular systems biology*, 3:145, 2007.

[58] Stephan Binder, Georg Schendzielorz, Norma Stäbler, Karin Krumbach, Kristina Hoffmann, Michael Bott, and Lothar Eggeling. A high-throughput approach to identify genomic variants of bacterial metabolite producers at the single-cell level. *Genome Biology*, 13(5):R40, 5 2012.

[59] Noah D Taylor, Alexander S Garruss, Rocco Moretti, Sum Chan, Mark Arbing, Duilio Cascio, Jameson K Rogers, Farren J Isaacs, Sriram Kosuri, David Baker, Stanley Fields, George M Church, and Srivatsan Raman. Engineering an allosteric transcription factor to respond to new ligands. *Nature methods*, In press(december), 2016.

[60] Clement T Y Chan, Jeong Wook Lee, D Ewen Cameron, Caleb J Bashor, and James J Collins. 'Deadman' and 'Passcode' microbial kill switches for bacterial containment. *Nature Chemical Biology*, 12(2):82–86, 12 2015.

[61] Andrew K D Younger, Neil C Dalvie, Austin G Rottinghaus, and Joshua N Leonard. Engineering Modular Biosensors to Confer Metabolite-Responsive Regulation of Transcription. *ACS Synthetic Biology*, 6(2):311–325, 2 2017.

[62] S. Tabor and C. C. Richardson. A bacteriophage T7 RNA polymerase/promoter system for controlled exclusive expression of specific genes. *Proceedings of the National Academy of Sciences of the United States of America*, 82(4):1074–1078, 2 1985.

[63] Li Zhou, Dan Dan Niu, Kang Ming Tian, Xian Zhong Chen, Bernard A. Prior, Wei Shen, Gui Yang Shi, Suren Singh, and Zheng Xiang Wang. Genetically switched d-lactate production in Escherichia coli. *Metabolic Engineering*, 14(5):560–568, 9 2012.

[64] Yuki Soma, Keigo Tsuruno, Masaru Wada, Atsushi Yokota, and Taizo Hanai. Metabolic flux redirection from a central metabolic pathway toward a synthetic pathway using a metabolic toggle switch. *Metabolic Engineering*, 23:175–184, 2014.

[65] Melissa B. Miller and Bonnie L. Bassler. Quorum Sensing in Bacteria. *Annual Review of Microbiology*, 55(1):165–199, 10 2001.

[66] Xinyuan He, Yan Chen, Quanfeng Liang, and Qingsheng Qi. Autoinduced AND Gate Controls Metabolic Pathway Dynamically in Response to Microbial Communities and Cell Physiological State. *ACS Synthetic Biology*, 6(3):463–470, 2017.

[67] William E. Bentley, Noushin Mirjalili, Dana C. Andersen, Robert H. Davis, and Dhinakar S. Kompala. Plasmid-encoded protein: The principal factor in the metabolic burden associated with recombinant bacteria. *Biotechnology and Bioengineering*, 35(7):668–681, 3 1990.

[68] Bernard R. Glick. Metabolic load and heterologous gene expression. *Biotechnology Advances*, 13(2):247–261, 1995.

[69] P. K.R. Kumar, H. E. Maschke, K. Friehs, and K. Schügerl. Strategies for improving plasmid stability in genetically modified bacteria in bioreactors. *Trends in Biotechnology*, 9(1):279–284, 1991.

[70] R. S. Donovan, C. W. Robinson, and B. R. Click. Review: Optimizing inducer and culture conditions for expression of foreign proteins under the control of the lac promoter, 1996.

[71] Savvas C Makrides. Strategies for Achieving High-Level Expression of Genes in Escherichia coli . Technical Report 3, 1996.

[72] Joan Miret, Ramón Román, Mario Benito, Antoni Casablancas, Marina Guillén, Gregorio Álvaro, and Glòria González. Development of a highly efficient production process for recombinant protein expression in Escherichia coli NEB10β. *Biochemical Engineering Journal*, page 107612, 4 2020.

[73] Luz-Maria Guzman, Dominique Belin, Michael J Carson, and Jon Beckwith. Tight Regulation, Modulation, and High-Level Expression by Vectors Containing the Arabinose P BAD Promoter. *JOURNAL OF BACTERIOLOGY*, 177(14):4121–4130, 1995.

[74] Germán L. Rosano and Eduardo A. Ceccarelli. Recombinant protein expression in Escherichia coli: Advances and challenges. *Frontiers in Microbiology*, 5(APR), 2014.

[75] F. William Studier. Stable expression clones and auto-induction for protein production in E. Coli. *Methods in Molecular Biology*, 1091:17–32, 2014.

[76] P. Neubauer, K. Hofmann, O. Holst, B. Mattiasson, and P. Kruschke. Maximizing the expression of a recombinant gene in Escherichia coli by manipulation of induction time using lactose as inducer. *Applied Microbiology and Biotechnology*, 36(6):739–744, 3 1992.

[77] Hugo G. Menzella and Hugo C. Gramajo. Recombinant Protein Production in High Cell Density Cultures of Escherichia coli with Galactose as a Gratuitous Inducer. *Biotechnology Progress*, 20(4):1263–1266, 1 2004.

[78] James P. Wynn, Robert Hanchar, Susanne Kleff, David Senyk, and Tonya Tiedje. Biobased technology commercialization: The importance of lab to pilot scale-up. In *Metabolic Engineering for Bioprocess Commercialization*, pages 101–119. Springer International Publishing, 1 2016.

[79] Anthony Burgard, Mark J. Burk, Robin Osterhout, Stephen Van Dien, and Harry Yim. Development of a commercial scale process for production of 1,4-butanediol from sugar, 12 2016.

[80] Matthew Hirsch and Thomas Elliott. Stationary-phase regulation of RpoS translation in Escherichia coli. *Journal of Bacteriology*, 187(21):7204–7213, 11 2005.

[81] Quanfeng Liang, Haojun Zhang, Shengnan Li, and Qingsheng Qi. Construction of stress-induced metabolic pathway from glucose to 1,3-propanediol in Escherichia coli. *Applied Microbiology and Biotechnology*, 89(1):57–62, 2011.

[82] Robert H Dahl, Fuzhong Zhang, Jorge Alonso-Gutierrez, Edward Baidoo, Tanveer S Batth, Alyssa M Redding-Johanson, Christopher J Petzold, Aindrila Mukhopadhyay, Taek Soon Lee, Paul D Adams, and Jay D Keasling. Engineering dynamic pathway regulation using stress-response promoters. *Nature Biotechnology*, 31(11):1039–1046, 2013.

[83] Frank Delvigne, Alison Brognaux, Nathalie Gorret, Peter Neubauer, Angélique Delafosse, Marie Laure Collignon, Dominique Toye, Michel Crine, Mathieu Boxus, and Philippe Thonart. Characterization of the response of GFP microbial biosensors sensitive to substrate limitation in scale-down bioreactors. *Biochemical Engineering Journal*, 55(2):131–139, 7 2011.

[84] John M. Leavitt, James M. Wagner, Cuong C. Tu, Alice Tong, Yanyi Liu, and Hal S. Alper. Biosensor-Enabled Directed Evolution to Improve Muconic Acid Production in <i>Saccharomyces cerevisiae</i>. *Biotechnology Journal*, 12(10):1600687, 10 2017.

[85] Stephanie J Doong, Apoorv Gupta, and Kristala L J Prather. Layered dynamic

regulation for improving metabolic pathway productivity in Escherichia coli. *Proceedings of the National Academy of Sciences*, 115(12):2964–2969, 2018.

[86] Di Liu, Trent Evans, and Fuzhong Zhang. Applications and advances of metabolite biosensors for metabolic engineering. *Metabolic engineering*, 31:35–43, 2015.

[87] Ahmad A. Mannan, Di Liu, Fuzhong Zhang, and Diego A. Oyarzún. Fundamental Design Principles for Transcription-Factor-Based Metabolite Biosensors. *ACS Synthetic Biology*, 6(10):1851–1859, 10 2017.

[88] Ye Chen, Joanne M.L. Ho, David L. Shis, Chinmaya Gupta, James Long, Daniel S. Wagner, William Ott, Kreimir Josić, and Matthew R. Bennett. Tuning the dynamic range of bacterial promoters regulated by ligand-inducible transcription factors. *Nature Communications*, 9(1), 12 2018.

[89] Heykel Trabelsi, Mathilde Koch, and JeanLoup Faulon. Building a minimal and generalizable model of transcription factorbased biosensors: Showcasing flavonoids. *Biotechnology and Bioengineering*, 115(9):2292–2304, 9 2018.

[90] Sarah Meinhardt, Michael W Manley, Nicole A Becker, Jacob A Hessman, L James Maher, and Liskin Swint-Kruse. Novel insights from hybrid LacI/GalR proteins: family-wide functional attributes and biologically significant variation in transcription repression. *Nucleic acids research*, 40(21):11139–54, 11 2012.

[91] Kevin J. Fox and Kristala L.J. Prather. Production of d-Glyceric acid from d-Galacturonate in Escherichia coli. *Journal of Industrial Microbiology and Biotechnology*, pages 1–7, 10 2020.

[92] Hiroshi Habe, Tokuma Fukuoka, Dai Kitamoto, and Keiji Sakaki. Biotechnological production of d-glyceric acid and its application, 9 2009.

[93] Judith Müller-Maatsch, Mariangela Bencivenni, Augusta Caligiani, Tullia Tedeschi, Geert Bruggeman, Montse Bosch, Janos Petrusan, Bart Van Droogenbroeck, Kathy Elst, and Stefano Sforza. Pectin content and composition from different food waste streams. *Food Chemistry*, 201:37–45, 6 2016.

[94] Peter Richard and Satu Hilditch. D-Galacturonic acid catabolism in microorganisms and its biotechnological relevance. *Applied Microbiology and Biotechnology*, 82(4):597–604, 3 2009.

[95] Ryan J. Protzko, Luke N. Latimer, Ze Martinho, Elise de Reus, Tanja Seibert, J. Philipp Benz, and John E. Dueber. Engineering Saccharomyces cerevisiae for co-utilization of d-galacturonic acid and d-glucose from citrus peel waste. *Nature Communications*, 9(1):1–10, 12 2018.

[96] Alessandra Biz, Maura Harumi Sugai-Guérios, Joosu Kuivanen, Hannu Maaheimo, Nadia Krieger, David Alexander Mitchell, and Peter Richard. The introduction of the fungal d-galacturonate pathway enables the consumption of d-galacturonic acid by Saccharomyces cerevisiae. *Microbial Cell Factories*, 15(1):144, 8 2016.

[97] Laura C. Valk, Jeroen Frank, Pilar de la Torre-Cortés, Max van 't Hof, Antonius J.A. van Maris, Jack T. Pronk, and Mark C.M. van Loosdrecht. Galacturonate metabolism in anaerobic chemostat enrichment cultures: Combined fermentation and acetogenesis by the dominant sp. nov. "Candidatus Galacturonibacter soehngenii.". *Applied and Environmental Microbiology*, 84(18), 9 2018.

[98] K R Mekjian, E M Bryan, B W Beall, and C P Moran. Regulation of hexuronate utilization in Bacillus subtilis. *Journal of bacteriology*, 181(2):426–33, 1 1999.

[99] Tomoya Baba, Takeshi Ara, Miki Hasegawa, Yuki Takai, Yoshiko Okumura, Miki Baba, Kirill A. Datsenko, Masaru Tomita, Barry L. Wanner, and Hirotada Mori. Construction of Escherichia coli K-12 in-frame, single-gene knockout mutants: The Keio collection. *Molecular Systems Biology*, 2:2006.0008, 5 2006.

[100] K. A. Datsenko and B. L. Wanner. One-step inactivation of chromosomal genes in Escherichia coli K-12 using PCR products. *Proceedings of the National Academy of Sciences*, 97(12):6640–6645, 6 2000.

[101] Michael E. Lee, William C. DeLoache, Bernardo Cervantes, and John E. Dueber. A Highly Characterized Yeast Toolkit for Modular, Multipart Assembly. *ACS Synthetic Biology*, 4(9):975–986, 2015.

[102] Registry of Standard Biological Parts.

[103] Dmitry A. Rodionov, Andrey A. Mironov, Alexandra B. Rakhmaninova, and Mikhail S. Gelfand. Transcriptional regulation of transport and utilization systems for hexuronides, hexuronates and hexonates in gamma purple bacteria. *Molecular Microbiology*, 38(4):673–683, 11 2000.

[104] K R Mekjian, E M Bryan, B W Beall, C P Moran, and Jr. Regulation of hexuronate utilization in Bacillus subtilis. *Journal of bacteriology*, 181(2):426–33, 1 1999.

[105] John R Sadler, Henri Sasmor, and Joan L Betzt. A perfectly symmetric lac operator binds the lac repressor very tightly (palindrome/protein-DNA interaction). *Biochemistry*, 80:6785–6789, 1983.

[106] RBS Calculator - De Novo DNA.

[107] Howard M Salis, Ethan A Mirsky, and Christopher A Voigt. Automated

design of synthetic ribosome binding sites to control protein expression. *Nature biotechnology*, 27(10):946–50, 10 2009.

[108] R Portalier, J Robert-Baudouy, and F Stoeber. Regulation of Escherichia coli K-12 hexuronate system genes: exu regulon. *Journal of bacteriology*, 143(3):1095–107, 9 1980.

[109] Maria N Tutukina, Anna V Potapova, Jeffrey A Cole, and Olga N Ozoline. Control of hexuronate metabolism in Escherichia coli by the two interdependent regulators, ExuR and UxuR: derepression by heterodimer formation. *Microbiology*, 162(7):1220–1231, 7 2016.

[110] Stefan Klumpp, Zhongge Zhang, and Terence Hwa. Growth Rate-Dependent Global Effects on Gene Expression in Bacteria. *Cell*, 139(7):1366–1375, 12 2009.

[111] Alessandra Procentese, Francesca Raganati, Giuseppe Olivieri, Maria Elena Russo, Marco de la Feld, and Antonio Marzocchella. Renewable feedstocks for biobutanol production by fermentation. *New Biotechnology*, 39:135–140, 10 2017.

[112] Karl Rumbold, Hugo J.J. van Buijsen, Karin M. Overkamp, Johan W. van Groenestijn, Peter J. Punt, and Mariët J.V.D. Werf. Microbial production host selection for converting second-generation feedstocks into bioproducts. *Microbial Cell Factories*, 8:64, 12 2009.

[113] Sumitra Ramachandran, Pierre Fontanille, Ashok Pandey, and Christian Larroche. Gluconic acid: Properties, applications and microbial production. *Food Technology and Biotechnology*, 44(2):185–195, 2006.

[114] Esra Uçkun Kiran, Antoine P. Trzcinski, Wun Jern Ng, and Yu Liu. Bioconversion of food waste to energy: A review. *Fuel*, 134:389–399, 10 2014.

[115] Sang Yup Lee, Hyun Uk Kim, Tong Un Chae, Jae Sung Cho, Je Woong Kim, Jae Ho Shin, Dong In Kim, Yoo Sung Ko, Woo Dae Jang, and Yu Sin Jang. A comprehensive metabolic map for production of bio-based chemicals. *Nature Catalysis 2019 2:1*, 2(1):18–33, 1 2019.

[116] Junichi Mano, Nian Liu, John H. Hammond, Devin H. Currie, and Gregory Stephanopoulos. Engineering Yarrowia lipolytica for the utilization of acid whey. *Metabolic Engineering*, 57:43–50, 1 2020.

[117] Theresah N.K. Zu, Sanchao Liu, Elliot S. Gerlach, Wais Mojadedi, and Christian J. Sund. Co-feeding glucose with either gluconate or galacturonate during clostridial fermentations provides metabolic fine-tuning capabilities. *Scientific Reports*, 11(1):29, 12 2021.

[118] Zhi Peng Wang, Xin Yue Zhang, Yan Ma, Jing Run Ye, Jing Jiang, Hai Ying

Wang, and Wei Chen. Whole conversion of agro-industrial wastes rich in galactose-based carbohydrates into lipid using oleaginous yeast Aureobasidium namibiae. *Biotechnology for Biofuels*, 14(1):1–11, 12 2021.

[119] Peter Dürre and Bernhard J. Eikmanns. C1-carbon sources for chemical and fuel production by microbial gas fermentation. *Current Opinion in Biotechnology*, 35:63–72, 12 2015.

[120] Cynthia Ni, Kevin J. Fox, and Kristala L.J. Prather. Substrate-activated expression of a biosynthetic pathway in Escherichia coli. *Biotechnology Journal*, 17(3):2000433, 3 2022.

[121] Y. Fujita, T. Fujita, Y. Miwa, J. Nihashi, and Y. Aratani. Organization of transcription of the gluconate operon, gnt, of Bacillus subtilis. *Journal of Biological Chemistry*, 261(29):13744–13753, 10 1986.

[122] Y. Fujita and T. Fujita. The gluconate operon gnt of Bacillus subtilis encodes its own transcriptional negative regulator. *Proceedings of the National Academy of Sciences of the United States of America*, 84(13):4524–4528, 1987.

[123] Y Fujita and Y Miwa. Identification of an operator sequence for the Bacillus subtilis gnt operon. *The Journal of biological chemistry*, 264(7):4201–6, 3 1989.

[124] Hatim Ahmed, Thijs J.G. Ettema, Britta Tjaden, Ans C.M. Geerling, John Van Der Oost, and Bettina Siebers. The semi-phosphorylative Entner-Doudoroff pathway in hyperthermophilic archaea: A re-evaluation. *Biochemical Journal*, 390(2):529–540, 9 2005.

[125] C L Buchanan, H Connaris, M J Danson, C D Reeve, and D W Hough. An extremely thermostable aldolase from Sulfolobus solfataricus with specificity for non-phosphorylated substrates. *The Biochemical journal*, 343 Pt 3(Pt 3):563–70, 11 1999.

[126] Iuliia Iermak, Oksana Degtjarik, Fabian Steffler, Volker Sieber, and Ivana Kuta Smatanova. Crystallization behaviour of glyceraldehyde dehydrogenase from Thermoplasma acidophilum. *Acta crystallographica. Section F, Structural biology communications*, 71(Pt 12):1475–80, 12 2015.

[127] Seonghun Kim and Sun Bok Lee. Identification and characterization of the bacterial d-gluconate dehydratase in Achromobacter xylosoxidans. *Biotechnology and Bioprocess Engineering*, 13(4):436–444, 9 2008.

[128] Apoorv Gupta. *Dynamic Regulation of Bacterial Metabolic Pathways using Autonomous, Pathway-Independent Control Strategies*. PhD thesis, 2017.

[129] Spencer R. Scott and Jeff Hasty. Quorum Sensing Communication Modules for Microbial Consortia. *ACS Synthetic Biology*, 5(9):969–977, 9 2016.

[130] Andrew D Halleran and Richard M Murray. Cell-Free and In Vivo Characterization of Lux, Las, and Rpa Quorum Activation Systems in E.ăcoli. *ACS Synthetic Biology*, 7(2):752–755, 2 2018.

[131] Nicolas Kylilis, Zoltan A. Tuza, Guy Bart Stan, and Karen M. Polizzi. Tools for engineering coordinated system behaviour in synthetic microbial consortia. *Nature Communications*, 9(1), 12 2018.

[132] Stefan J. Tekel, Christina L. Smith, Brianna Lopez, Amber Mani, Christopher Connot, Xylaan Livingstone, and Karmella A. Haynes. Engineered Orthogonal Quorum Sensing Systems for Synthetic Gene Regulation in Escherichia coli. *Frontiers in Bioengineering and Biotechnology*, 7(MAR):80, 4 2019.

[133] Wei Jiang, Xinyuan He, Yue Luo, Yunlan Mu, Fei Gu, Quanfeng Liang, and Qingsheng Qi. Two Completely Orthogonal Quorum Sensing Systems with Self-Produced Autoinducers Enable Automatic Delayed Cascade Control. *ACS Synthetic Biology*, 9(9):2588–2599, 9 2020.

[134] Junjun Wu, Meijiao Bao, Xuguo Duan, Peng Zhou, Caiwen Chen, Jiahua Gao, Shiyao Cheng, Qianqian Zhuang, and Zhijun Zhao. Developing a pathway-independent and full-autonomous global resource allocation strategy to dynamically switching phenotypic states. *Nature Communications*, 11(1):1–14, 12 2020.

[135] Claudia Elena, Pablo Ravasi, María E. Castelli, Salvador Peirú, and Hugo G. Menzella. Expression of codon optimized genes in microbial systems: Current industrial applications and perspectives. *Frontiers in Microbiology*, 5(FEB):21, 2014.

[136] Michael Stadler and Andrew Fire. Wobble base-pairing slows in vivo translation elongation in metazoans. *RNA*, 17(12):2063–2073, 12 2011.

[137] Hans Peter Sørensen and Kim Kusk Mortensen. Soluble expression of recombinant proteins in the cytoplasm of Escherichia coli. *Microbial Cell Factories*, 4(1):1–8, 1 2005.

[138] Jin Hwa Jung and Sun Bok Lee. Identification and characterization of Thermoplasma acidophilum glyceraldehyde dehydrogenase: a new class of NADP+-specific aldehyde dehydrogenase. *Biochemical Journal*, 397(Pt 1):131, 7 2006.

[139] Silviya R. Macwan, Bhumika K. Dabhi, S.C. Parmar, and K.D. Aparnathi. Whey and its Utilization. *International Journal of Current Microbiology and Applied Sciences*, 5(8):134–155, 8 2016.

[140] John K. Henske, St Elmo Wilken, Kevin V. Solomon, Chuck R. Smallwood, Vaithiyalingam Shutthanandan, James E. Evans, Michael K. Theodorou, and

Michelle A. O'Malley. Metabolic characterization of anaerobic fungi provides a path forward for bioprocessing of crude lignocellulose. *Biotechnology and Bioengineering*, 115(4):874–884, 4 2018.

[141] Felix Moser, Amin Espah Borujeni, Amar N. Ghodasara, Ewen Cameron, Yongjin Park, and Christopher A. Voigt. Dynamic control of endogenous metabolism with combinatorial logic circuits. *Molecular Systems Biology*, 14(11), 11 2018.

[142] Christina V. Dinh, Xingyu Chen, and Kristala L. J. Prather. Development of a quorum-sensing based circuit for control of co-culture population composition in a naringenin production system. *ACS Synthetic Biology*, 2 2020.

[143] Pauli S. Losoi, Ville P. Santala, and Suvi M. Santala. Enhanced Population Control in a Synthetic Bacterial Consortium by Interconnected Carbon Cross-Feeding. *ACS Synthetic Biology*, 8(12):2642–2650, 12 2019.

[144] Wentao Kong, David R. Meldgin, James J. Collins, and Ting Lu. Designing microbial consortia with defined social interactions. *Nature Chemical Biology*, 14(8):821–829, 8 2018.

[145] Peter L. Singer. Federally Supported Innovations: 22 Examples of Major Technology Advances That Stem From Federal Research Support. Technical report, Information Technology & Innovation Foundation, Washington, DC, 2 2014.

[146] Paul Ellwood, Ceri Williams, and John Egan. Crossing the valley of death: Five underlying innovation processes. *Technovation*, 109, 1 2022.

[147] Gregory F. Nemet, Vera Zipperer, and Martina Kraus. The valley of death, the technology pork barrel, and public support for large demonstration projects. *Energy Policy*, 119:154–167, 8 2018.